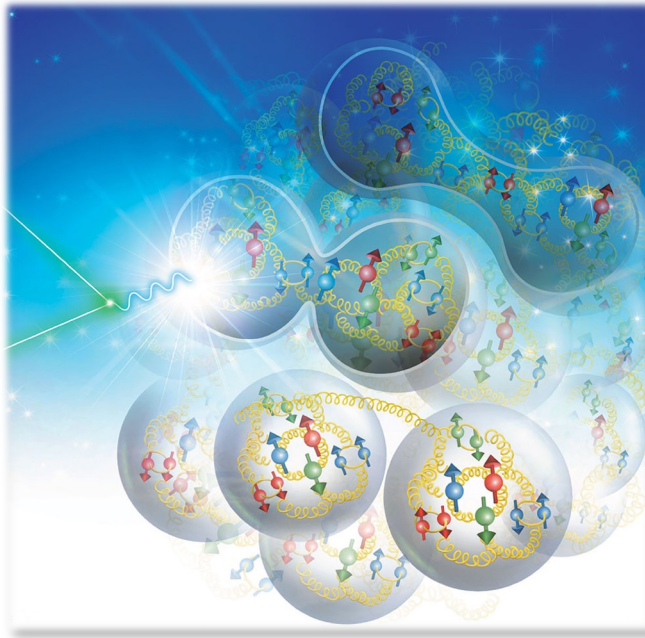


Imagining bound nucleons

John Terry

Los Alamos National Lab

Based on *Phys. Rev. Lett.* 129 (2022) 24, 242001, *JHEP* 10 (2023) 013,
JHEP 05 (2024) 066, *JHEP* 02 (2025) 102



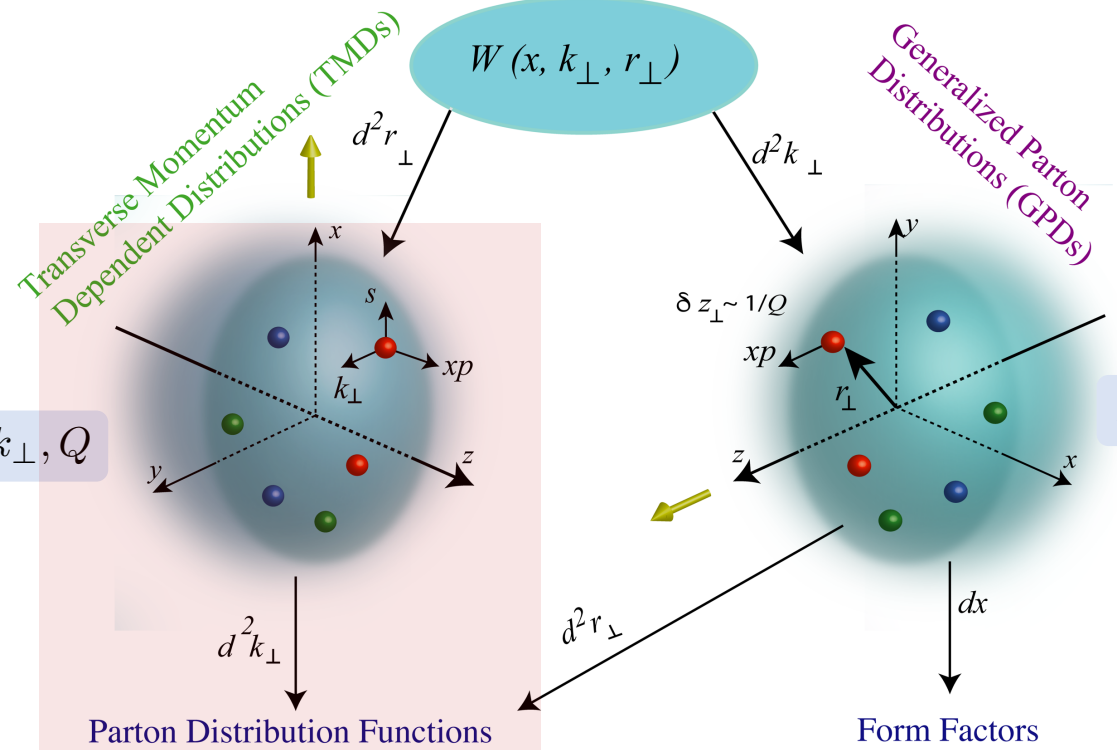
Motivation

The structure of matter in the vacuum

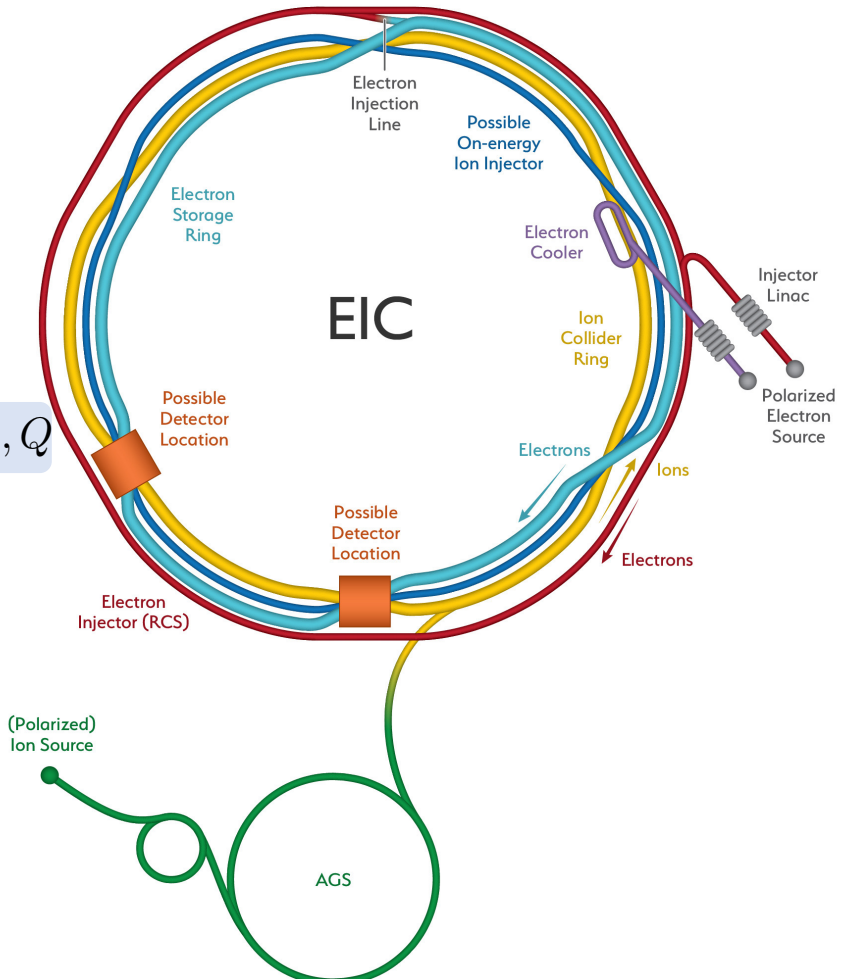
Distributions of partons in hadrons

Wigner Distributions

$\Lambda_{\text{QCD}}, k_\perp, 1/r_\perp, Q$



Highly differential distributions require high luminosity



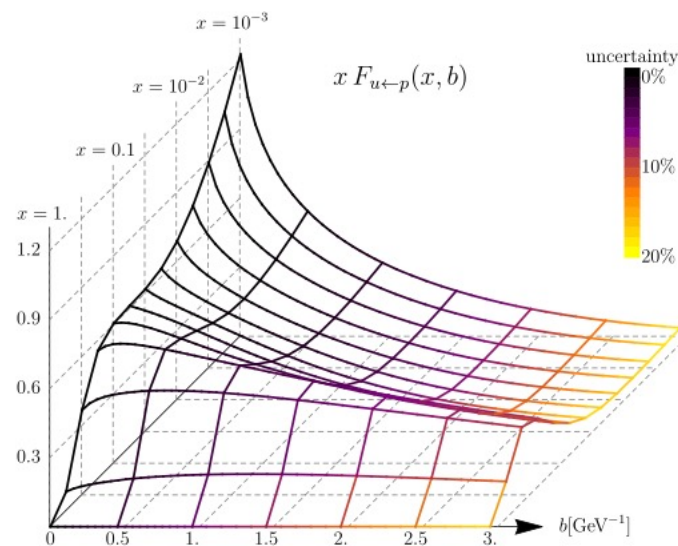
Images of proton structure

Global extraction from data requires evolution equations for TMDs

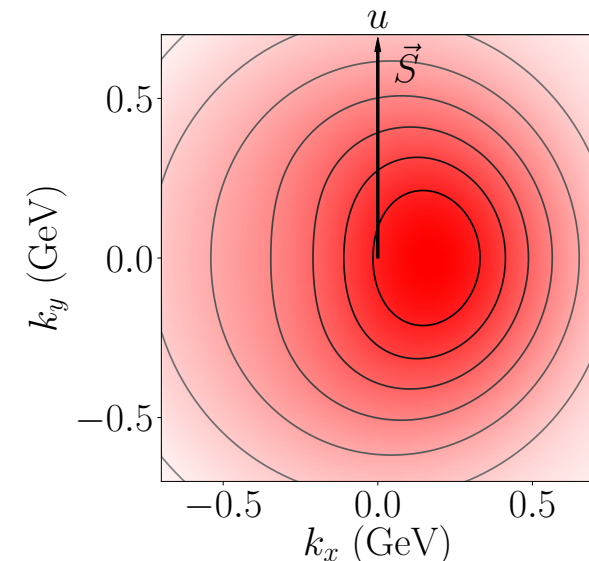
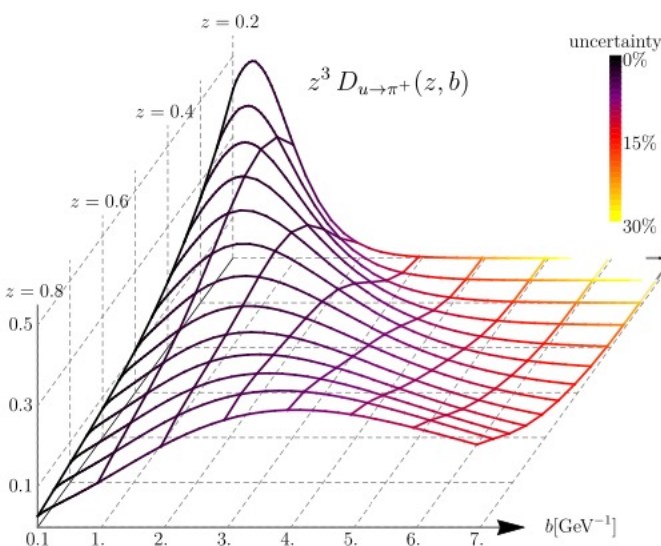
$$\frac{d}{d \ln \mu} \ln F(w, b, \mu, \zeta) = \gamma_\mu (\mu, \zeta) , \quad \frac{d}{d \ln \zeta} \ln F(w, b, \mu, \zeta) = \gamma_\zeta (b, \mu) ,$$

Approximations to N⁴LL TMDs have been extracted in *Moos, Scimemi, Vladimirov, Zurita (2023)*

True N⁴LL requires full 5 loop cusp anomalous dimension and evolution of PDF at N³LO



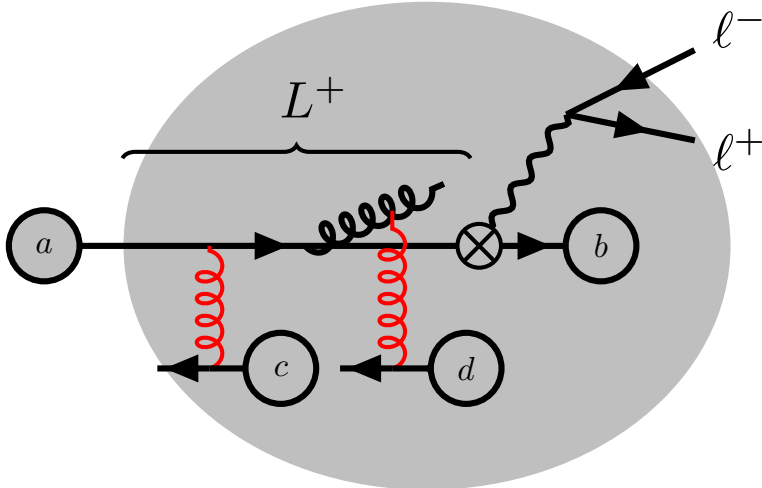
Gutierrez-Reyes, Scimemi, Vladimirov (2020)



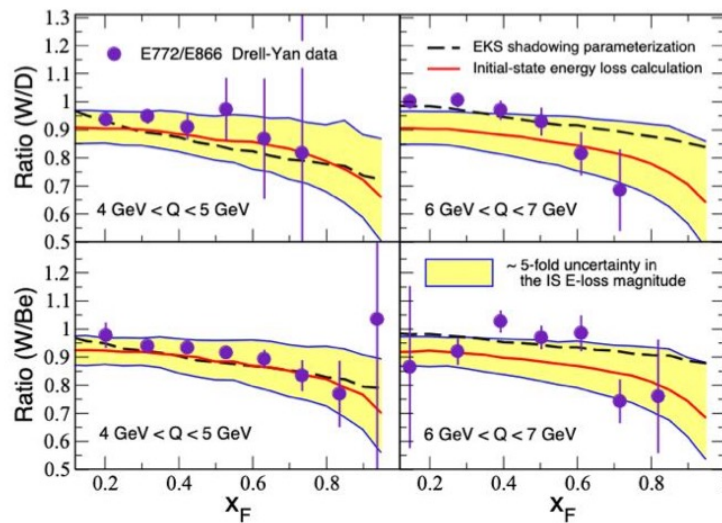
Echevarria, Kang, JT (2020)

How does nuclear matter alter TMDs

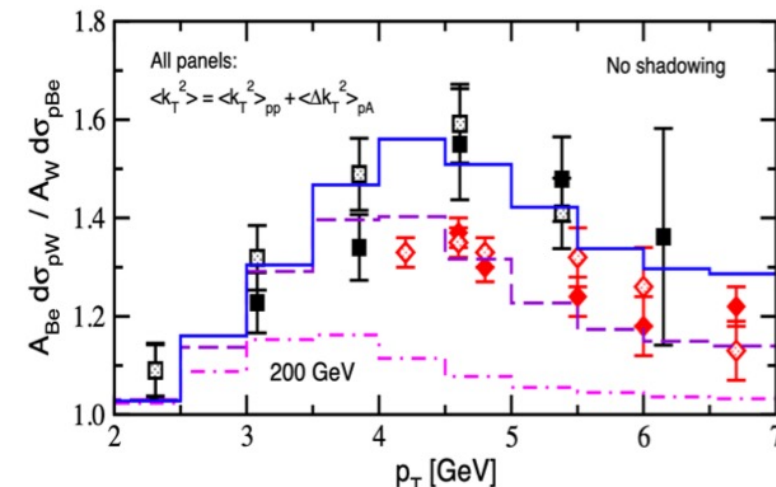
Example process



Stimulated emissions in Drell-Yan result in energy loss



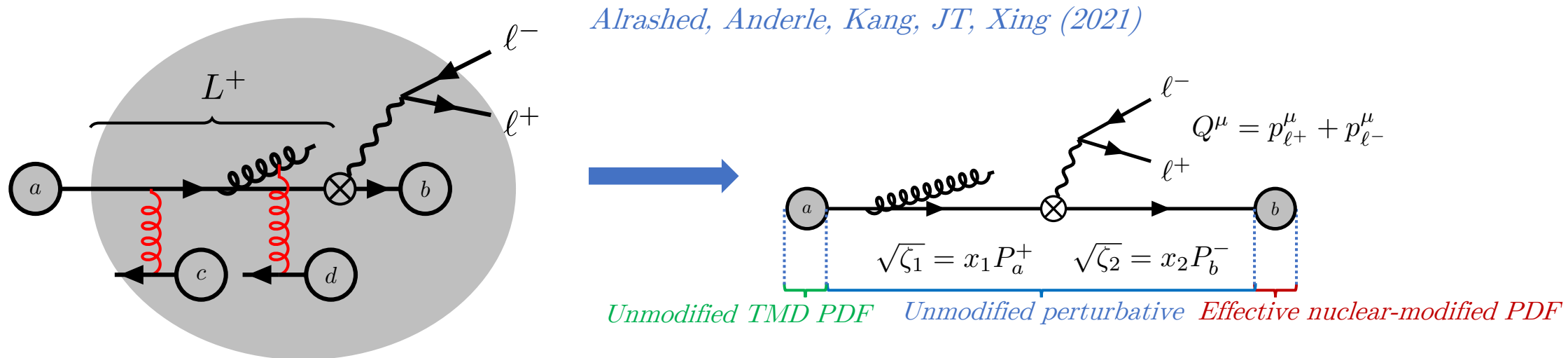
Stimulated emissions also generate additional transverse momentum



Past work

The structure of matter in the medium: an approximation

nTMDs were originally defined using an approximate scheme by these two



Non-perturbative parameterization is modified to account for nuclear medium effects

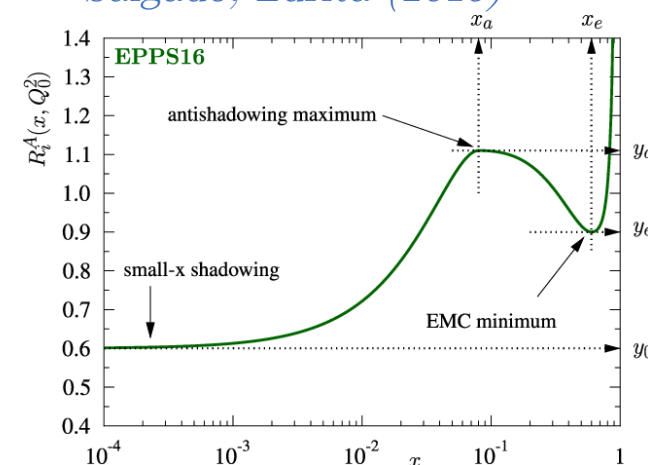
$$f_{1q/A}(x, b, \mu, \zeta) = [C \otimes f]_{q/A}(x, b, \mu_i, \zeta_i) U(\mu_i, \mu; \zeta) Z(b, \zeta_i, \zeta; \mu_i) U_{\text{NP}}^{fA}(x, b, \zeta, A)$$

$$D_{1h/q}^A(z, b, \mu, \zeta) = \frac{1}{z^2} [\hat{C} \otimes D^A]_{h/q}(z, b, \mu_i, \zeta_i) U(\mu_i, \mu; \zeta) Z(b, \zeta_i, \zeta; \mu_i) U_{\text{NP}}^{DA}(z, b, \zeta, A)$$

Perturbative

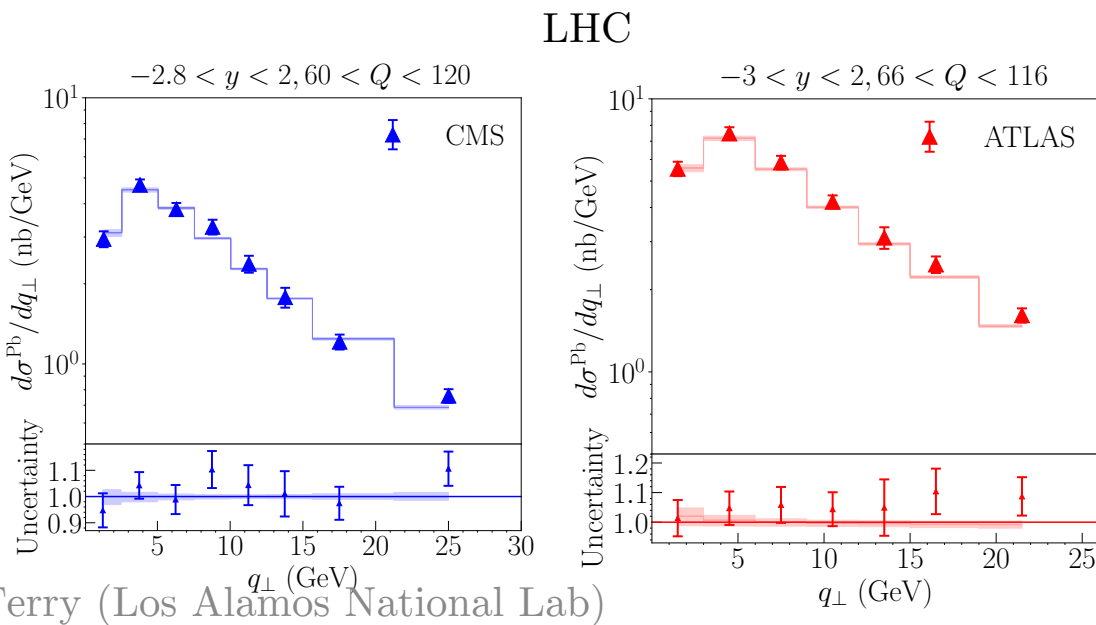
Non-perturbative

Armesto, Paukkunen, Penín, Salgado, Zurita (2015)

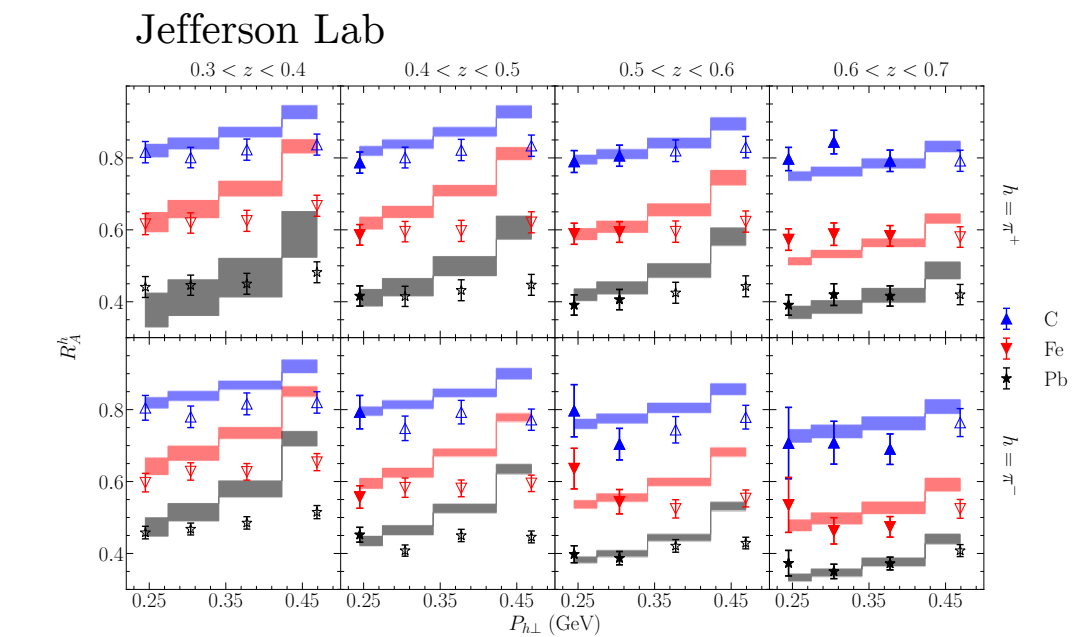
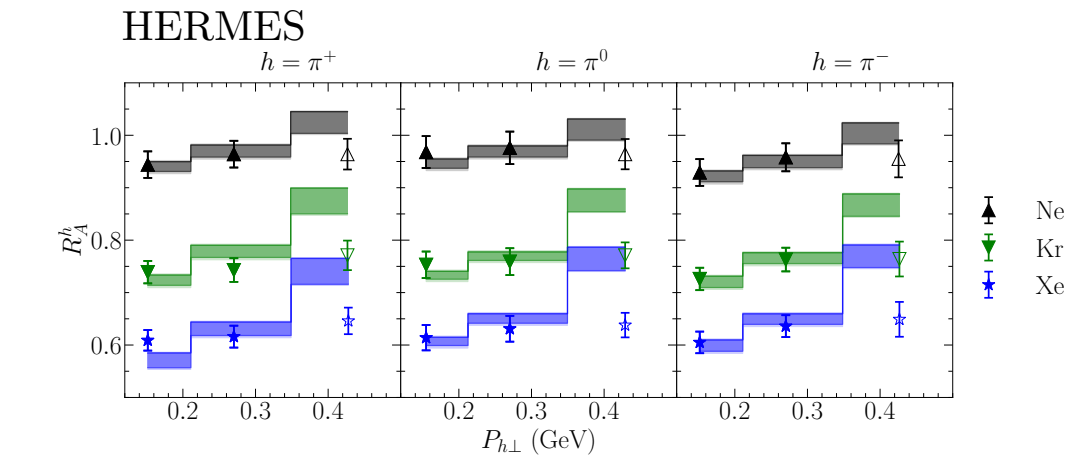


Description of the experimental data

Collaboration	Process	Baseline	Nuclei	N _{data}	χ^2
JLAB [49]	SIDIS(π)	D	C, Fe, Pb	36	41.7
HERMES [40]	SIDIS(π)	D	Ne, Kr, Xe	18	10.2
RHIC [43]	DY	p	Au	4	1.3
E772 [41]	DY	D	C, Fe, W	16	40.2
E866 [42]	DY	Be	Fe, W	28	20.6
CMS [63]	γ^*/Z	N/A	Pb	8	10.4
ATLAS [83]	γ^*/Z	N/A	Pb	7	13.3
Total				117	137.8



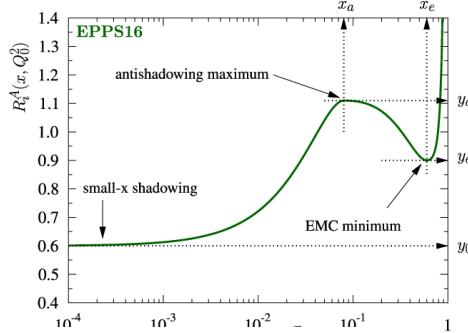
John Terry (Los Alamos National Lab)



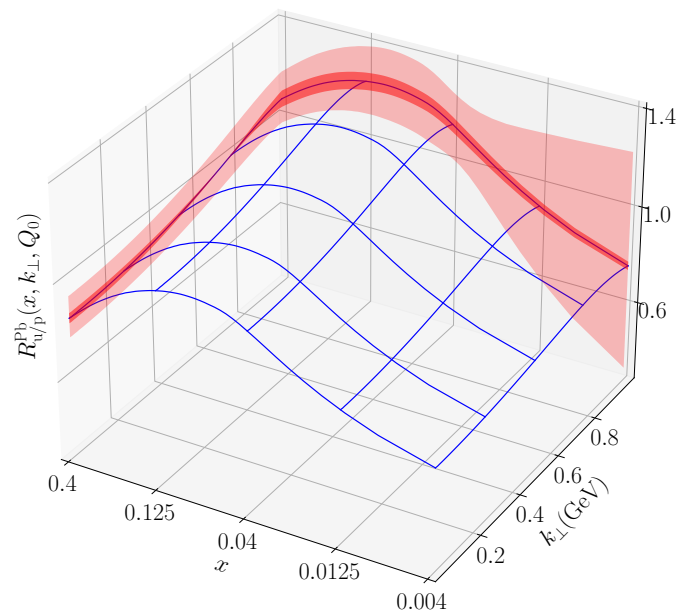
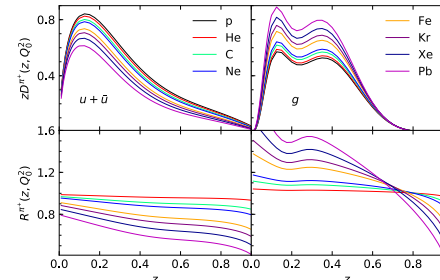
Three-dimensional images

Ratios defined for nPDF and nFF Alrashed, JT et al: Phys. Rev. Lett. 129 (2022)

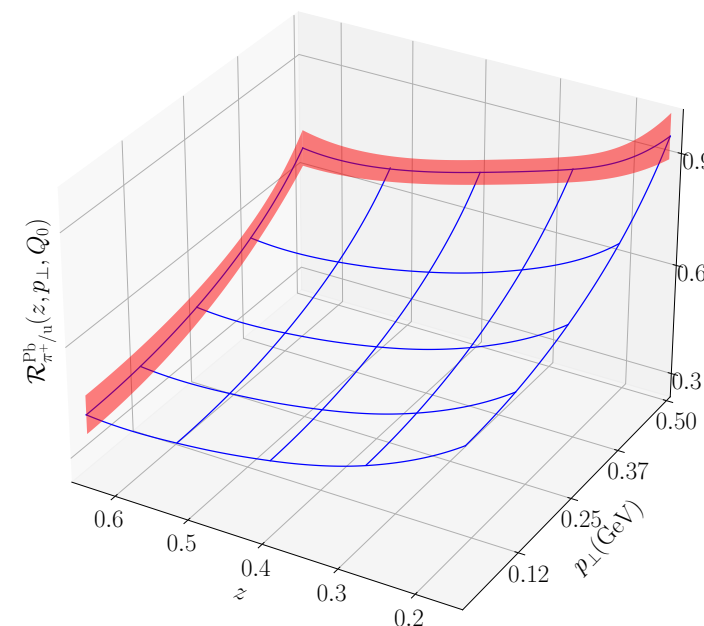
$$R_i^A(x, Q_0^2) = \frac{f_{i/p}^A(x, Q_0^2)}{f_{i/p}(x, Q_0^2)}$$



$$R_i^A(z, Q_0^2) = \frac{D_{h/i}^A(z, Q_0^2)}{D_{h/i}(z, Q_0^2)}$$



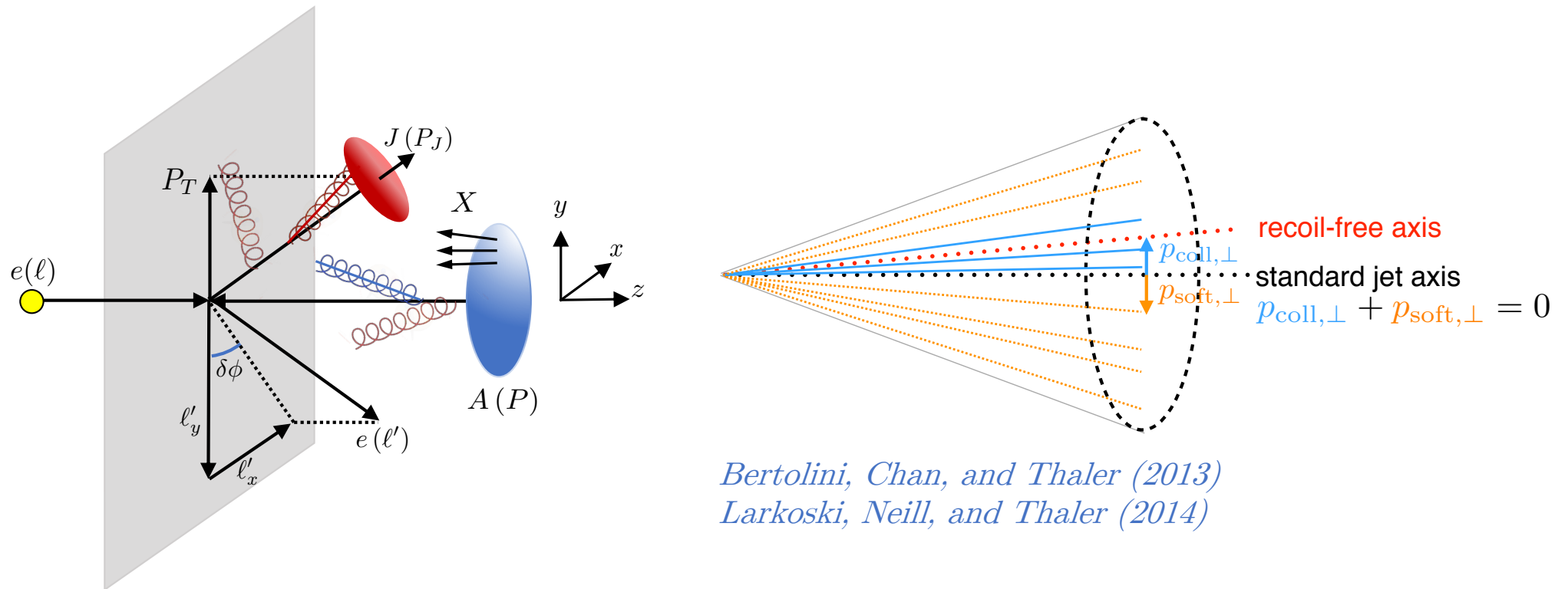
$$R_{u/p}^{Pb}(x, k_\perp, Q_0) = \frac{f_{u/p}^{Pb}(x, k_\perp, Q_0, Q_0^2)}{f_{u/p}(x, k_\perp, Q_0, Q_0^2)}$$



$$R_{\pi^+/u}^{Pb}(z, p_\perp, Q_0) = \frac{D_{\pi^+/u}^{Pb}(z, p_\perp, Q_0, Q_0^2)}{D_{\pi^+/u}(z, p_\perp, Q_0, Q_0^2)}$$

Back-to-back lepton-jet production

Process proposed by: *Liu, Ringer, Vogelsang, Yuan (2019)*



Factorization using recoil-free jets: *Fang, Ke, Shao, JT (2023)*

Hard: $P_{JT}(1, 1, 1)$

Collinear: $P_{JT}(\lambda^2, 1, \lambda)$

Jet: $P_{JT}(1, \lambda^2, \lambda)$

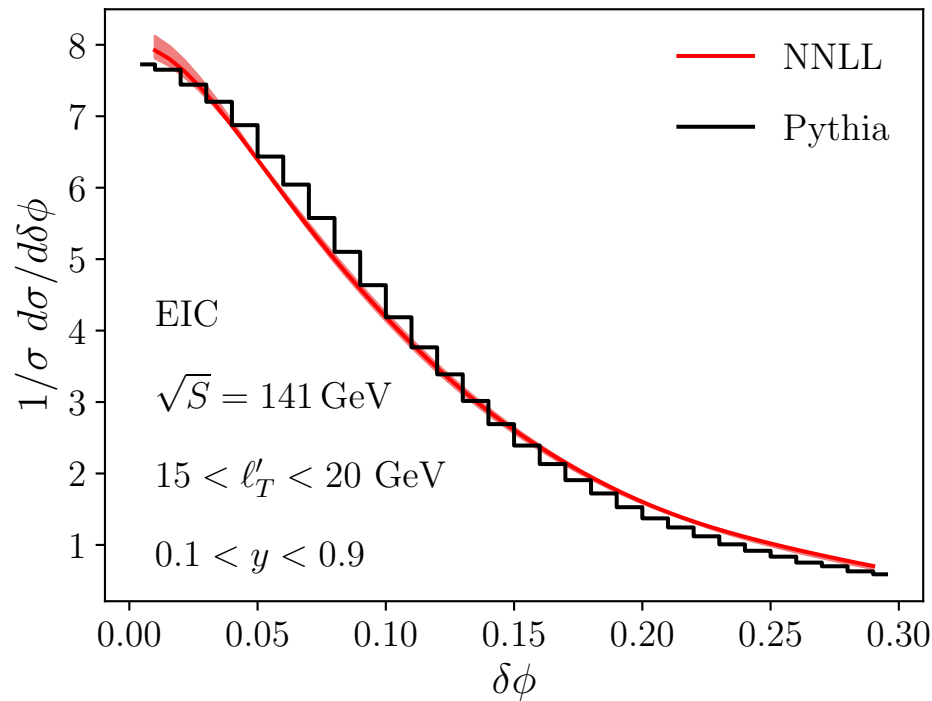
Global soft: $P_{JT}(\lambda, \lambda, \lambda)$

$$\frac{d\sigma_p}{d^2\ell'_T dy d\delta\phi} = \frac{\sigma_0 \ell'_T}{1-y} H(Q, \mu_H) \int \frac{db}{2\pi} \cos(b\ell'_T \delta\phi) \sum_q e_q^2 f_{q/p}(x_B, b, \mu_H, \zeta_B) \mathcal{J}_q(b, \mu_H, \zeta_J)$$

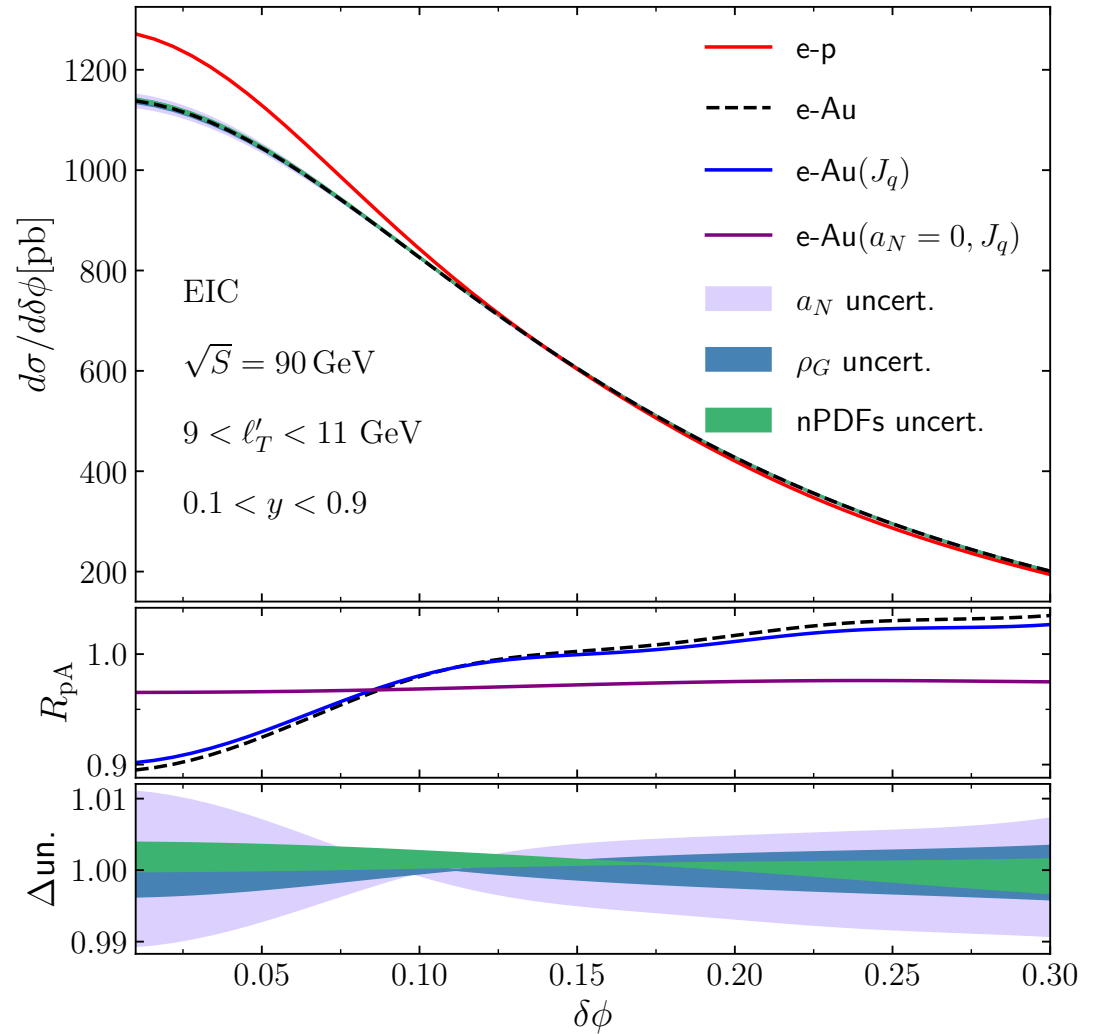
$$\frac{d\sigma_A}{d^2\ell'_T dy d\delta\phi} = \frac{\sigma_0 \ell'_T}{1-y} H(Q, \mu_H) \int \frac{db}{2\pi} \cos(b\ell'_T \delta\phi) \sum_q e_q^2 f_{q/A}(x_B, b, \mu_H, \zeta_B) \mathcal{J}_q^A(b, \mu_H, \zeta_J)$$

Predictions at the EIC

Comparison of our results with Pythia at NNLL

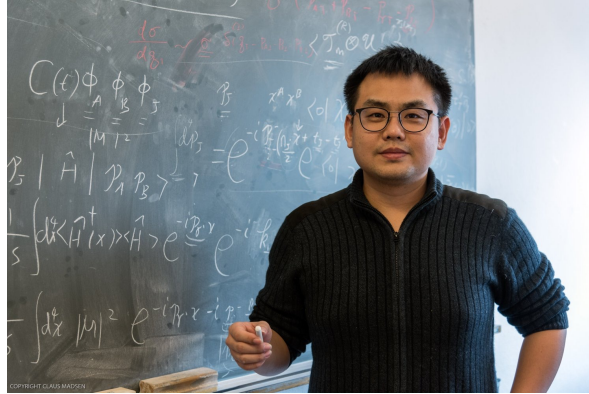


Perturbative ingredients are known to have N³LL accuracy.
Only missing the 3-loop jet function and the 5-loop
cusp anomalous dimension to reach N⁴LL

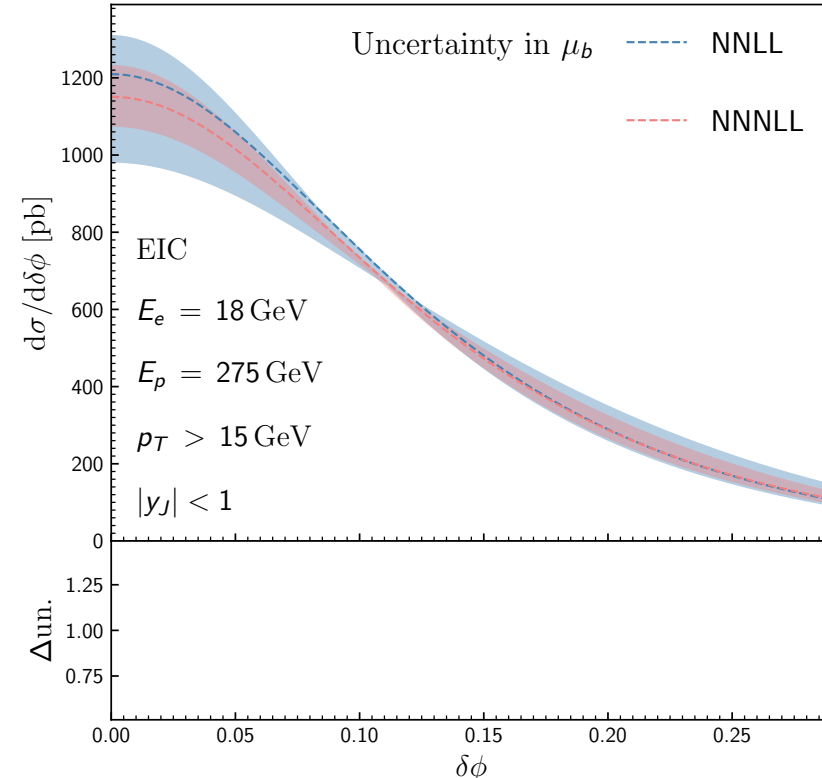


Higher order results

Results have been taken one step higher by: *Fang, Gao, Li, Shao (2024)*



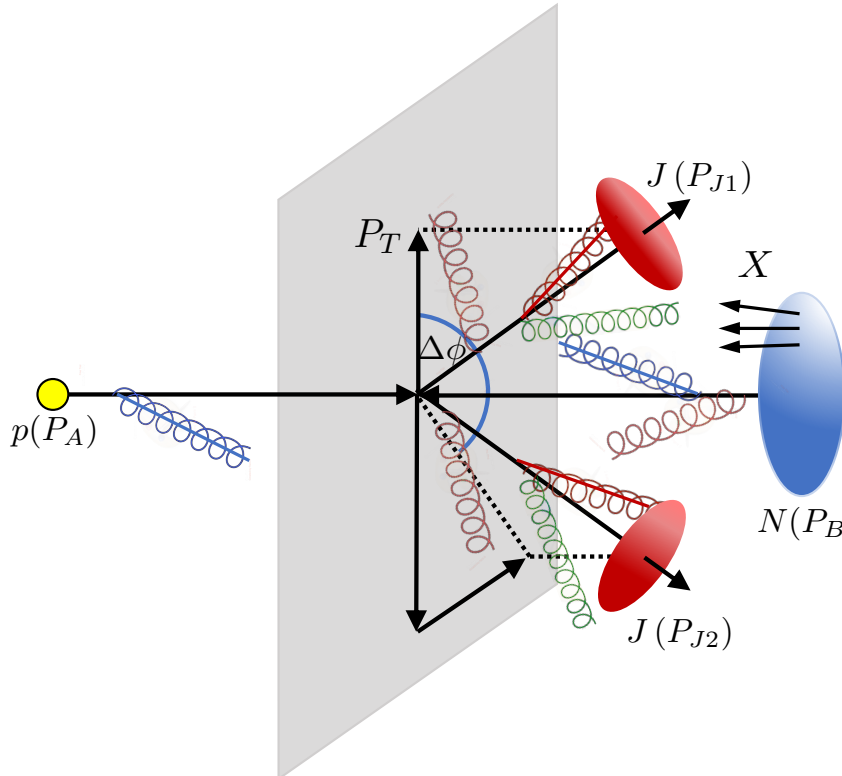
$$\begin{aligned}
 J_q(b, \mu, \zeta) = & 1 + \frac{\alpha_s C_F}{4\pi} \left[-L_b^2 + L_b(3 + 2L_\zeta) - \frac{5\pi^2}{6} + 7 - 6\ln 2 \right] \\
 & + \left(\frac{\alpha_s}{4\pi} \right)^2 \left\{ C_F^2 \left[\frac{L_b^4}{2} - L_b^3(3 + 2L_\zeta) + L_b^2 \left(2L_\zeta^2 + 6L_\zeta - \frac{5}{2} + 6\ln 2 + \frac{5\pi^2}{6} \right) \right. \right. \\
 & + L_b \left(L_\zeta \left(14 - 12\ln 2 - \frac{5\pi^2}{3} \right) + \frac{45}{2} - 18\ln 2 - \frac{9\pi^2}{2} + 24\zeta_3 \right) \left. \right] \\
 & + C_F C_A \left[-\frac{22}{9} L_b^3 + L_b^2 \left(\frac{11}{3} L_\zeta - \frac{35}{18} + \frac{\pi^2}{3} \right) + L_\zeta \left(\frac{404}{27} - 14\zeta_3 \right) \right. \\
 & + L_b \left(L_\zeta \left(\frac{134}{9} - \frac{2\pi^2}{3} \right) + \frac{57}{2} - 22\ln 2 - \frac{11\pi^2}{9} - 12\zeta_3 \right) \left. \right] \\
 & + C_F T_F n_f \left[\frac{8}{9} L_b^3 + L_b^2 \left(\frac{2}{9} - \frac{4}{3} L_\zeta \right) + L_b \left(-\frac{40}{9} L_\zeta - 10 + 8\ln 2 + \frac{4\pi^2}{9} \right) \right. \\
 & \left. \left. - \frac{112}{27} L_\zeta \right] + j_2 \right\}, \quad \text{Constant that was obtained numerically}
 \end{aligned}$$



Gutierrez-Reyes, Scimemi, Waalewijn, Zoppi (2019)

Factorization in pp and pA

Azimuthal angle decorrelations of di-jets measured at the CMS, are sensitive to nTMDs



Factorization and resummation derived in a SCET framework

$$\text{hard} : p_h^\mu \sim p_T(1, 1, 1)$$

$$n_{a,b}\text{-collinear} : p_{c_i}^\mu \sim p_T(\delta\phi^2, 1, \delta\phi)_{n_i \bar{n}_i},$$

$$\text{soft} : p_s^\mu \sim p_T(\delta\phi, \delta\phi, \delta\phi),$$

$$n_{c,d}\text{-jet} : p_{c_i}^\mu \sim p_T(R^2, 1, R)_{n_i \bar{n}_i},$$

$$n_{c,d}\text{-collinear-soft} : p_{cs_i}^\mu \sim \frac{p_T \delta\phi}{R} (R^2, 1, R)_{n_i \bar{n}_i},$$

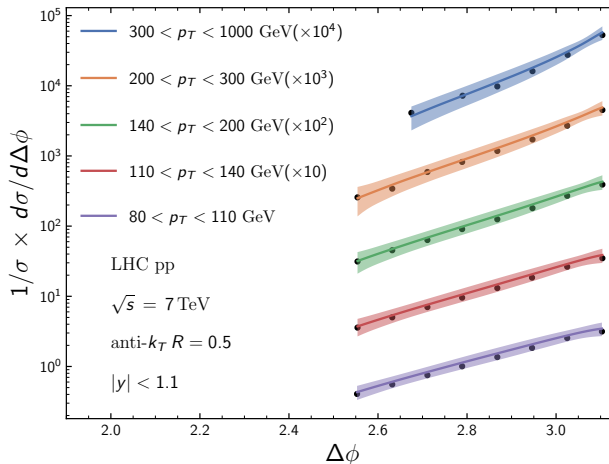
$$\begin{aligned} \frac{d^4\sigma_{pA}}{dy_c dy_d dp_T^2 d\delta\phi} &= \sum_{abcd} \frac{p_T}{16\pi\hat{s}^2} \frac{1}{1 + \delta_{cd}} \int_0^\infty \frac{2db}{\pi} \cos(bp_T\delta\phi) x_a \tilde{f}_{a/p}(x_a, \mu_{b_*}) x_b \tilde{f}_{b/A}(x_b, \mu_{b_*}) \\ &\times \exp \left\{ - \int_{\mu_{b_*}}^{\mu_h} \frac{d\mu}{\mu} \left[\gamma_{\text{cusp}}(\alpha_s) C_H \ln \frac{\hat{s}}{\mu^2} + 2\gamma_H(\alpha_s) \right] \right\} \\ &\times \sum_{KK'} \exp \left[- \int_{\mu_{b_*}}^{\mu_h} \frac{d\mu}{\mu} \gamma_{\text{cusp}}(\alpha_s) (\lambda_K + \lambda_{K'}^*) \right] H_{KK'}(\hat{s}, \hat{t}, \mu_h) W_{K'K}(b_*, \mu_{b_*}) \\ &\times \exp \left[- \int_{\mu_{b_*}}^{\mu_j} \frac{d\mu}{\mu} \Gamma^{J_c}(\alpha_s) - \int_{\mu_{b_*}}^{\mu_j} \frac{d\mu}{\mu} \Gamma^{J_d}(\alpha_s) \right] U_{\text{NG}}^c(\mu_{b_*}, \mu_j) U_{\text{NG}}^d(\mu_{b_*}, \mu_j) \\ &\times \exp \left[-S_{\text{NP}}^a(b, Q_0, \sqrt{\hat{s}}) - S_{\text{NP}}^{b,A}(b, Q_0, \sqrt{\hat{s}}) \right] \end{aligned}$$

Description of pp and pA data

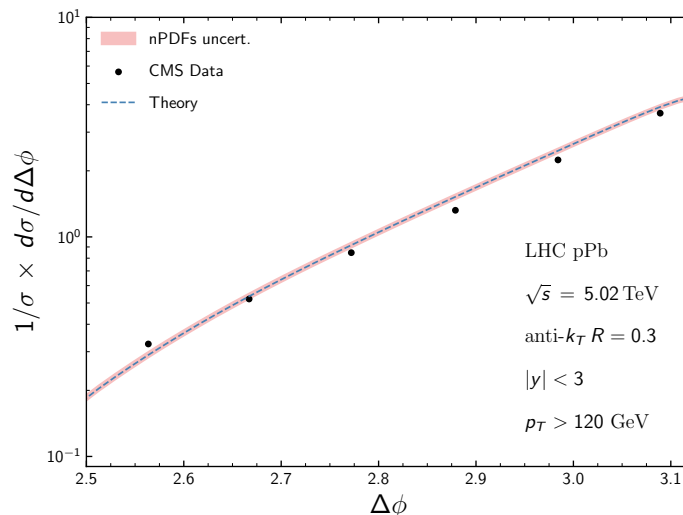
Strong consistency with the CMS measurements of the azimuthal angle decorrelation in pA and the ratio of the integrated azimuthal angle decorrelation.

$$\frac{d^4\sigma_{pp}}{dy_c dy_d dp_T^2 d\Delta\phi}$$

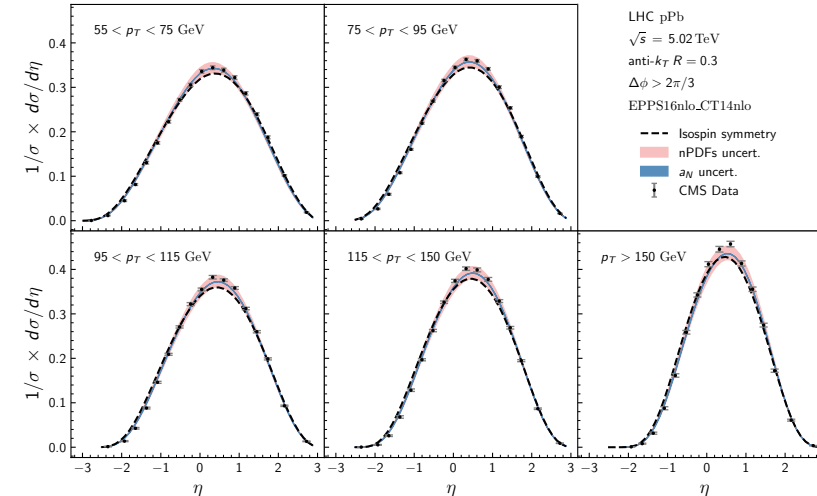
Phys. Rev. Lett. 106:122003, 2011



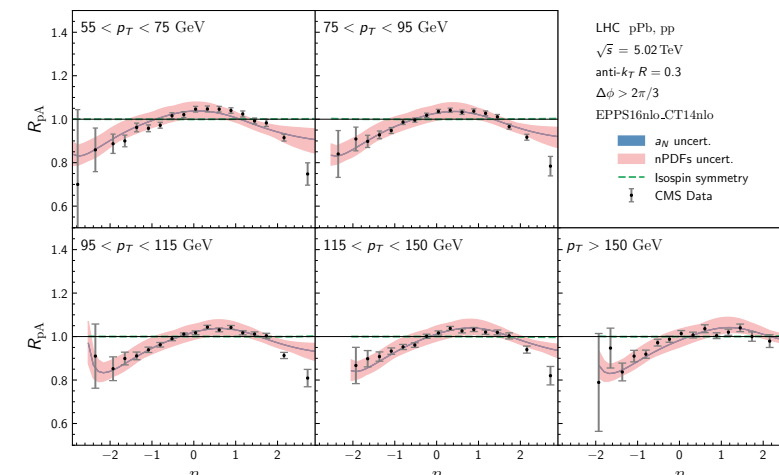
$$\frac{d^4\sigma_{pA}}{dy_c dy_d dp_T^2 d\Delta\phi}$$



Phys. Rev. Lett. 121, 062002 (2018)



$$R_{pA} = \frac{1}{A} \frac{d^4\sigma_{pA}}{dy_c dy_d dp_T^2 d\Delta\phi} / \frac{d^4\sigma_{pp}}{dy_c dy_d dp_T^2 d\Delta\phi}$$



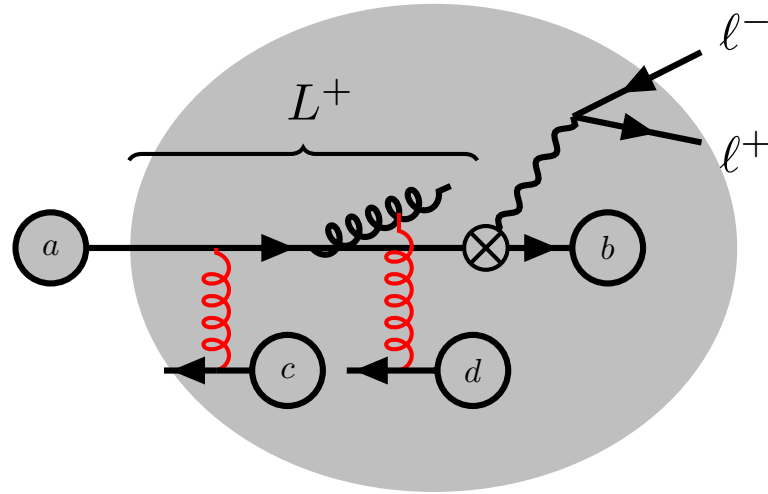
Eur. Phys. J. C 74 (2014) 2951

Phys. Rev. Lett. 121, 062002 (2018)

Towards first principles

The structure of matter in the medium

Spectrum of energy and transverse momentum in matter is modified in a non-trivial way in QCD



Cross section can be written as an expansion in the opacity

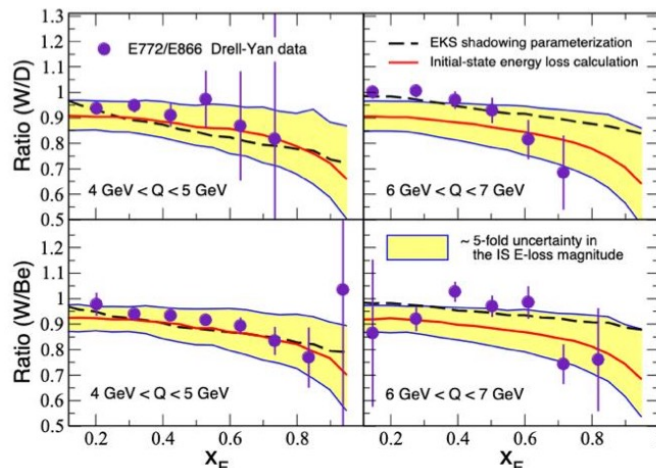
$$\frac{d\sigma}{d\mathcal{PS}} = \sum_{n=0}^{\infty} \frac{1}{n!} \chi^n \frac{d\sigma_n}{d\mathcal{PS}}$$

χ^n is the average number of active partons that contribute

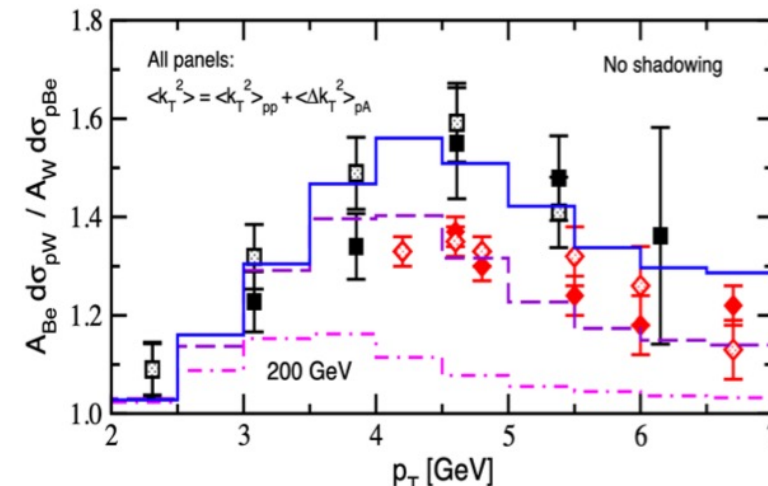
$$\chi^n \ll 1$$

Gyulassy-Levai-Vitev (2000) Guo, Wang (2000)

Stimulated emissions in Drell-Yan result in energy loss

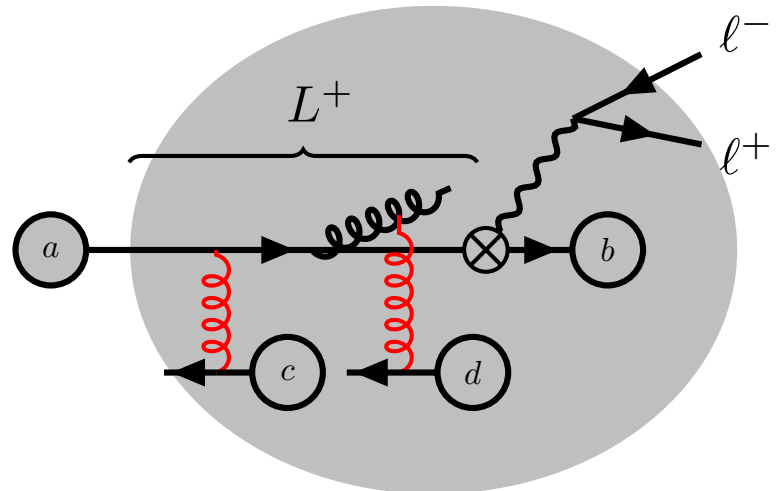


Stimulated emissions also generate additional transverse momentum



The Landau–Pomeranchuk–Migdal effect

Spectrum of energy and transverse momentum in matter is modified in a non-trivial way in QCD



Cross section can be written as an expansion in the opacity

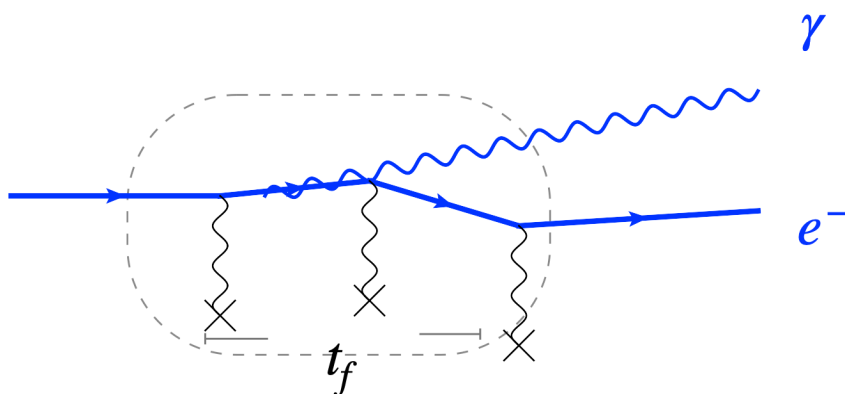
$$\frac{d\sigma}{d\mathcal{PS}} = \sum_{n=0}^{\infty} \frac{1}{n!} \chi^n \frac{d\sigma_n}{d\mathcal{PS}}$$

$$\chi^n \ll 1$$

χ^n is the average number of active partons that contribute

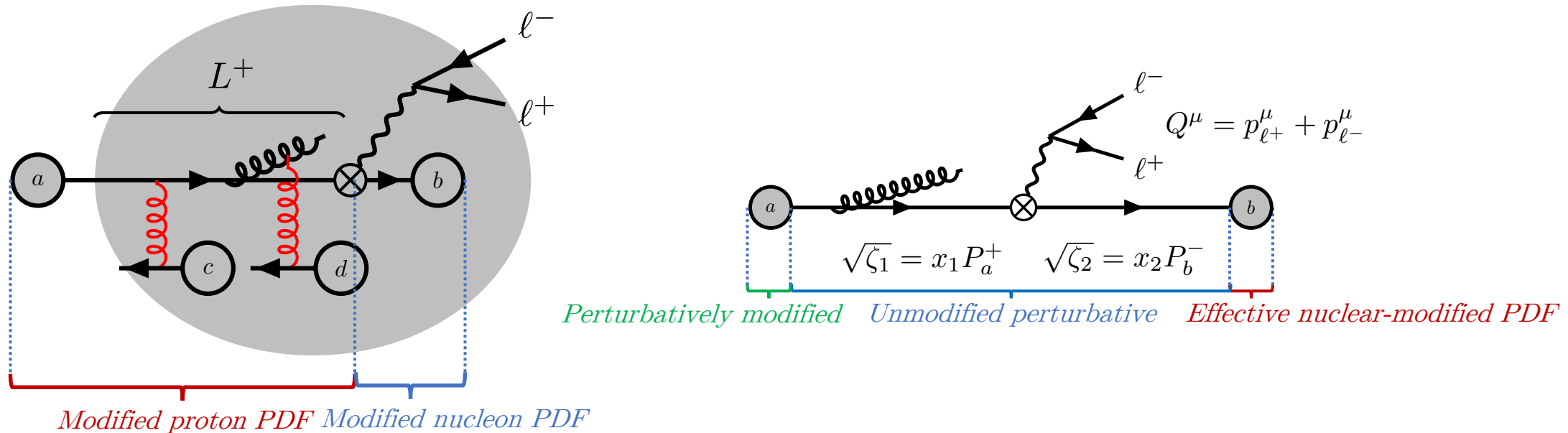
Spectrum of energy and transverse momentum in matter is modified in a non-trivial way in QCD

Landau et al (1953), Migdal (1956)



The structure of matter in the medium: modified beam function

Spectrum of energy and transverse momentum in matter is modified in a non-trivial way in QCD



We consider the first-order opacity correction to the incoming beam function

$$\frac{d\sigma}{d\mathcal{PS}} = \sum_{n=0}^{\infty} \frac{1}{n!} \chi^n \frac{d\sigma_n}{d\mathcal{PS}}$$

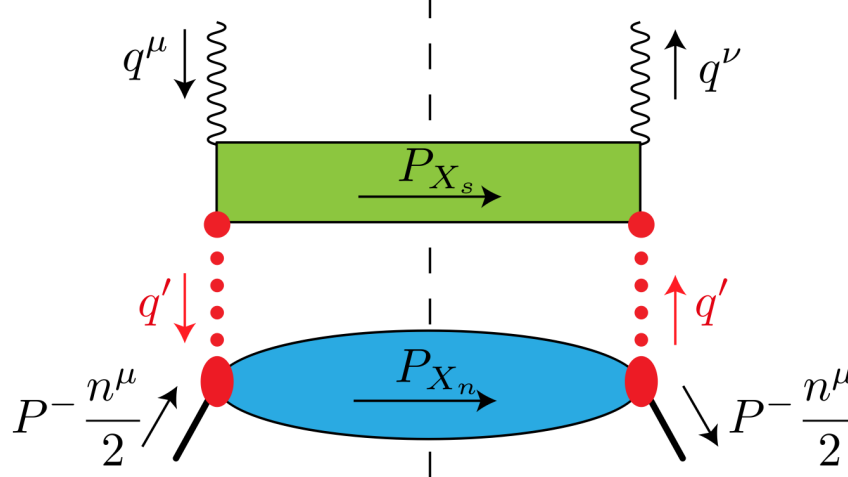
$$\frac{d\sigma_1}{d\mathcal{PS}} = \frac{4\pi\alpha_{\text{em}}^2}{3N_c Q^2 s} H(Q, \mu) \sum_q c_q(Q) \int \frac{d^2 \mathbf{b}}{(2\pi)^2} e^{i \mathbf{P}_T \cdot \mathbf{b}} \\ \times \sum_{N \in A} \mathcal{B}_{q/p, 1} \left(x_1, b, \mu, \frac{\zeta_1}{\nu^2}; \mu_E, \mathcal{L}_1 \right) \mathcal{B}_{\bar{q}/N} \left(x_2, b, \mu, \frac{\zeta_2}{\nu^2} \right) S(b, \mu, \nu)$$

The focus of this talk

Soft-Collinear Effective Theory with Glaubers

SCET with Glauber gluons has been applied to pp and DIS

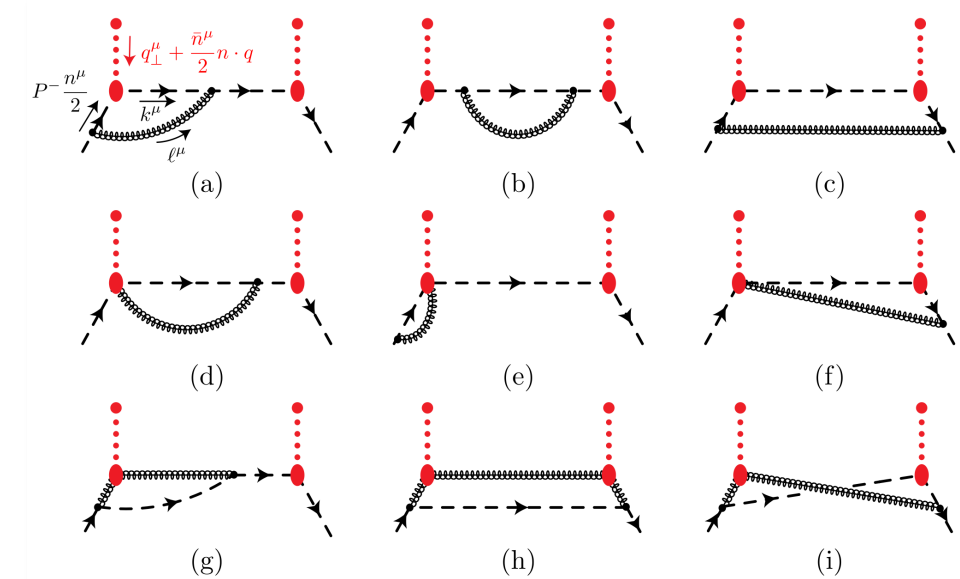
$$S_G = \sum_{i,j} \int d^4x \mathcal{O}_{ns}^{ij}(x), \quad \mathcal{O}_{ns}^{ij}(x) = 8\pi\alpha_s e^{-ix\cdot P} \mathcal{O}_n^{iA}(\tilde{x}) \frac{1}{P_\perp^2} \mathcal{O}_s^{j_n A}(\tilde{x}),$$



$$p_{\bar{n}} \sim \sqrt{s} \left(\underbrace{1}_{p^+}, \underbrace{\lambda^2}_{p^-}, \underbrace{\lambda}_{p_\perp} \right)$$

$$k_s \sim \sqrt{s} \left(\underbrace{\lambda}_{p^+}, \underbrace{\lambda}_{p^-}, \underbrace{\lambda}_{p_\perp} \right)$$

$$p_n \sim \sqrt{s} \left(\underbrace{\lambda^2}_{p^+}, \underbrace{1}_{p^-}, \underbrace{\lambda}_{p_\perp} \right)$$



Was shown that rapidity divergences of the collinear function give rise to the BFKL evolution equation

$$\nu \frac{d}{d\nu} C \left(\frac{\nu}{\bar{n} \cdot P}, q_\perp, \epsilon \right) = -C \left(\frac{\nu}{\bar{n} \cdot P}, q_\perp, \epsilon \right)$$

Ovanesyan, Vitev (2011)

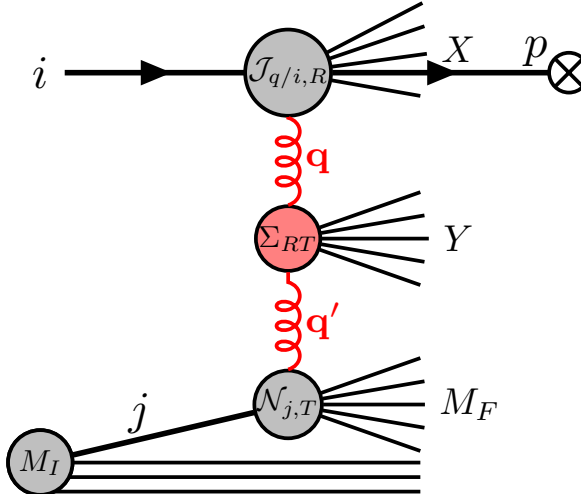
Rothstein, Stewart (2016)

Neill, Pathak, Stewart (2022)

$$- 2 \frac{\alpha_s C_A}{\pi} \nu^\epsilon \mu^{2\epsilon} \int \frac{d^{2-2\epsilon} k_\perp}{(2\pi)^{1-2\epsilon}} \left\{ \frac{C \left(\frac{\nu}{\bar{n} \cdot P}, \vec{k}_\perp, \epsilon \right)}{(\vec{q}_\perp - \vec{k}_\perp)^2} - \frac{\vec{q}_\perp^2}{2 \vec{k}_\perp^2 (\vec{q}_\perp - \vec{k}_\perp)^2} C \left(\frac{\nu}{\bar{n} \cdot P}, q_\perp, \epsilon \right) \right\}$$

Overview of graphs at one loop

In this paper, we study the correlations between the incoming proton and the medium



$$\mathcal{B}_{q/p,1} = \sum_{i=q,g} \sum_{j=q,\bar{q},g} \sigma_{q/i,j} \otimes f_{i/p} \otimes f_{j/N} \cdot \rho_0^- L^+,$$

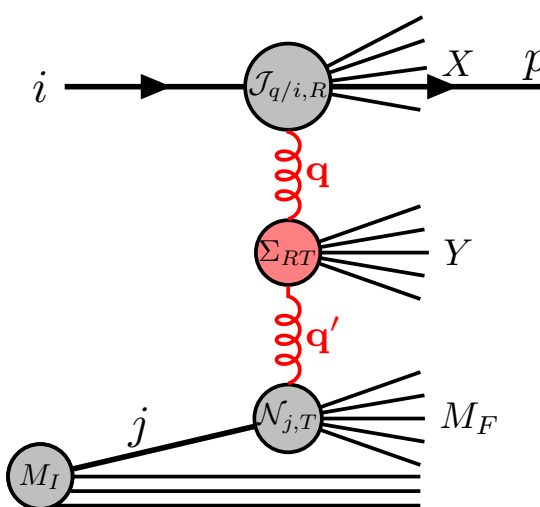
$$\begin{aligned} \sigma_{q/q,j}^{(0)} + \sigma_{q/q,j}^{(1)} &= \left(\mathcal{J}_{q/q,F}^{(0)} + \mathcal{J}_{q/q,F}^{(1),\text{rap}} \right) \otimes_{\perp} \Sigma_{FT}^{(0)} \otimes_{\perp} \mathcal{N}_{j,T}^{(0)} + \\ &+ \mathcal{J}_{q/q,F}^{(1),\text{coll}} \otimes_{\perp} \Sigma_{FT}^{(0)} \otimes_{\perp} \mathcal{N}_{j,T}^{(0)} + \mathcal{J}_{q/q,A}^{(1),\text{coll}} \otimes_{\perp} \Sigma_{AT}^{(0)} \otimes_{\perp} \mathcal{N}_{j,T}^{(0)} \\ &+ \mathcal{J}_{q/q,A}^{(1),\text{rap}} \otimes_{\perp} \Sigma_{AT}^{(0)} \otimes_{\perp} \mathcal{N}_{j,T}^{(0)} + \mathcal{J}_{q/q,F}^{(0)} \otimes_{\perp} \Sigma_{FT}^{(1)} \otimes_{\perp} \mathcal{N}_{j,T}^{(0)} + \mathcal{J}_{q/q,F}^{(0)} \otimes_{\perp} \Sigma_{FT}^{(0)} \otimes_{\perp} \mathcal{N}_{j,T}^{(1)} \\ &+ \Delta\sigma_{q/q,j}^{\text{NLO}}, \end{aligned}$$

Here we use the short-hand

$$\begin{aligned} [\mathcal{J}_{q/i,R} \otimes_{\perp} \Sigma_{RT} \otimes_{\perp} \mathcal{N}_{j,T}] (x_1, \mathbf{p}, \mu) &= \int \frac{d^{2-2\epsilon} \mathbf{q}}{(2\pi)^{2-2\epsilon}} \frac{d^{2-2\epsilon} \mathbf{q}'}{(2\pi)^{2-2\epsilon}} \left[\mathcal{J}_{q/i,R}(x_1, \mathbf{p}, \mathbf{q}, \mu, \nu) \frac{g_s^2}{\mathbf{q}^2} \right] \\ &\times \left[\left(\frac{g_s^2}{\mathbf{q}^2} \right)^{-1} \Sigma_{RT}(\mathbf{q}, \mathbf{q}', \nu, \nu') \left(\frac{g_s^2}{\mathbf{q}'^2} \right)^{-1} \right] \times \left[\frac{g_s^2}{\mathbf{q}'^2} \mathcal{N}_{j,T}(\mathbf{q}', \nu') \right] \end{aligned}$$

Overview of graphs at one loop

In this paper, we study the correlations between the incoming proton and the medium

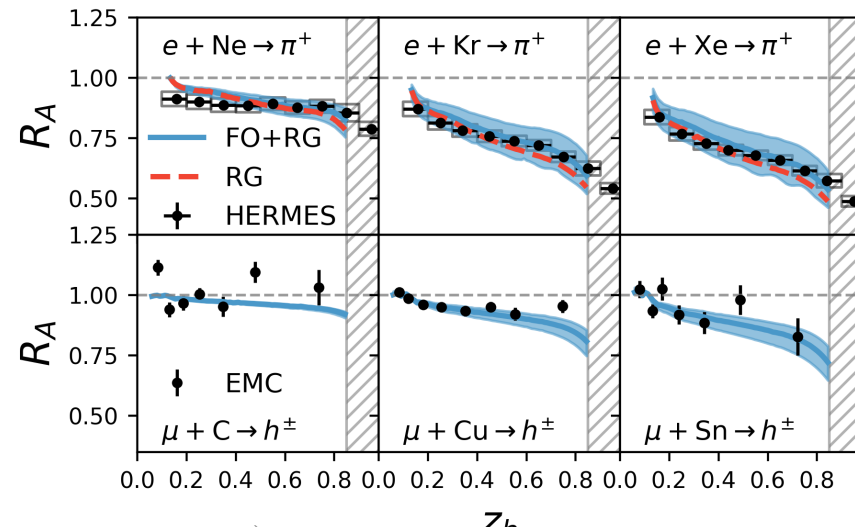


$$\mathcal{B}_{q/p,1} = \sum_{i=q,g} \sum_{j=q,\bar{q},g} \sigma_{q/i,j} \otimes f_{i/p} \otimes f_{j/N} \cdot \rho_0^- L^+,$$

$$\begin{aligned} \sigma_{q/q,j}^{(0)} + \sigma_{q/q,j}^{(1)} &= \left(\mathcal{J}_{q/q,F}^{(0)} + \mathcal{J}_{q/q,F}^{(1),\text{rap}} \right) \otimes_{\perp} \Sigma_{FT}^{(0)} \otimes_{\perp} \mathcal{N}_{j,T}^{(0)} + \\ &+ \mathcal{J}_{q/q,F}^{(1),\text{coll}} \otimes_{\perp} \Sigma_{FT}^{(0)} \otimes_{\perp} \mathcal{N}_{j,T}^{(0)} + \mathcal{J}_{q/q,A}^{(1),\text{coll}} \otimes_{\perp} \Sigma_{AT}^{(0)} \otimes_{\perp} \mathcal{N}_{j,T}^{(0)} \\ &+ \mathcal{J}_{q/q,A}^{(1),\text{rap}} \otimes_{\perp} \Sigma_{AT}^{(0)} \otimes_{\perp} \mathcal{N}_{j,T}^{(0)} + \mathcal{J}_{q/q,F}^{(0)} \otimes_{\perp} \Sigma_{FT}^{(1)} \otimes_{\perp} \mathcal{N}_{j,T}^{(0)} + \mathcal{J}_{q/q,F}^{(0)} \otimes_{\perp} \Sigma_{FT}^{(0)} \otimes_{\perp} \mathcal{N}_{j,T}^{(1)} \\ &+ \Delta\sigma_{q/q,j}^{\text{NLO}}, \end{aligned}$$

Collinear divergent terms

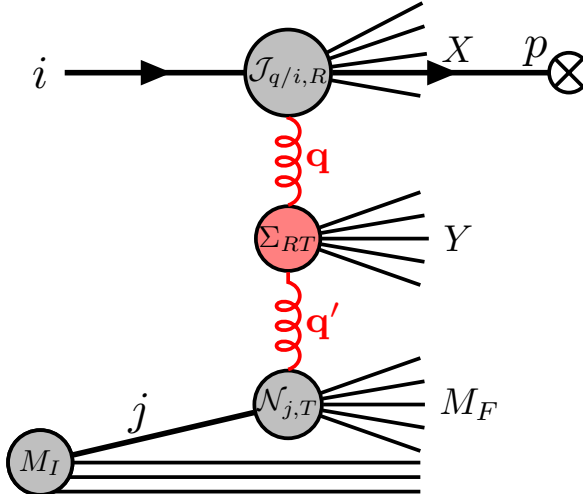
Collinear divergent terms have been considered in Semi-Inclusive DIS



Ke, Vitev (2023)

Overview of graphs at one loop

In this paper, we study the correlations between the incoming proton and the medium



$$\mathcal{B}_{q/p,1} = \sum_{i=q,g} \sum_{j=q,\bar{q},g} \sigma_{q/i,j} \otimes f_{i/p} \otimes f_{j/N} \cdot \rho_0^- L^+,$$

$$\begin{aligned} \sigma_{q/q,j}^{(0)} + \sigma_{q/q,j}^{(1)} &= \left(\mathcal{J}_{q/q,F}^{(0)} + \mathcal{J}_{q/q,F}^{(1),\text{rap}} \right) \otimes_{\perp} \Sigma_{FT}^{(0)} \otimes_{\perp} \mathcal{N}_{j,T}^{(0)} + \\ &+ \mathcal{J}_{q/q,F}^{(1),\text{coll}} \otimes_{\perp} \Sigma_{FT}^{(0)} \otimes_{\perp} \mathcal{N}_{j,T}^{(0)} + \mathcal{J}_{q/q,A}^{(1),\text{coll}} \otimes_{\perp} \Sigma_{AT}^{(0)} \otimes_{\perp} \mathcal{N}_{j,T}^{(0)} \\ &+ \mathcal{J}_{q/q,A}^{(1),\text{rap}} \otimes_{\perp} \Sigma_{AT}^{(0)} \otimes_{\perp} \mathcal{N}_{j,T}^{(0)} + \mathcal{J}_{q/q,F}^{(0)} \otimes_{\perp} \Sigma_{FT}^{(1)} \otimes_{\perp} \mathcal{N}_{j,T}^{(0)} + \mathcal{J}_{q/q,F}^{(0)} \otimes_{\perp} \Sigma_{FT}^{(0)} \otimes_{\perp} \mathcal{N}_{j,T}^{(1)} \\ &+ \Delta\sigma_{q/q,j}^{\text{NLO}}, \end{aligned}$$

Collinear divergent terms

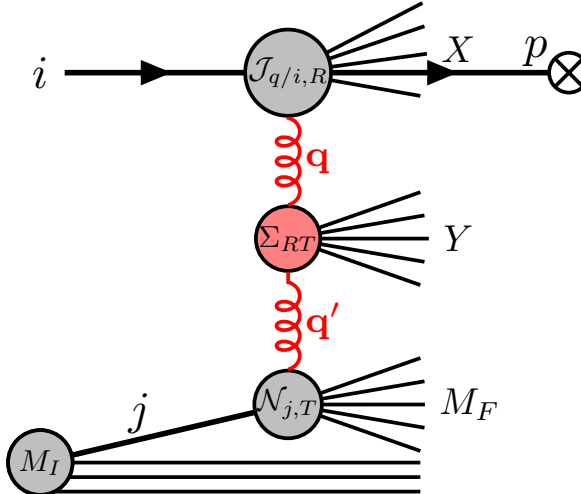
Collinear rapidity divergent terms

Here we use the short-hand

$$\begin{aligned} [\mathcal{J}_{q/i,R} \otimes_{\perp} \Sigma_{RT} \otimes_{\perp} \mathcal{N}_{j,T}] (x_1, \mathbf{p}, \mu) &= \int \frac{d^{2-2\epsilon} \mathbf{q}}{(2\pi)^{2-2\epsilon}} \frac{d^{2-2\epsilon} \mathbf{q}'}{(2\pi)^{2-2\epsilon}} \left[\mathcal{J}_{q/i,R}(x_1, \mathbf{p}, \mathbf{q}, \mu, \nu) \frac{g_s^2}{\mathbf{q}^2} \right] \\ &\times \left[\left(\frac{g_s^2}{\mathbf{q}^2} \right)^{-1} \Sigma_{RT}(\mathbf{q}, \mathbf{q}', \nu, \nu') \left(\frac{g_s^2}{\mathbf{q}'^2} \right)^{-1} \right] \times \left[\frac{g_s^2}{\mathbf{q}'^2} \mathcal{N}_{j,T}(\mathbf{q}', \nu') \right] \end{aligned}$$

Overview of graphs at one loop

In this paper, we study the correlations between the incoming proton and the medium



$$\mathcal{B}_{q/p,1} = \sum_{i=q,g} \sum_{j=q,\bar{q},g} \sigma_{q/i,j} \otimes f_{i/p} \otimes f_{j/N} \cdot \rho_0^- L^+,$$

$$\begin{aligned} \sigma_{q/q,j}^{(0)} + \sigma_{q/q,j}^{(1)} &= \left(\mathcal{J}_{q/q,F}^{(0)} + \mathcal{J}_{q/q,F}^{(1),\text{rap}} \right) \otimes_{\perp} \Sigma_{FT}^{(0)} \otimes_{\perp} \mathcal{N}_{j,T}^{(0)} + \\ &+ \mathcal{J}_{q/q,F}^{(1),\text{coll}} \otimes_{\perp} \Sigma_{FT}^{(0)} \otimes_{\perp} \mathcal{N}_{j,T}^{(0)} + \mathcal{J}_{q/q,A}^{(1),\text{coll}} \otimes_{\perp} \Sigma_{AT}^{(0)} \otimes_{\perp} \mathcal{N}_{j,T}^{(0)} \\ &+ \mathcal{J}_{q/q,A}^{(1),\text{rap}} \otimes_{\perp} \Sigma_{AT}^{(0)} \otimes_{\perp} \mathcal{N}_{j,T}^{(0)} + \mathcal{J}_{q/q,F}^{(0)} \otimes_{\perp} \Sigma_{FT}^{(1)} \otimes_{\perp} \mathcal{N}_{j,T}^{(0)} + \mathcal{J}_{q/q,F}^{(0)} \otimes_{\perp} \Sigma_{FT}^{(0)} \otimes_{\perp} \mathcal{N}_{j,T}^{(1)} \\ &+ \Delta\sigma_{q/q,j}^{\text{NLO}}, \end{aligned}$$

Collinear divergent terms

Collinear rapidity divergent terms

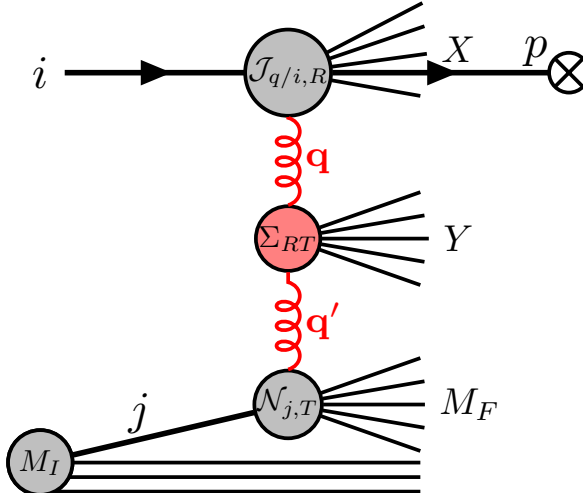
Soft and anti-collinear rapidity divergent terms

Here we use the short-hand

$$\begin{aligned} [\mathcal{J}_{q/i,R} \otimes_{\perp} \Sigma_{RT} \otimes_{\perp} \mathcal{N}_{j,T}] (x_1, \mathbf{p}, \mu) &= \int \frac{d^{2-2\epsilon} \mathbf{q}}{(2\pi)^{2-2\epsilon}} \frac{d^{2-2\epsilon} \mathbf{q}'}{(2\pi)^{2-2\epsilon}} \left[\mathcal{J}_{q/i,R}(x_1, \mathbf{p}, \mathbf{q}, \mu, \nu) \frac{g_s^2}{\mathbf{q}^2} \right] \\ &\times \left[\left(\frac{g_s^2}{\mathbf{q}^2} \right)^{-1} \Sigma_{RT}(\mathbf{q}, \mathbf{q}', \nu, \nu') \left(\frac{g_s^2}{\mathbf{q}'^2} \right)^{-1} \right] \times \left[\frac{g_s^2}{\mathbf{q}'^2} \mathcal{N}_{j,T}(\mathbf{q}', \nu') \right] \end{aligned}$$

Overview of graphs at one loop

In this paper, we study the correlations between the incoming proton and the medium



$$\mathcal{B}_{q/p,1} = \sum_{i=q,g} \sum_{j=q,\bar{q},g} \sigma_{q/i,j} \otimes f_{i/p} \otimes f_{j/N} \cdot \rho_0^- L^+,$$

$$\begin{aligned} \sigma_{q/q,j}^{(0)} + \sigma_{q/q,j}^{(1)} &= \left(\mathcal{J}_{q/q,F}^{(0)} + \mathcal{J}_{q/q,F}^{(1),\text{rap}} \right) \otimes_{\perp} \Sigma_{FT}^{(0)} \otimes_{\perp} \mathcal{N}_{j,T}^{(0)} + \\ &+ \mathcal{J}_{q/q,F}^{(1),\text{coll}} \otimes_{\perp} \Sigma_{FT}^{(0)} \otimes_{\perp} \mathcal{N}_{j,T}^{(0)} + \mathcal{J}_{q/q,A}^{(1),\text{coll}} \otimes_{\perp} \Sigma_{AT}^{(0)} \otimes_{\perp} \mathcal{N}_{j,T}^{(0)} \\ &+ \mathcal{J}_{q/q,A}^{(1),\text{rap}} \otimes_{\perp} \Sigma_{AT}^{(0)} \otimes_{\perp} \mathcal{N}_{j,T}^{(0)} + \mathcal{J}_{q/q,F}^{(0)} \otimes_{\perp} \Sigma_{FT}^{(1)} \otimes_{\perp} \mathcal{N}_{j,T}^{(0)} + \mathcal{J}_{q/q,F}^{(0)} \otimes_{\perp} \Sigma_{FT}^{(0)} \otimes_{\perp} \mathcal{N}_{j,T}^{(1)} \\ &+ \Delta\sigma_{q/q,j}^{\text{NLO}}, \end{aligned}$$

Collinear divergent terms

Collinear rapidity divergent terms

Soft and anti-collinear rapidity divergent terms

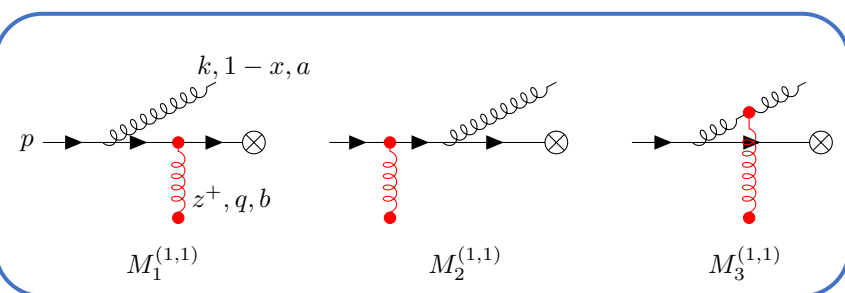
Finite terms

Here we use the short-hand

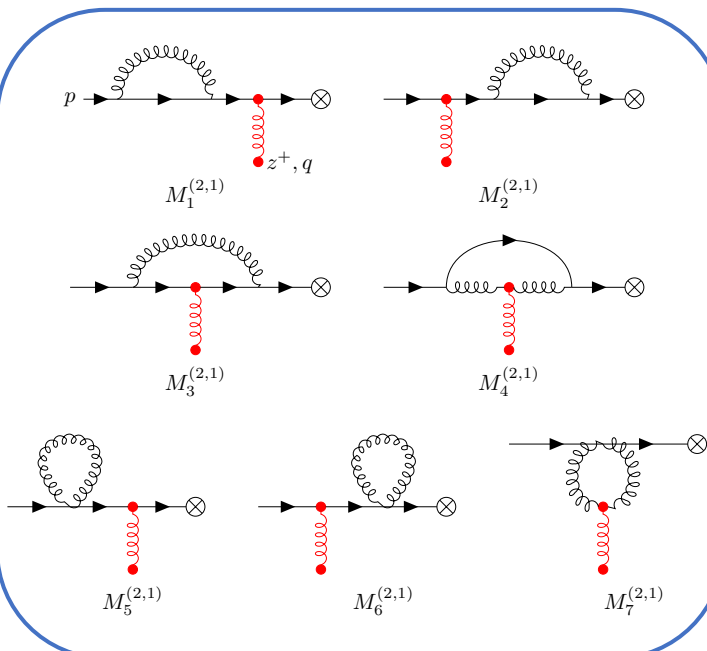
$$\begin{aligned} [\mathcal{J}_{q/i,R} \otimes_{\perp} \Sigma_{RT} \otimes_{\perp} \mathcal{N}_{j,T}] (x_1, \mathbf{p}, \mu) &= \int \frac{d^{2-2\epsilon} \mathbf{q}}{(2\pi)^{2-2\epsilon}} \frac{d^{2-2\epsilon} \mathbf{q}'}{(2\pi)^{2-2\epsilon}} \left[\mathcal{J}_{q/i,R}(x_1, \mathbf{p}, \mathbf{q}, \mu, \nu) \frac{g_s^2}{\mathbf{q}^2} \right] \\ &\times \left[\left(\frac{g_s^2}{\mathbf{q}^2} \right)^{-1} \Sigma_{RT}(\mathbf{q}, \mathbf{q}', \nu, \nu') \left(\frac{g_s^2}{\mathbf{q}'^2} \right)^{-1} \right] \times \left[\frac{g_s^2}{\mathbf{q}'^2} \mathcal{N}_{j,T}(\mathbf{q}', \nu') \right] \end{aligned}$$

Graphs at one loop for the matching function

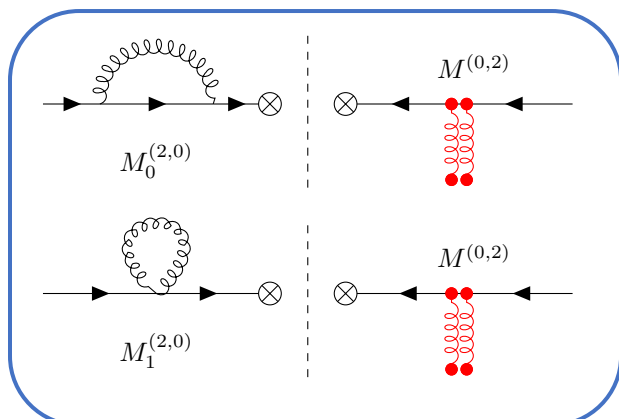
One loop graphs can be organized by the type of integration



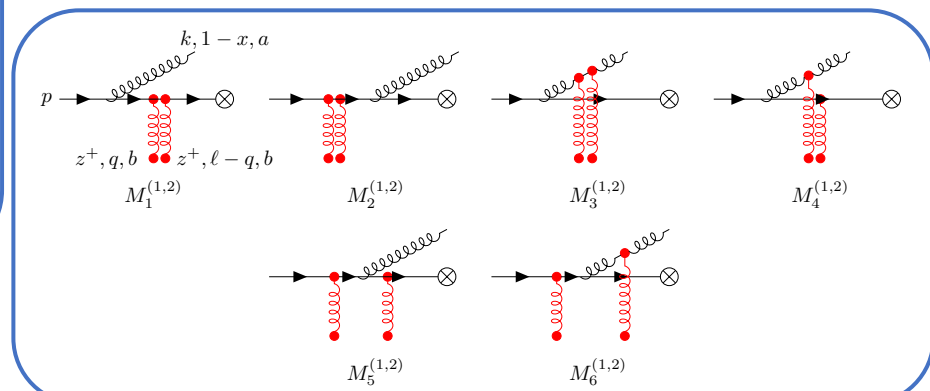
Single Glauber, real emission



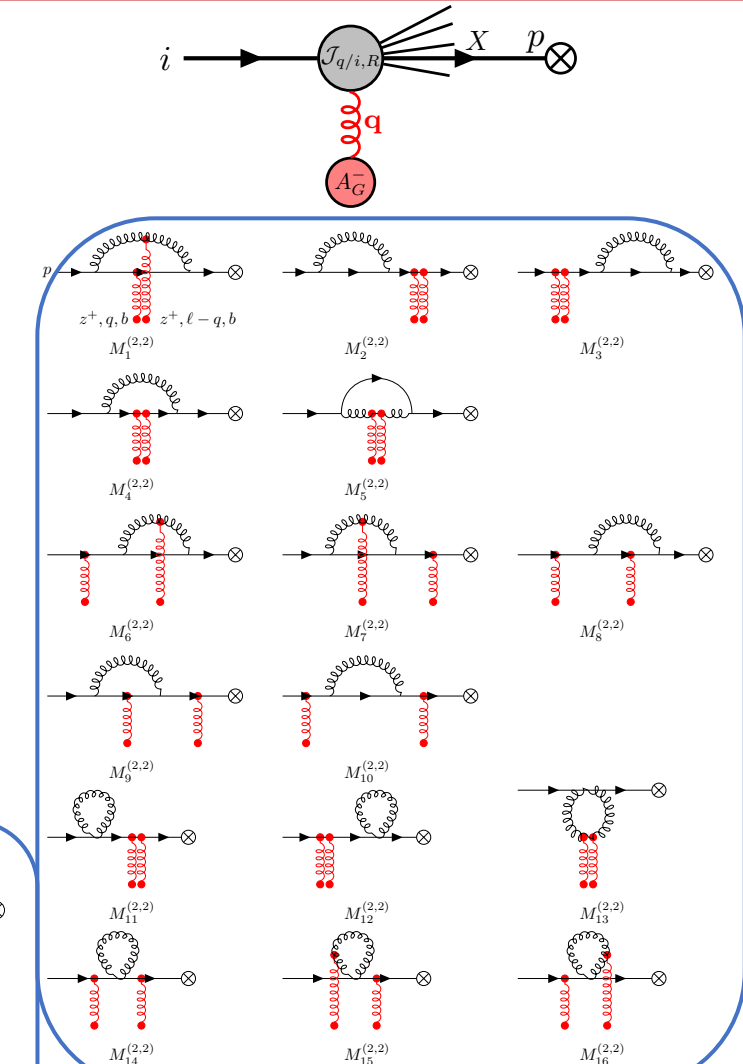
Single Glauber, virtual loop



Wave function



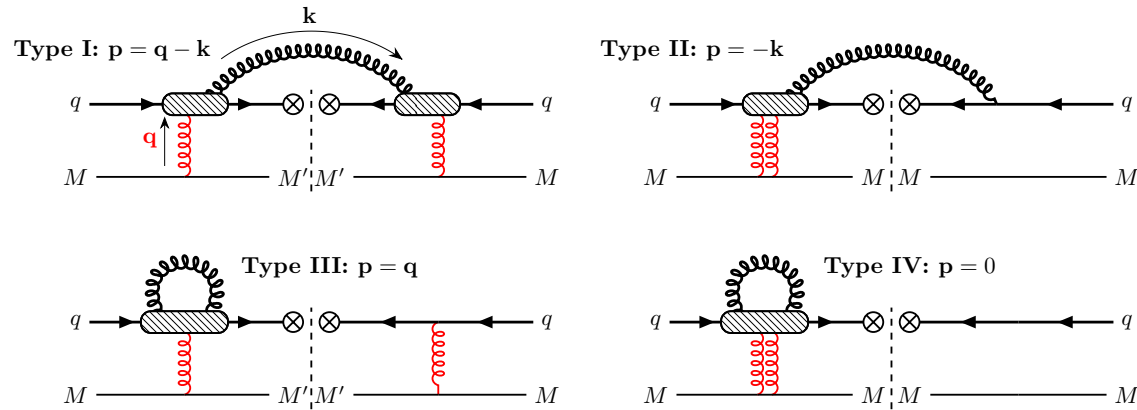
Double Glauber, real emission



Double Glauber, virtual emission

Collinear matching function at one loop

The finite contributions to the collinear function can be organized based on the type of emission



We use the short-hand

Type K	$\mathcal{I}_{K,F}(x, \mathbf{k}, \mathbf{q})$	$\mathcal{I}_{K,A}(x, \mathbf{k}, \mathbf{q})$
I	$\frac{1}{\mathbf{Q}_1^2} + 2 \frac{\mathbf{Q}_2}{\mathbf{Q}_2^2} \cdot \left(\frac{\mathbf{Q}_2}{\mathbf{Q}_2^2} - \frac{\mathbf{Q}_1}{\mathbf{Q}_1^2} \right) \phi_2$	$\frac{1}{\mathbf{Q}_3^2} - \frac{\mathbf{Q}_1}{\mathbf{Q}_1^2} \cdot \frac{\mathbf{Q}_3}{\mathbf{Q}_3^2} + \frac{\mathbf{Q}_2}{\mathbf{Q}_2^2} \cdot \left(\frac{\mathbf{Q}_1}{\mathbf{Q}_1^2} - \frac{\mathbf{Q}_3}{\mathbf{Q}_3^2} \right) \phi_2$
II	$-\frac{1}{\mathbf{Q}_1^2}$	$\frac{\mathbf{Q}_1}{\mathbf{Q}_1^2} \cdot \left(\frac{\mathbf{Q}_1}{\mathbf{Q}_1^2} - \frac{\mathbf{Q}_3}{\mathbf{Q}_3^2} \right) (\phi_1 - 1)$
III	$-2 \frac{\mathbf{Q}_2}{\mathbf{Q}_2^2} \cdot \left(\frac{\mathbf{Q}_2}{\mathbf{Q}_2^2} - \frac{\mathbf{Q}_1}{\mathbf{Q}_1^2} \right) \phi_2$	$-\frac{\mathbf{Q}_1 \cdot \mathbf{Q}_2}{\mathbf{Q}_1^2 \mathbf{Q}_2^2} \phi_2 + \frac{\mathbf{Q}_1}{\mathbf{Q}_1^2} \cdot \frac{\mathbf{Q}_4}{\mathbf{Q}_4^2} \phi_4$
IV	0	$-\frac{1}{\mathbf{Q}_1^2} \phi_1 + \frac{\mathbf{Q}_1}{\mathbf{Q}_1^2} \cdot \frac{\mathbf{Q}_3}{\mathbf{Q}_3^2} \phi_3$

The finite contributions to the collinear function can be organized based on the type of emission

$$\begin{aligned} \mathcal{J}_{q/q,R}^{(1)}(x, \mathbf{p}, \mathbf{q}) &= \frac{g_s^2 C_F}{2\pi} p_{qq,\epsilon}(x) \int d^{2-2\epsilon} \mathbf{k} \left[\delta^{(2-2\epsilon)}(\mathbf{p} - \mathbf{q} + \mathbf{k}) \mathcal{I}_{I,R} + \delta^{(2-2\epsilon)}(\mathbf{p} + \mathbf{k}) \mathcal{I}_{II,R} \right] \\ &+ \frac{g_s^2 C_F}{2\pi} \delta(1-x) \int_0^1 dx' p_{qq,\epsilon}(x') \int d^{2-2\epsilon} \mathbf{k} \left[\delta^{(2-2\epsilon)}(\mathbf{p} - \mathbf{q}) \mathcal{I}_{III,R} + \delta^{(2-2\epsilon)}(\mathbf{p}) \mathcal{I}_{IV,R} \right] \end{aligned}$$

$$\mathbf{Q}_1 = x\mathbf{k} - (1-x)(\mathbf{p}_0 - \mathbf{k})$$

$$\mathbf{Q}_2 = x\mathbf{k} - (1-x)(\mathbf{p}_0 - \mathbf{k} + \mathbf{q})$$

$$\mathbf{Q}_3 = x(\mathbf{k} - \mathbf{q}) - (1-x)(\mathbf{p}_0 - \mathbf{k} + \mathbf{q})$$

$$\mathbf{Q}_4 = x(\mathbf{k} + \mathbf{q}) - (1-x)(\mathbf{p}_0 - \mathbf{k})$$

Generate collinear divergences

Generate rapidity divergences (focus of this talk)

Coherence in the scattering

There are two competing time-scales in the process

$$\tau_f \sim \frac{1}{p^-}$$

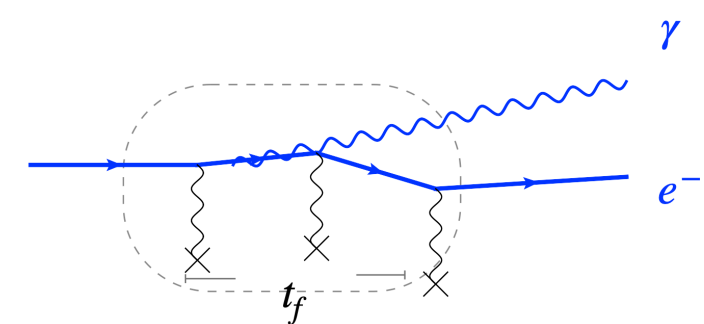
Time-scale for emission

$$L^+$$

Time-scale for traversing the medium

$$e^{iL^+/\tau_f}$$

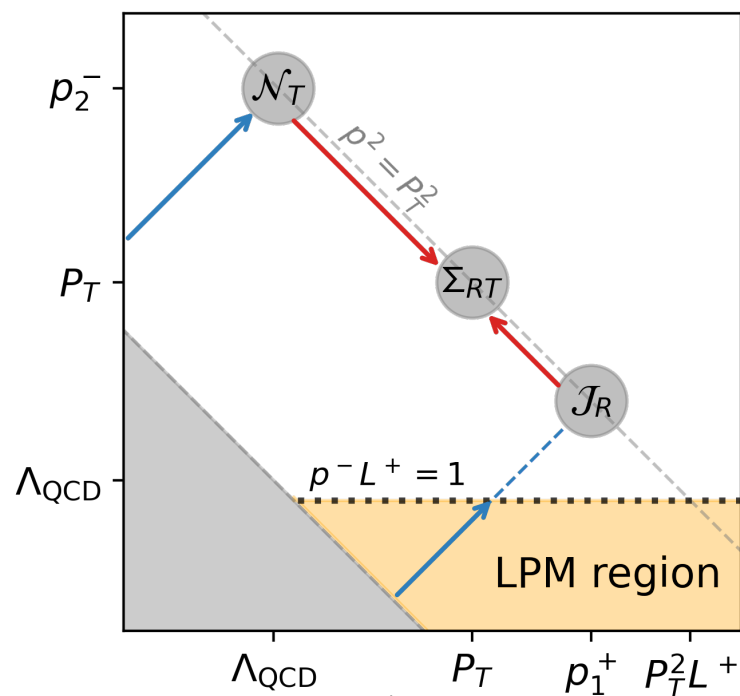
LPM phase



There are two regions with distinct power countings

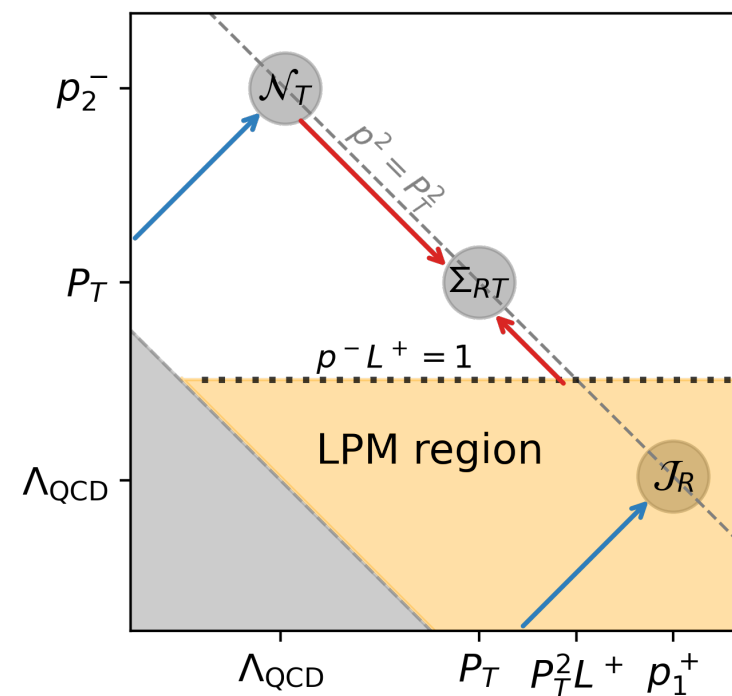
$$\tau_f \ll L^+$$

Emissions break coherence (GB region)



$$\tau_f \gg L^+$$

Coherence is unbroken (LPM region)

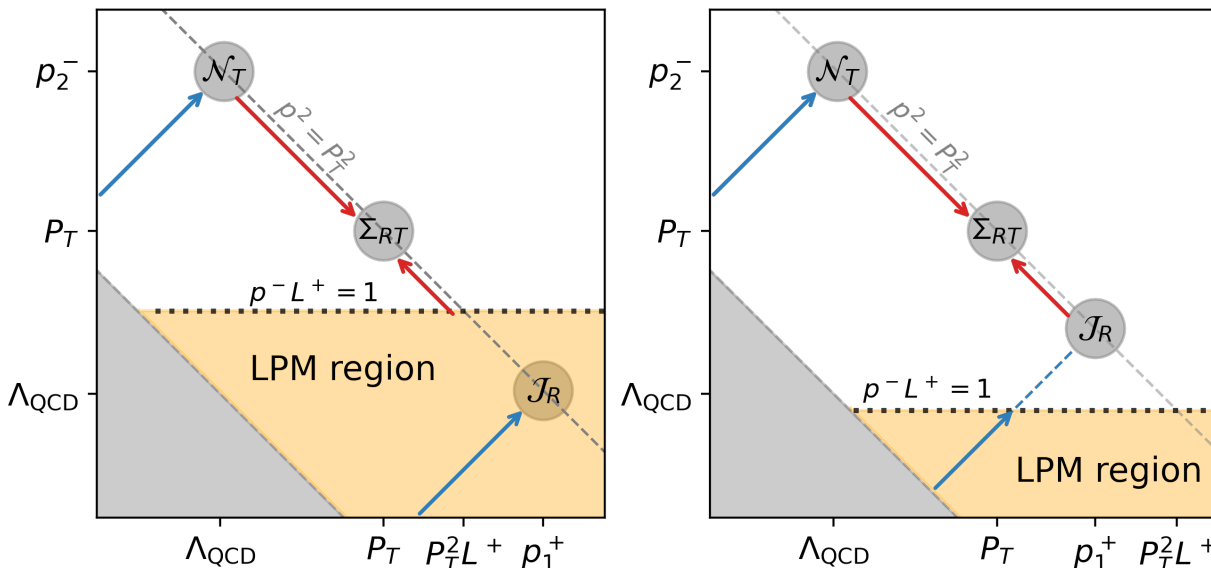


Rapidity divergence in the collinear function

The one loop contribution to the collinear function takes on a simple form

$$\begin{aligned} \mathcal{J}_{q/q,F}^{(0)} \otimes_{\perp} \Sigma_{FT}^{(0)} \otimes_{\perp} \mathcal{N}_{j,T}^{(0)} + \mathcal{J}_{q/q,A}^{(1),\text{rap}} \otimes_{\perp} \Sigma_{AT}^{(0)} \otimes_{\perp} \mathcal{N}_{j,T}^{(0)} &= \int \frac{d^{2-2\epsilon} \mathbf{p}}{(2\pi)^{2-2\epsilon}} e^{-i\mathbf{p}\cdot\mathbf{b}} \int \frac{d^{2-2\epsilon} \mathbf{q}}{(2\pi)^{2-2\epsilon}} \int \frac{d^{2-2\epsilon} \mathbf{q}'}{(2\pi)^{2-2\epsilon}} \quad \eta(x) = \left(\frac{(1-x)p_1^+}{\nu} \right)^{-\tau} \\ &\times \left[1 + \left(-\frac{1}{\tau} + \mathcal{L}_n \right) \hat{\mathcal{C}} \right] \left[\frac{\mathcal{J}_{q/q,F}^{(0)}}{\mathbf{q}^2} \right] \mathbf{q}^2 \mathbf{q}'^2 \Sigma_{FT}^{(0)} \frac{\mathcal{N}_{j,T}^{(0)}}{\mathbf{q}'^2} \\ \hat{\mathcal{C}}[v(\mathbf{q}^2)] &= \frac{g_s^2 C_A}{\pi} \int \frac{d^{2-2\epsilon} \mathbf{k}}{(2\pi)^{2-2\epsilon}} \left[\frac{1}{(\mathbf{q}-\mathbf{k})^2} v(\mathbf{k}^2) - \frac{\mathbf{q}^2}{2\mathbf{k}^2(\mathbf{q}-\mathbf{k})^2} v(\mathbf{q}^2) \right] \end{aligned}$$

The one loop contribution to the collinear function takes on a simple form

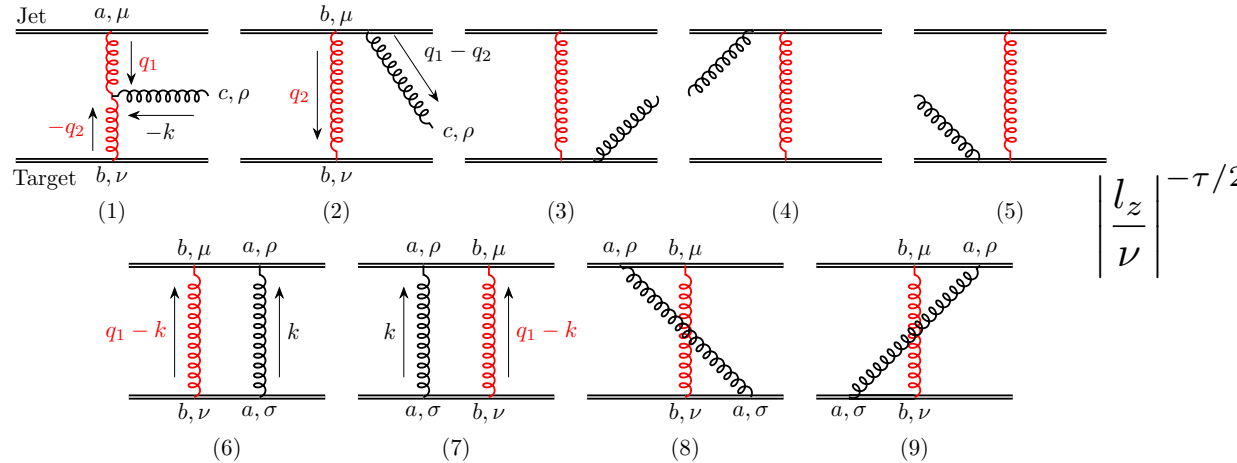


Different natural rapidity scale enters into the different regions

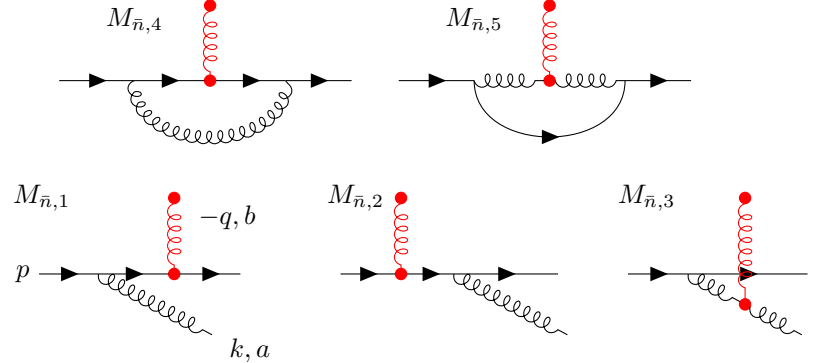
$$\mathcal{L}_n \sim \ln \frac{\min\{2L^+ \mu_b^2, x_1 P_a^+\}}{\nu}$$

Soft and anti-collinear contribution

Graphs from the soft sector $l^\mu \sim Q(\lambda, \lambda, \lambda)$



Graphs from the anti-collinear sector



Double Glauber exchange graphs are scaleless

Soft and collinear functions at one loop

$$\begin{aligned} & \mathcal{J}_{q/q,F}^{(0)} \otimes_{\perp} \Sigma_{FT}^{(1)} \otimes_{\perp} \mathcal{N}_{j,T}^{(0)} \\ &= \int \frac{d^{2-2\epsilon} \mathbf{p}}{(2\pi)^{-2\epsilon}} e^{-i\mathbf{p}\cdot\mathbf{b}} \int \frac{d^{2-2\epsilon} \mathbf{q}}{(2\pi)^{2-2\epsilon}} \int \frac{d^{2-2\epsilon} \mathbf{q}'}{(2\pi)^{2-2\epsilon}} \frac{\mathcal{J}_{q/q,F}^{(0)}}{\mathbf{q}^2} \left(\frac{2}{\tau} + \mathcal{L}_s \right) \hat{\mathcal{C}} \left[\mathbf{q}^2 \mathbf{q}'^2 \Sigma_{FT}^{(0)} \right] \frac{\mathcal{N}_{j,T}^{(0)}}{\mathbf{q}'^2} \quad \mathcal{L}_s \sim \ln \left(\frac{\mu_b^2}{\nu^2} \right) \end{aligned}$$

$$\mathcal{J}_{q/q,F}^{(0)} \otimes_{\perp} \Sigma_{FT}^{(0)} \otimes_{\perp} \mathcal{N}_{j,T}^{(1)}$$

$$= \int \frac{d^{2-2\epsilon} \mathbf{p}}{(2\pi)^{-2\epsilon}} e^{-i\mathbf{p}\cdot\mathbf{b}} \int \frac{d^{2-2\epsilon} \mathbf{q}}{(2\pi)^{2-2\epsilon}} \int \frac{d^{2-2\epsilon} \mathbf{q}'}{(2\pi)^{2-2\epsilon}} \frac{\mathcal{J}_{q/q,F}^{(0)}}{\mathbf{q}^2} \mathbf{q}^2 \mathbf{q}'^2 \Sigma_{FT}^{(0)} \left(-\frac{1}{\tau} + \mathcal{L}_{\bar{n}} \right) \hat{\mathcal{C}} \left[\frac{\mathcal{N}_{j,T}^{(0)}}{\mathbf{q}'^2} \right]$$

The BFKL evolution equations

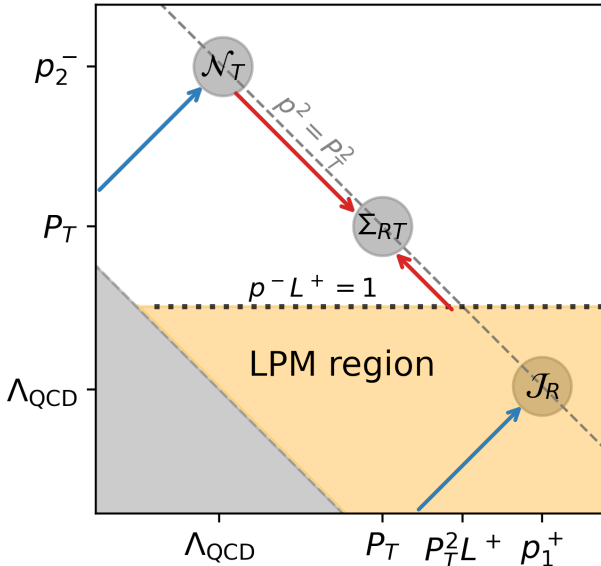
Each sector obeys a BFKL evolution equation

$$\frac{g_s^2}{\mathbf{q}^2} \frac{\partial \mathcal{J}_{q/i,R}(x, \mathbf{p}, \mathbf{q}; \nu)}{\partial \ln \nu} = -\hat{\mathcal{C}} \left[\frac{g_s^2}{\mathbf{q}^2} \mathcal{J}_{q/i,R}(x, \mathbf{p}, \mathbf{q}; \nu) \right],$$

$$\frac{g_s^2}{\mathbf{q}'^2} \frac{\partial \mathcal{N}_{j,T}(\mathbf{q}'; \nu')}{\partial \ln \nu'} = -\hat{\mathcal{C}} \left[\frac{g_s^2}{\mathbf{q}'^2} \mathcal{N}_{j,T}(\mathbf{q}'; \nu') \right],$$

$$\left(\frac{g_s^2}{\mathbf{q}^2} \right)^{-1} \left(\frac{g_s^2}{\mathbf{q}'^2} \right)^{-1} \frac{\partial \Sigma_{RT}(\mathbf{q}, \mathbf{q}'; \nu, \nu')}{\partial \ln \nu} = \hat{\mathcal{C}} \left[\left(\frac{g_s^2}{\mathbf{q}^2} \right)^{-1} \left(\frac{g_s^2}{\mathbf{q}'^2} \right)^{-1} \Sigma_{RT}(\mathbf{q}, \mathbf{q}'; \nu, \nu') \right].$$

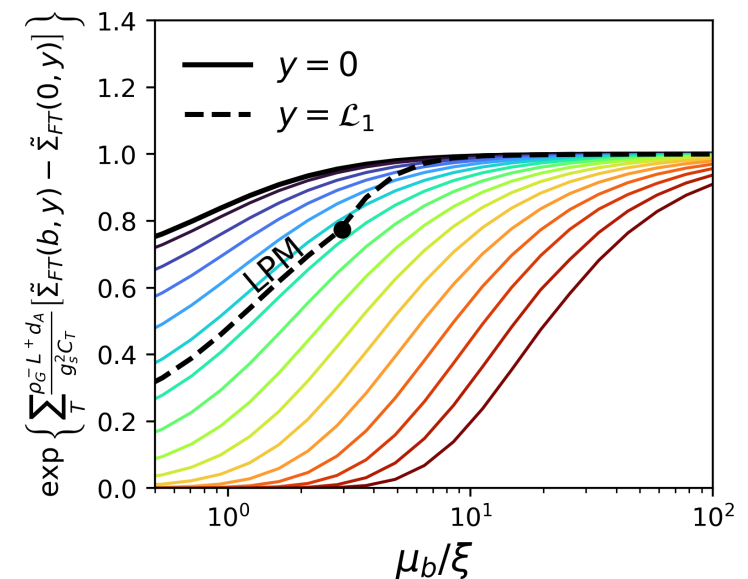
$$\frac{\partial}{\partial \ln \nu} [\mathcal{J}_{q/i,R} \otimes_{\perp} \Sigma_{RT} \otimes_{\perp} \mathcal{N}_{j,T}] (x_1, \mathbf{p}, \mu) = 0$$



Each sector obeys a BFKL evolution equation

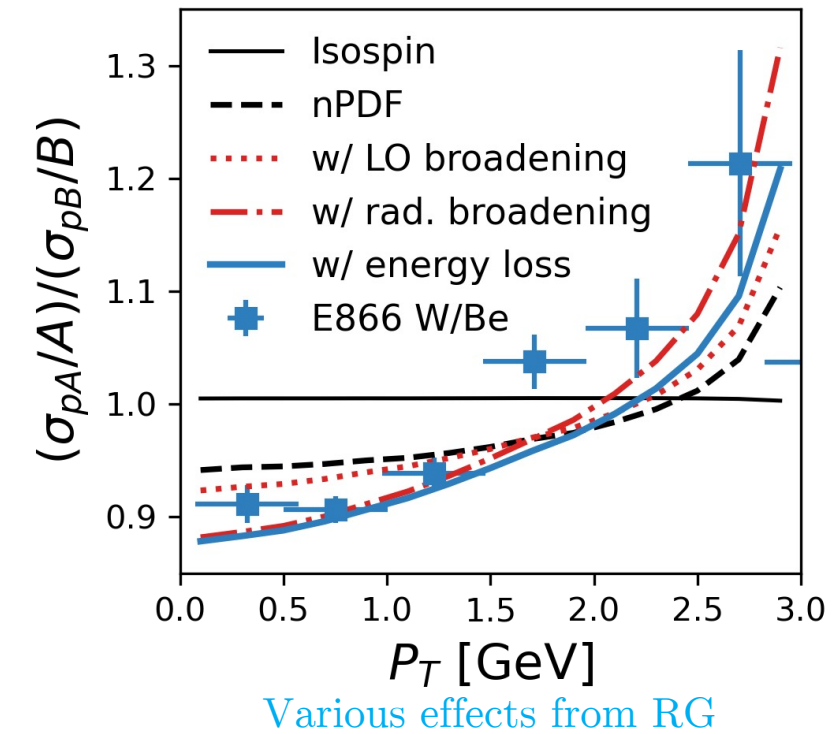
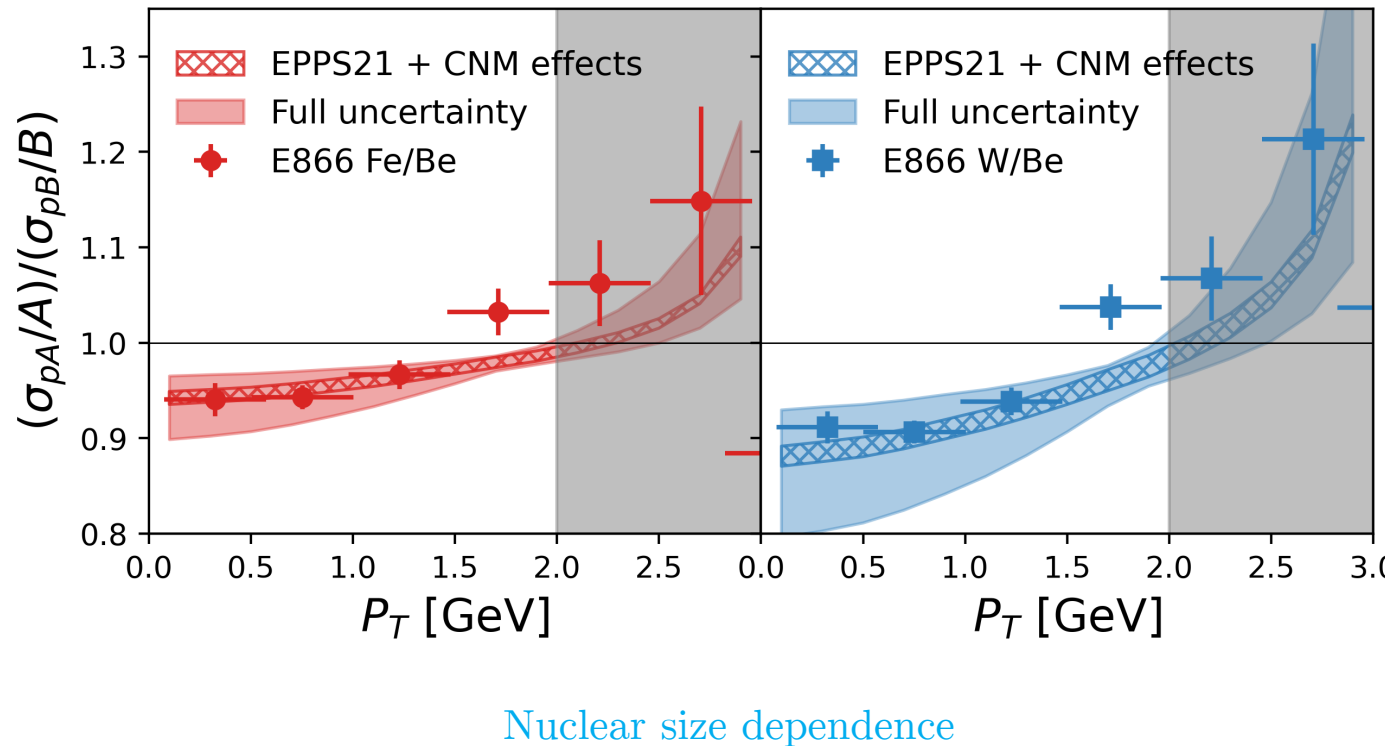
$$\begin{aligned} & \mathcal{B}_{q/i,0}^{(0)} + \chi \mathcal{B}_{q/i,1}^{(0)} + \dots \\ &= \delta(1-x_1) \exp \left\{ \sum_j \rho_0^- L^+ \int dx_t f_{j/N}(x_t) \mathcal{N}_{j,T}^{(0)} \left[\tilde{\Sigma}_{FT}^{(0)}(b) - \tilde{\Sigma}_{FT}^{(0)}(0) \right] \right\} \end{aligned}$$

$$\tilde{\Sigma}_{RT}(b, y) = \int d^2 \mathbf{b}' \tilde{v}_R(\mathbf{b} - \mathbf{b}', 0) \tilde{v}_T(\mathbf{b}', y)$$



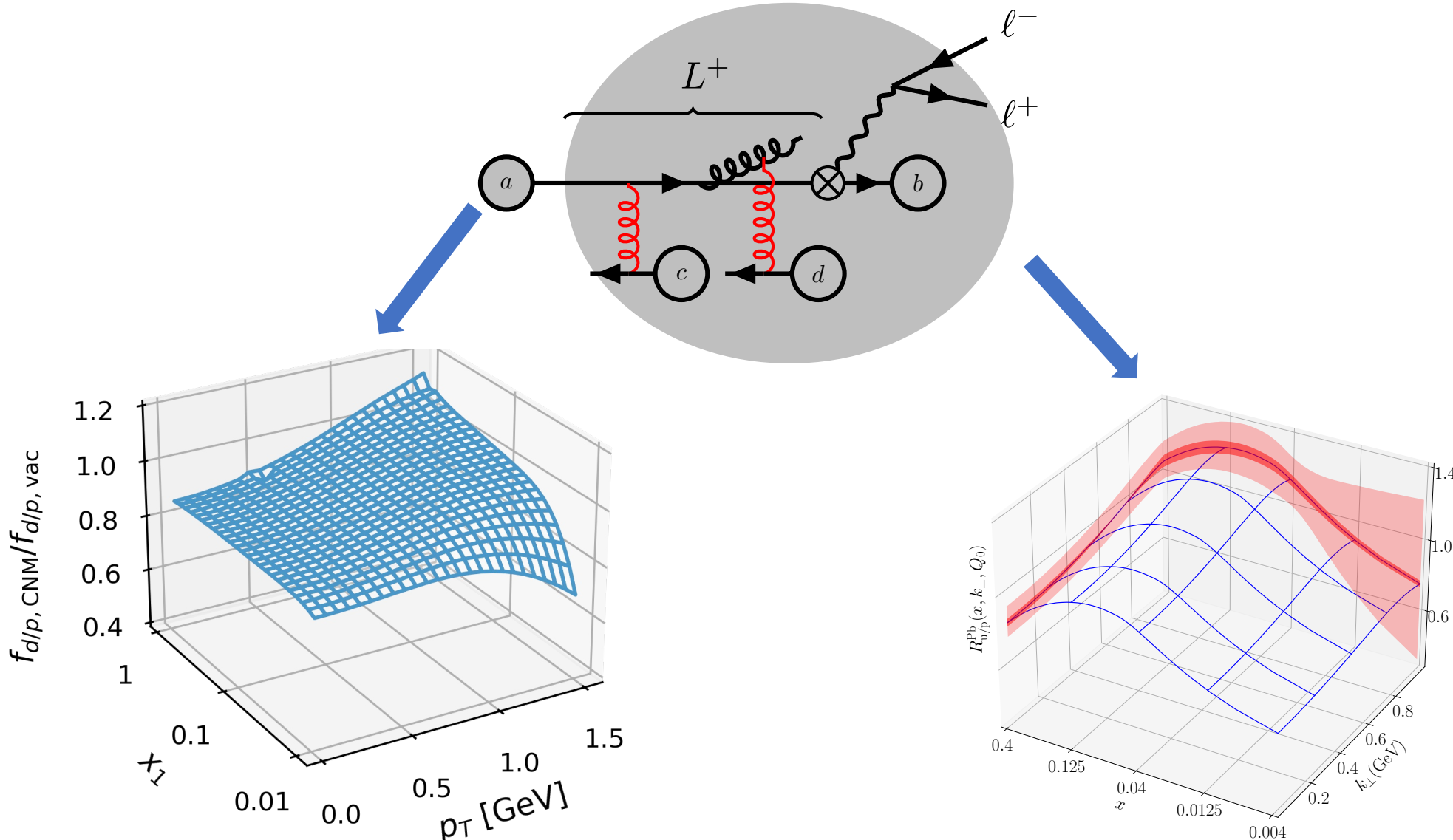
Example description of data

First principle description of data. Small improvements can be made by adding non-perturbative effects and investigating other perturbative effects



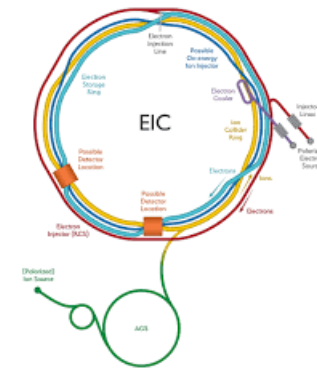
Three dimensional pictures

The medium modified beam function and the pheno extracted nuclear modified TMD PDF have been obtained



Future opportunities

Upcoming measurements at the LHCb, Jlab, and the EIC



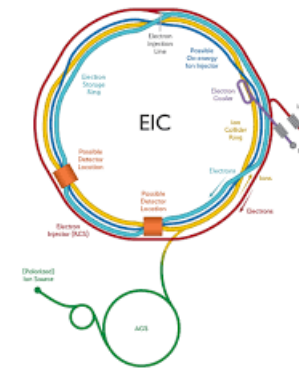
Future opportunities

Upcoming measurements at the LHCb, Jlab, and the EIC

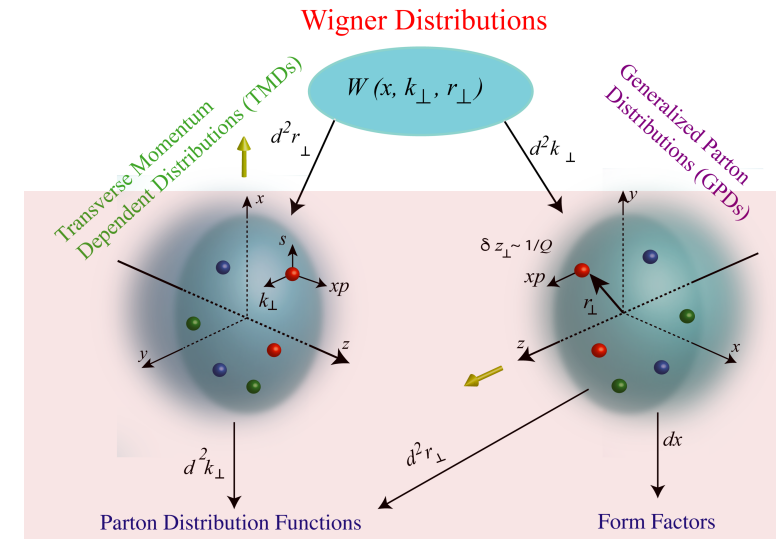




Jefferson Lab

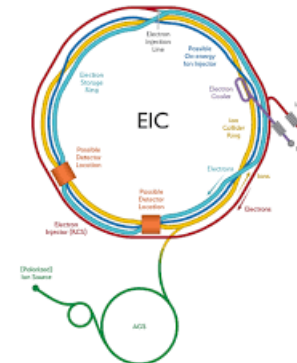


Cold matter modifications can be considered in GPDs

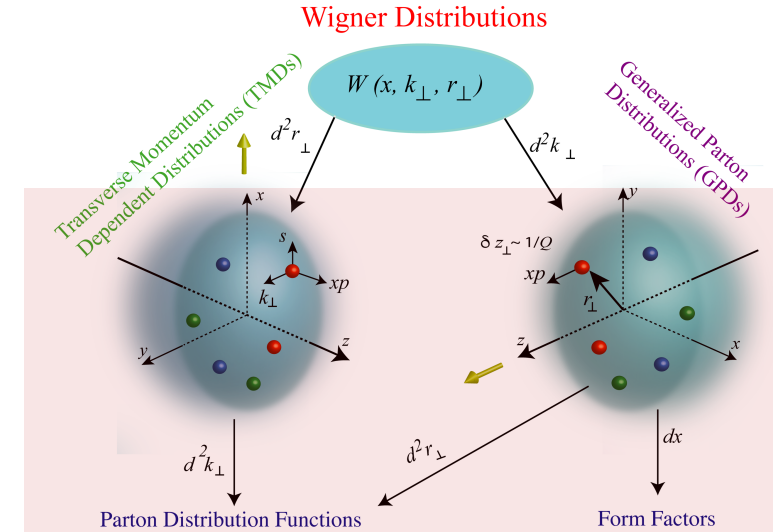


Future opportunities

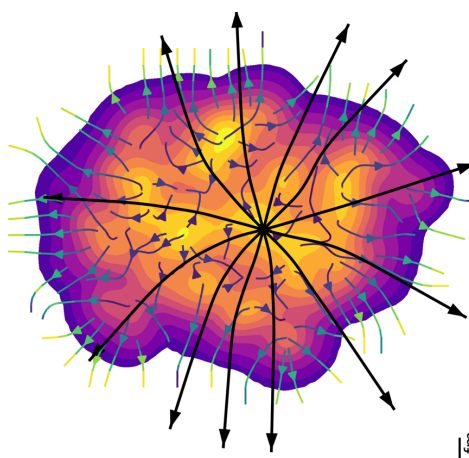
Upcoming measurements at the LHCb, Jlab, and the EIC



Cold matter modifications can be considered in GPDs

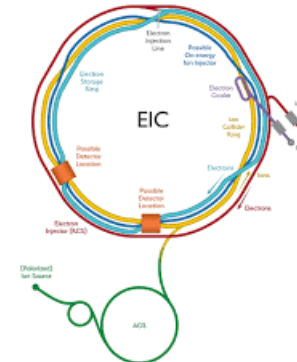


Medium modifications to beam function can be used to probe properties of a QGP

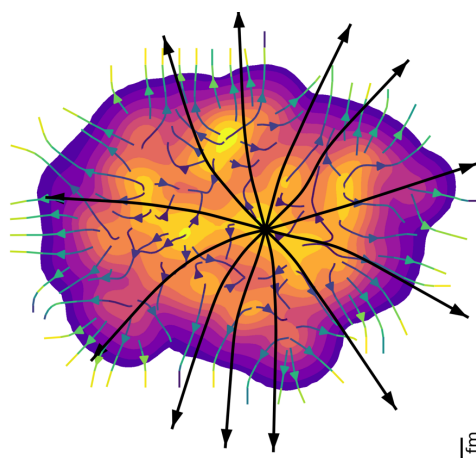


Future opportunities

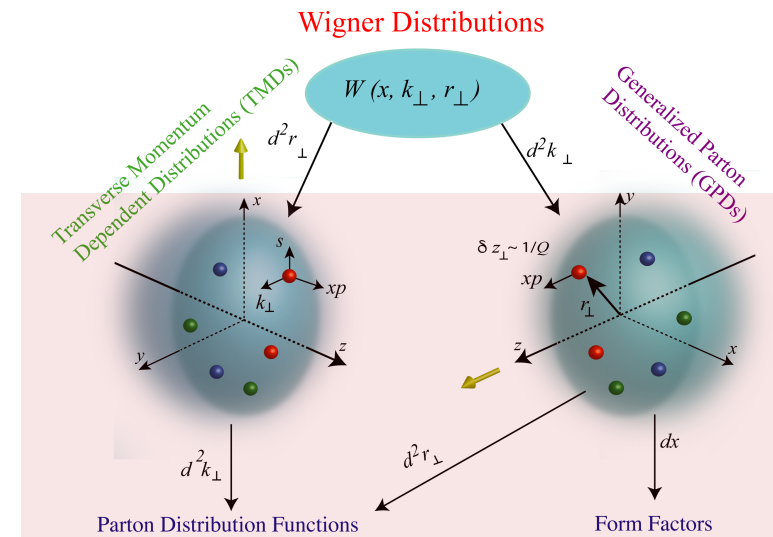
Upcoming measurements at the LHCb, Jlab, and the EIC



Medium modifications to beam function can be used to probe properties of a QGP

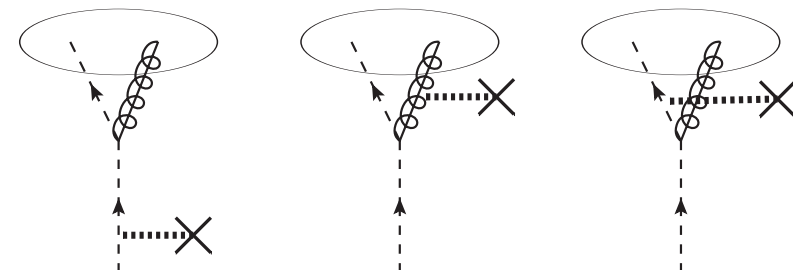


Cold matter modifications can be considered in GPDs



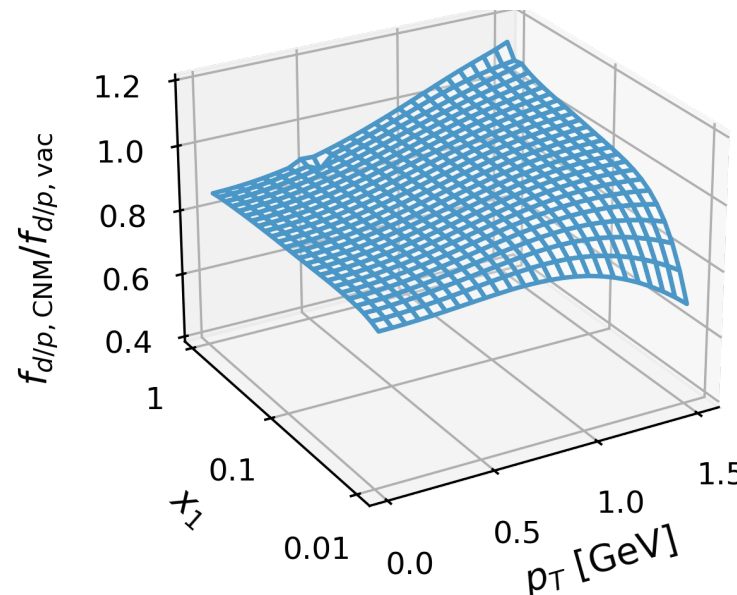
Wide variety of applications to jet functions

- Medium modifications to jet function
- Heavy flavor contribution
- Hadron in jet
- Jet substructure



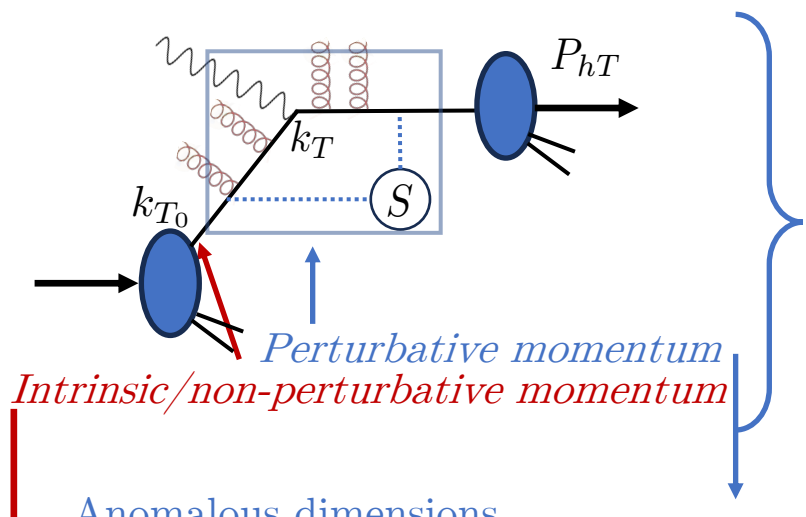
Conclusion

- We have introduced the idea of nuclear modified TMDs.
- We have performed the first extraction of these distributions in an approximate scheme.
- We have used SCET with Glauber gluons to derive the one-loop expression for the proton beam function.
- We have demonstrated that collinear and rapidity divergences give rise to the energy loss and transverse momentum broadening of the TMDs.
- Demonstrated that the broadening effect is governed by a BFKL evolution equation.



Perturbative background

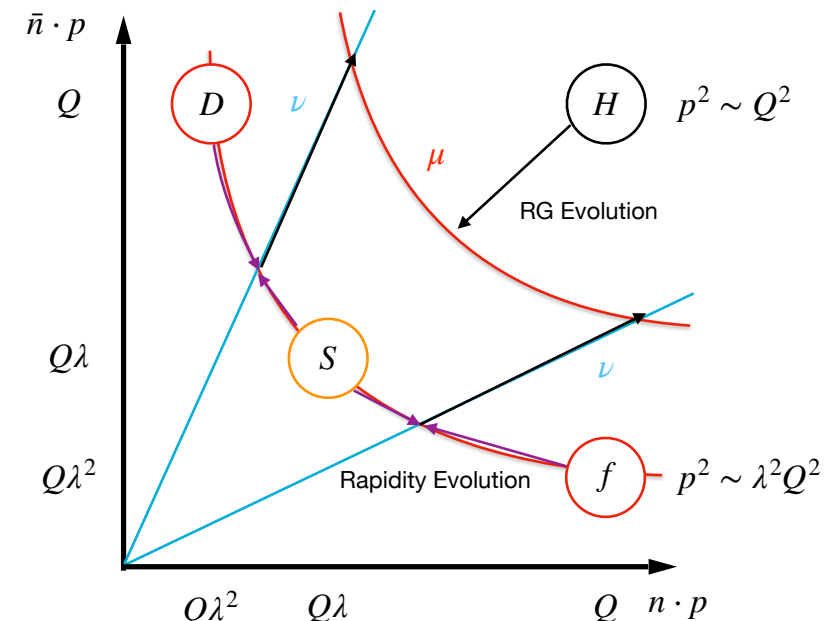
Perturbative Sudakov: accounts for transverse momenta generated from soft and collinear emissions



$$\mu \frac{d}{d\mu} \ln F(Q, \mu, \nu) = \gamma_F^q(Q, \mu, \nu) \quad F \in \{H, f, D, S\}$$

$$\nu \frac{d}{d\nu} \ln G(Q, \mu, \nu) = \gamma_G^q(Q, \mu, \nu) \quad G \in \{f, D, S\}$$

Experiments involve mixture of Perturbative and non-perturbative momentum



Obtain intrinsic momentum through a fit to data

Available perturbative accuracy

Anomalous dimensions

$$\mu \frac{d}{d\mu} \ln F(Q, \mu, \nu) = \gamma_F^q(Q, \mu, \nu)$$

$$F \in \{H, f, D, S\}$$

$$\mu \frac{d}{d\nu} \ln G(Q, \mu, \nu) = \gamma_G^q(Q, \mu, \nu)$$

$$G \in \{f, D, S\}$$

Anomalous dimensions are almost known up to N⁴LL at this point (no 5-loop cusp)

Accuracy	H, \mathcal{J}	$\Gamma_{\text{cusp}}(\alpha_s)$	$\gamma_H^q(\alpha_s)$	$\gamma_r^q(\alpha_s)$	$\beta(\alpha_s)$
LL	Tree level	1-loop			1-loop
NLL	Tree level	2-loop	1-loop	1-loop	2-loop
NLL'	1-loop	2-loop	1-loop	1-loop	2-loop
NNLL	1-loop	3-loop	2-loop	2-loop	3-loop
NNLL'	2-loop	3-loop	2-loop	2-loop	3-loop
N^3LL	2-loop	4-loop	3-loop	3-loop	4-loop
N^3LL'	3-loop	4-loop	3-loop	3-loop	4-loop
N^4LL	3-loop	5-loop	4-loop	4-loop	5-loop
N^4LL'	4-loop	5-loop	4-loop	4-loop	5-loop

Lee, Smirnov, and Smirnov (2010)

Gehrmann, Glover, Huber, Ikizlerli, and Studerus (2010)

Ebert, Mistlberger, Vita (2020)

Ebert, Mistlberger, Vita (2020)

Agarwal, von Manteuffel, Panzer, and Schabinger (2021)

Duhr, Mistlberger, Vita (2022)

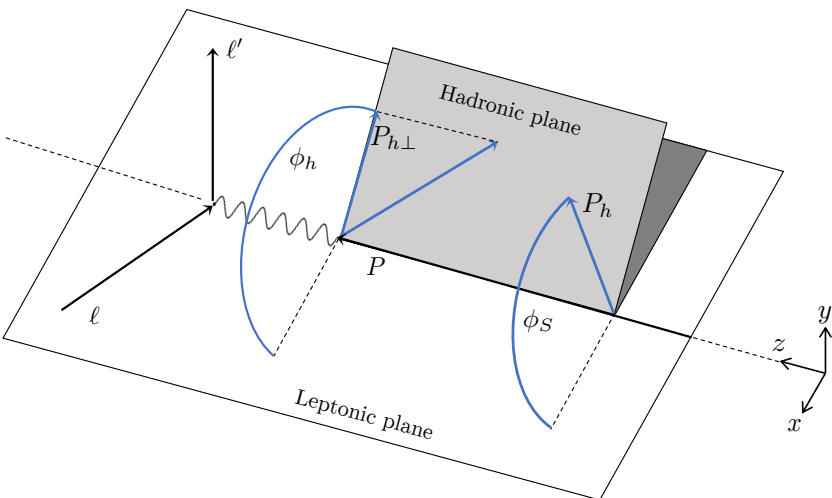
Moult, Zhu, Zhu (2022)

Herzog, Moch, Ruijl, Ueda, Vermaseren, and Vogt (2019)

Baikov, Chetyrkin, and Kuhn (2017)

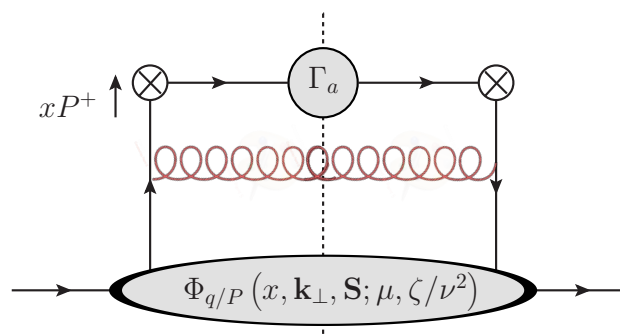
Factorization of physics at different scales

Factorization of the cross section in an OPE



Factorization of IR modes

$$q_T \gtrsim \Lambda_{\text{QCD}}$$



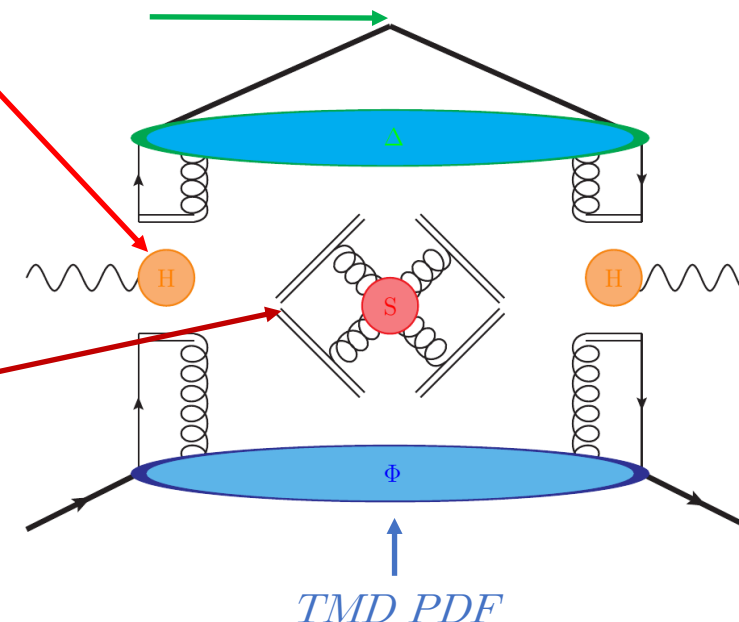
John Terry

$$Q \gg q_T \gtrsim \Lambda_{\text{QCD}}$$

TMD FF

Hard

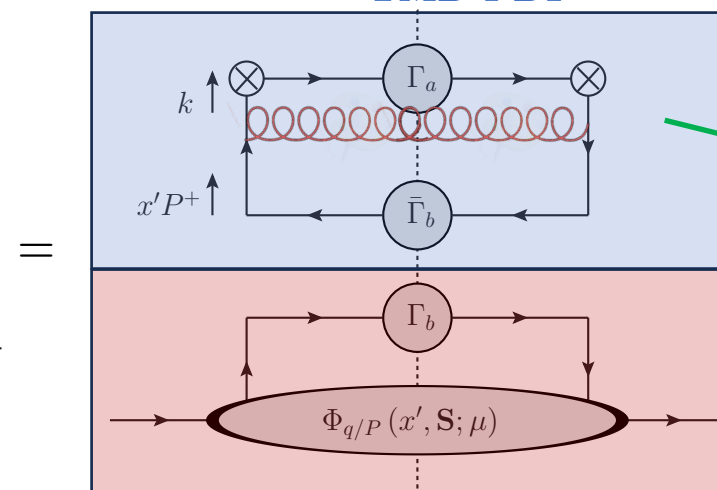
Soft



$$d\sigma \sim \sum_i |C(Q; \mu)| f \otimes D \otimes S(q_T, \mu)$$

Contains fixed order and large logs

$$\ln \left(\frac{Q}{\mu} \right)$$



Matching coefficient contains fixed order and large logs

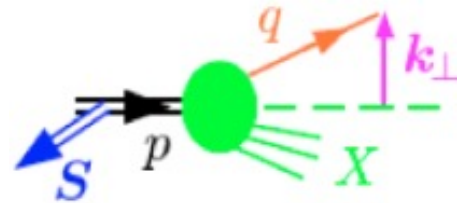
$$\ln \left(\frac{q_T}{\mu} \right)$$

$$f(x, q_T, \mu) \sim [C \otimes f](x, q_T, \mu)$$

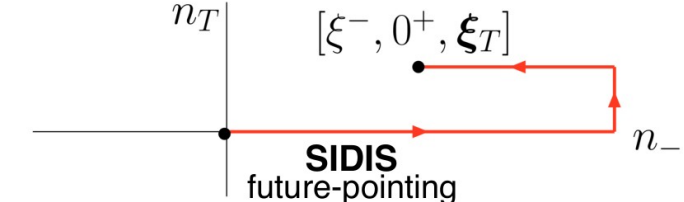
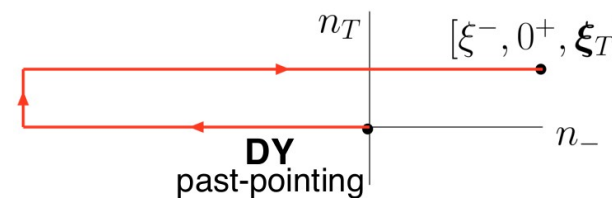
Collinear PDF

Intro to the Sivers effect

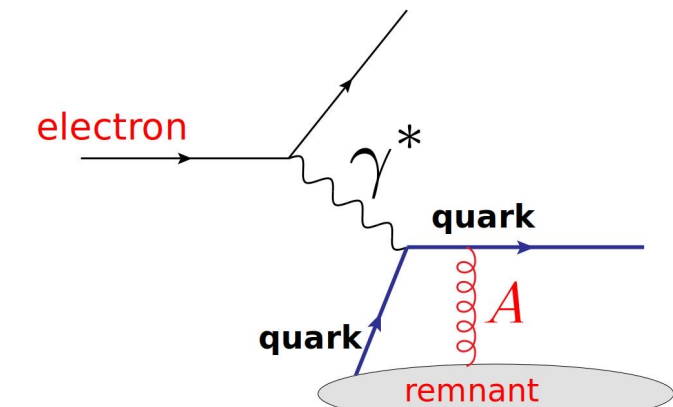
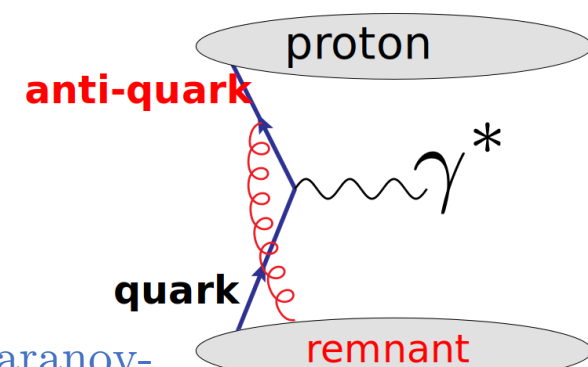
Anomalous dimensions



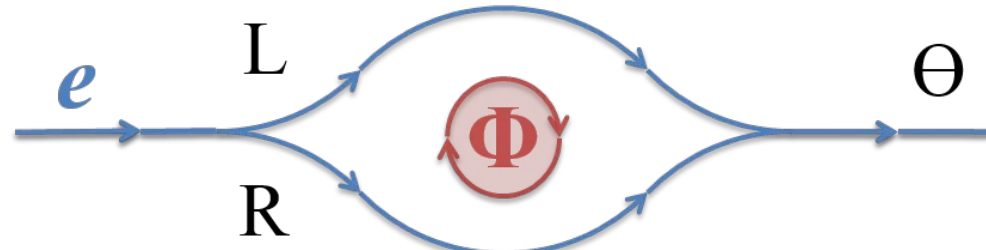
The Sivers function is process dependent



$$\Phi_{q/p}(x, \mathbf{k}_\perp, \mathbf{S}, \mu, \zeta) = f_{1q/p}(x, k_\perp, \mu, \zeta) - \frac{\epsilon_{\perp}^{\rho\sigma} k_{\perp\rho} S_{\perp\sigma}}{M} f_{1Tq/p}^\perp(x, k_\perp, \mu, \zeta)$$



This long-range correlation is similar to the Aharonov-Bohm effect



$$U^{\bar{n}}(0, \xi^-) = \mathcal{P} \exp \left[-ig \int_0^{\xi^-} d\bar{n} \cdot x n \cdot A(x) \right]$$

$$\psi(\mathbf{r}, t) \rightarrow \psi(\mathbf{r}, t) \exp \left(iq \int_C \mathbf{A} \cdot d\mathbf{r} \right)$$

Factorization and resummation

Differential cross section for Semi-Inclusive DIS is given by

$$F_{UU}(x, z, \mathbf{P}_{h\perp}) = \underbrace{H_{\text{DIS}}(Q, \mu)}_{\text{Hard}} \sum_q e_q^2 \int \frac{bdb}{2\pi} J_0\left(\frac{b P_{h\perp}}{z}\right) \underbrace{f_{1q/p}(x, b, \mu, \zeta_1)}_{\text{TMD PDF}} \underbrace{D_{1h/q}(z, b, \mu, \zeta_2)}_{\text{TMD FF}}$$

$$F_{UT}^{\sin \phi_h - \phi_s}(x, z, \mathbf{P}_{h\perp}) = \underbrace{H_{\text{DIS}}(Q, \mu)}_{\text{Hard}} \sum_q e_q^2 \int \frac{b^2 db}{2\pi} J_1\left(\frac{b P_{h\perp}}{z}\right) \underbrace{f_{1Tq/p}^\perp(x, b, \mu, \zeta_1)}_{\text{Sivers function}} \underbrace{D_{1h/q}(z, b, \mu, \zeta_2)}_{\text{TMD FF}}$$

TMDs can be matched onto the collinear distributions

$$f_{1q/p}(x, b, \mu, \zeta) = [C \otimes f](x, b, \mu_i, \zeta_i) U(\mu_i, \mu; \zeta) Z(b, \zeta_i, \zeta; \mu_i) U_{\text{NP}}^f(x, b, \zeta)$$

$$D_{1h/q}(z, b, \mu, \zeta) = \frac{1}{z^2} [\hat{C} \otimes D](z, b, \mu_i, \zeta_i) U(\mu_i, \mu; \zeta) Z(b, \zeta_i, \zeta; \mu_i) U_{\text{NP}}^D(z, b, \zeta).$$


Large logarithms are resummed to all orders in the perturbative Sudakov

$$U(\mu_i, \mu; \zeta) = \exp \left[\int_{\mu_i}^{\mu} \frac{d\mu'}{\mu'} \gamma_{\mu}(\mu', \zeta) \right], Z(b, \mu_i, \mu; \zeta) = \left(\frac{\zeta}{\zeta_i} \right)^{\gamma_{\zeta}(b, \mu_i)}$$

Matching of the Sivers function

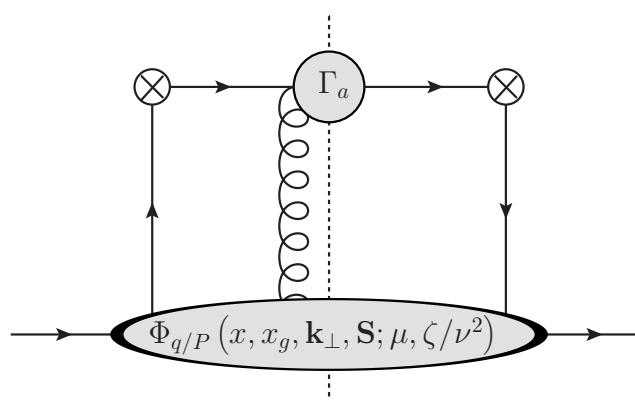
Differential cross section for Semi-Inclusive DIS is given by

$$F_{\text{UT}}^{\sin \phi_h - \phi_s} (x, z, \mathbf{P}_{h\perp}) = \underbrace{H_{\text{DIS}}(Q, \mu)}_{\text{Hard}} \sum_q e_q^2 \int \frac{b^2 db}{2\pi} J_1 \left(\frac{b P_{h\perp}}{z} \right) \underbrace{f_{1T,q/p}^\perp(x, b, \mu, \zeta_1)}_{\text{Sivers function}} \underbrace{D_{1h/q}(z, b, \mu, \zeta_2)}_{\text{TMD FF}}$$

TMDs can be matched onto the collinear distributions

$$f_{1T,q/p}^\perp(x, b, \mu, \zeta) = [\bar{C} \otimes T_F]_{q/p}(x, b, \mu_i, \zeta_i) \underbrace{U(\mu_i, \mu; \zeta) Z(b, \zeta_i, \zeta; \mu_i)}_{\text{Same as the unpolarized}} \underbrace{U_{\text{NP}}^{f_{1T}^\perp}(x, b, \zeta)}_{\text{Transverse momentum dependence}}$$

Collinear dependence



$$T_{F,q/p}(x, x_g, \mu_0) = \mathcal{N}_q(x) f_{q/p}(x, \mu_0)$$

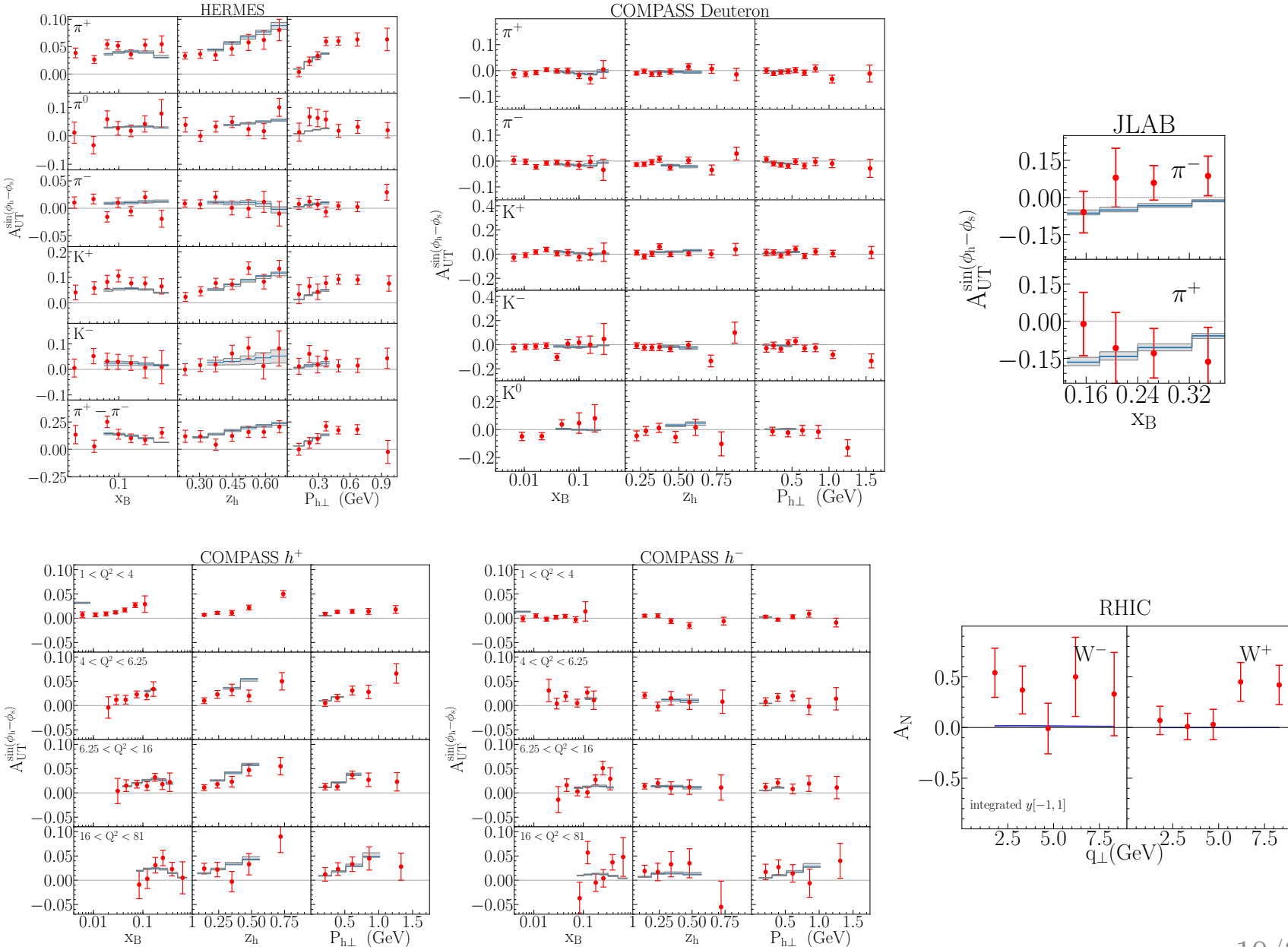
$$\mathcal{N}_q(x) = N_q \frac{(\alpha_q + \beta_q)^{(\alpha_q + \beta_q)}}{\alpha_q^{\alpha_q} \beta_q^{\beta_q}} x^{\alpha_q} (1-x)^{\beta_q}$$

$$U_{\text{NP}}^{f_{1T}^\perp}(x, b, \zeta) = g_1^{f_{1T}^\perp} b^2 + \frac{g_2}{4} \ln \left(\frac{\zeta}{\zeta_0} \right) \ln \left(\frac{b}{b_*} \right)$$

11 params in total

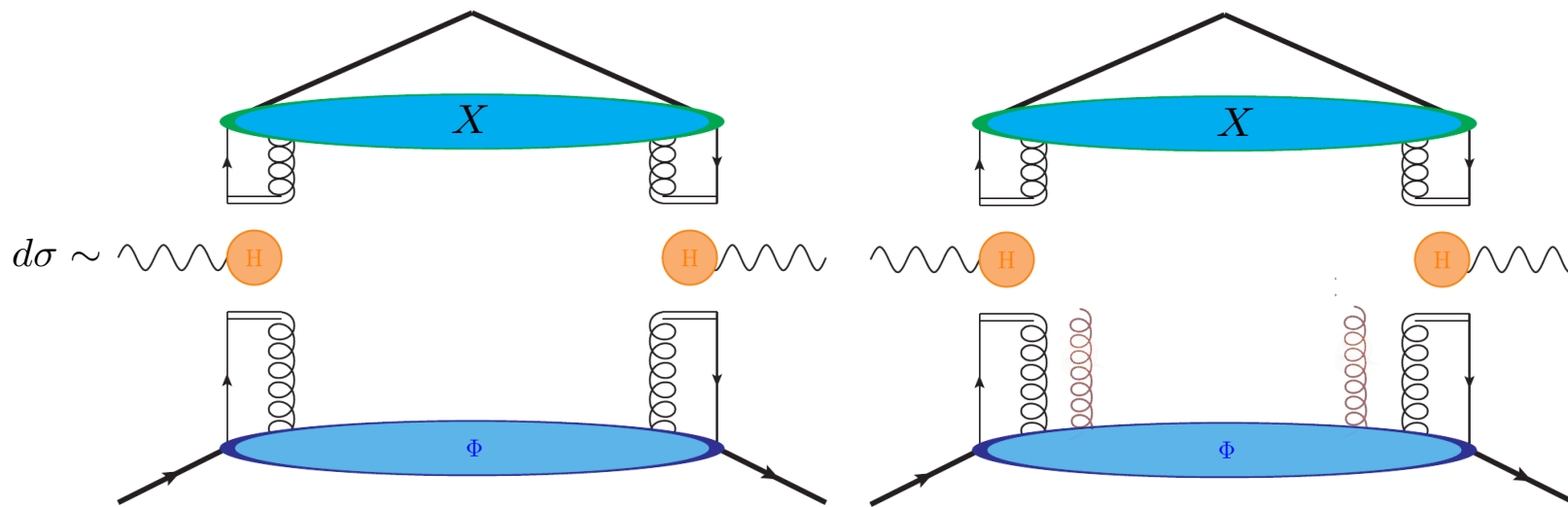
Data description

Collab	Ref	Process	Q_{avg}	N_{data}	χ^2/N_{data}
COMPASS	[44]	$ld \rightarrow lK^0X$	2.52	7	0.770
		$ld \rightarrow lK^-X$	2.80	11	1.325
		$ld \rightarrow lK^+X$	1.73	13	0.749
		$ld \rightarrow l\pi^-X$	2.50	11	0.719
		$ld \rightarrow l\pi^+X$	1.69	12	0.578
	[43]	$lp \rightarrow lh^-X$	4.02	31	1.055
		$lp \rightarrow lh^+X$	3.93	34	0.898
HERMES	[41]	$lp \rightarrow lK^-X$	1.70	14	0.376
		$lp \rightarrow lK^+X$	1.73	14	1.339
		$lp \rightarrow l\pi^0X$	1.76	13	0.997
		$lp \rightarrow l(\pi^+ - \pi^-)X$	1.73	15	1.252
		$lp \rightarrow l\pi^-X$	1.67	14	1.498
		$lp \rightarrow l\pi^+X$	1.69	14	1.697
		$lN \rightarrow l\pi^+X$	1.41	4	0.508
JLAB	[45]	$lN \rightarrow l\pi^-X$	1.69	4	1.048
		$pp \rightarrow W^+X$	M_W	8	2.189
	[47]	$pp \rightarrow W^-X$	M_W	8	1.684
		$pp \rightarrow Z^0X$	M_Z	1	3.270
Total				226	0.989

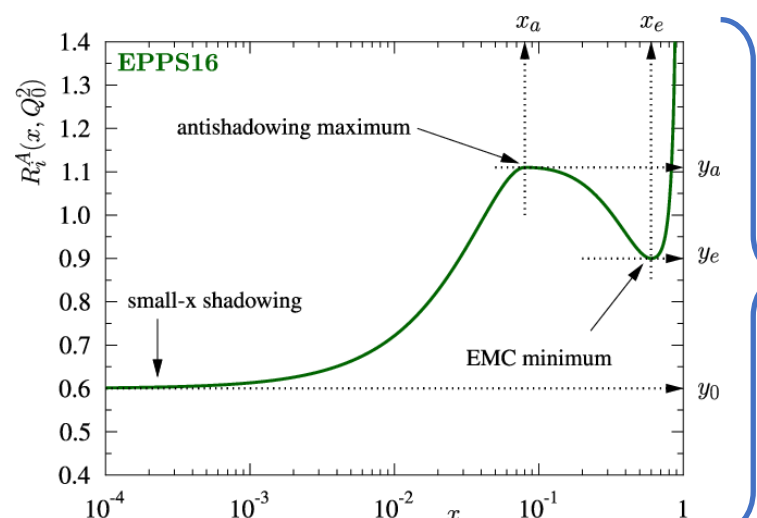


Nuclear modifications to collinear PDFs

Nuclear medium modification via higher twist



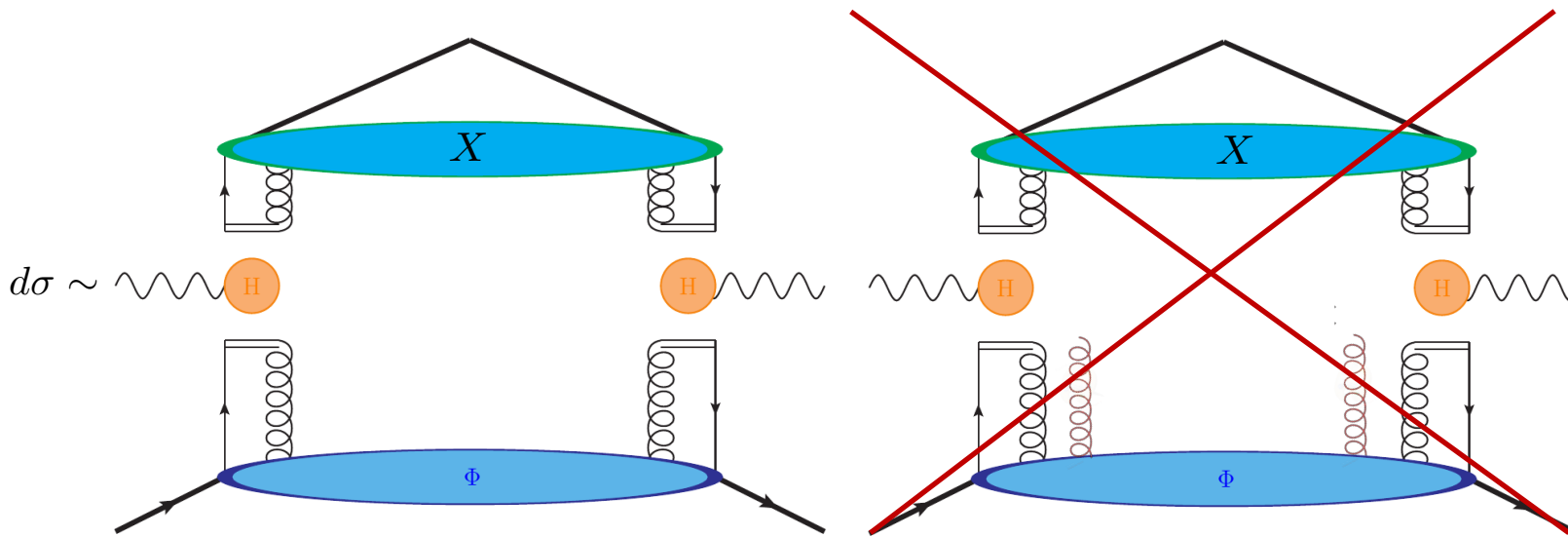
LP TMD factorization cannot address how multiple partons are correlated with one another



Eskola, Kolhinen, Ruuskanen (1998)
Eskola, Paakkinen, Paukkunen, Salgado (2017)

Method of treating nuclear modifications

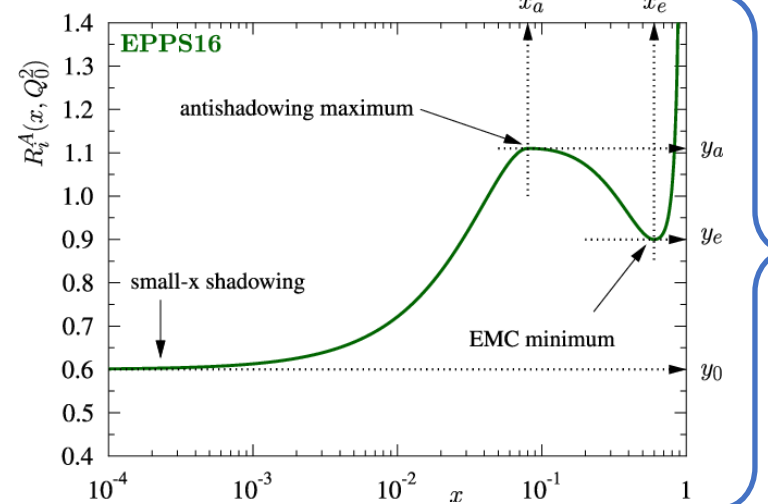
Nuclear medium modification via higher twist



LP TMD factorization cannot address how multiple partons are correlated with one another

$$R_i^A(x, Q) = \frac{f_{i/p}^A(x; Q)}{f_{i/p}(x; Q)}$$

$$R_i^A(x, Q_0^2) = \begin{cases} a_0 + a_1(x - x_a)^2 & x \leq x_a \\ b_0 + b_1x^\alpha + b_2x^{2\alpha} + b_3x^{3\alpha} & x_a \leq x \leq x_e \\ c_0 + (c_1 - c_2x)(1 - x)^{-\beta} & x_e \leq x \leq 1, \end{cases}$$



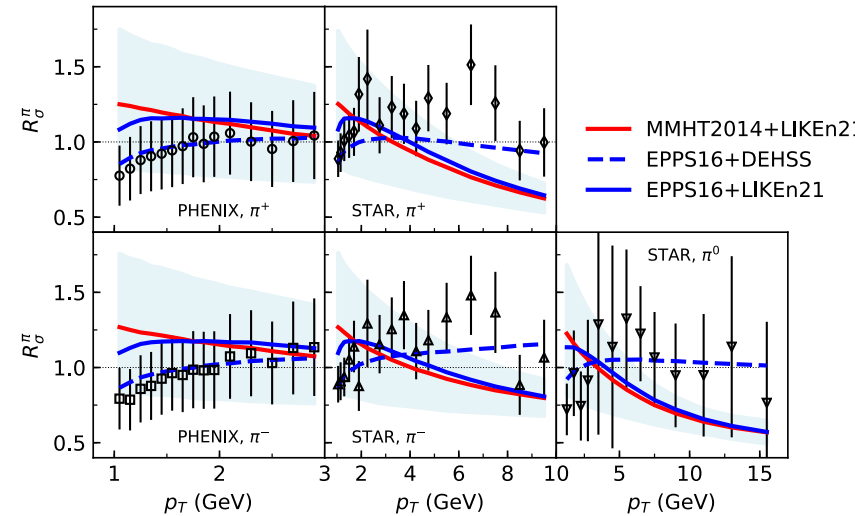
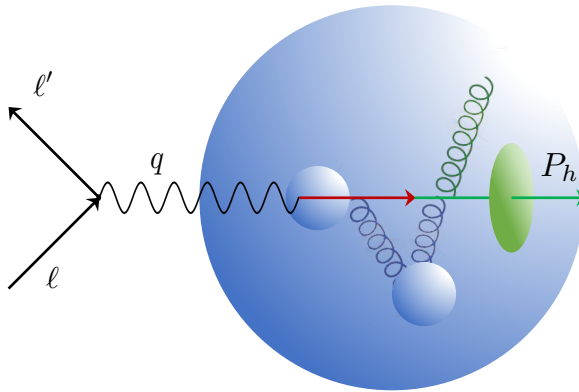
Eskola, Kolhinen, Ruuskanen (1998)

Eskola, Paakkinen, Paukkunen, Salgado (2017)

Nuclear modifications are absorbed into the non-perturbative parameterization.

Effective treatment of medium modifications

Ejected quark undergoes multiple scattering in the nuclear medium, modifies the fragmentation functions



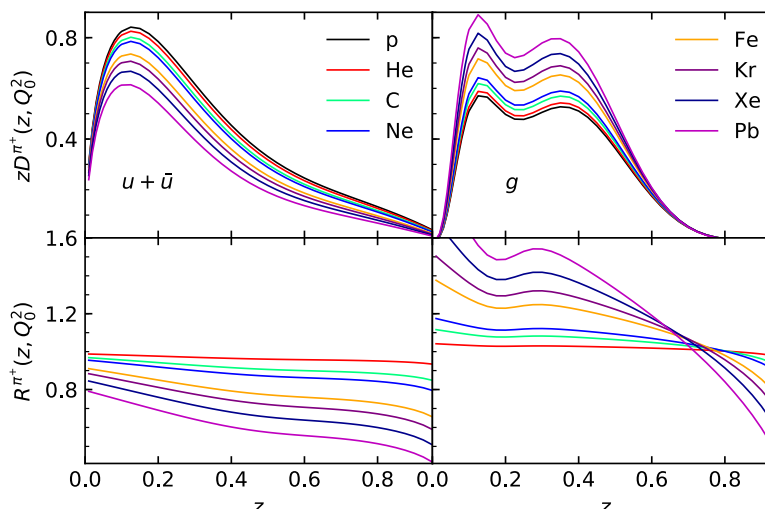
D. de Florian and R. Sassot (2004)
Zurita (2021)

Simultaneous extraction from hadroproduction in p-A collisions from PHENIX and STAR, and Semi-Inclusive DIS (collinear) from HERMES

$$D_i^h(z, Q_0) = \tilde{N}_i z^{\alpha_i} (1-z)^{\beta_i} \left[1 + \gamma_i (1-z)^{\delta_i} \right]$$

$$\tilde{N}_i \rightarrow \tilde{N}_i \left[1 + N_{i,1} (1 - A^{N_{i,2}}) \right]$$

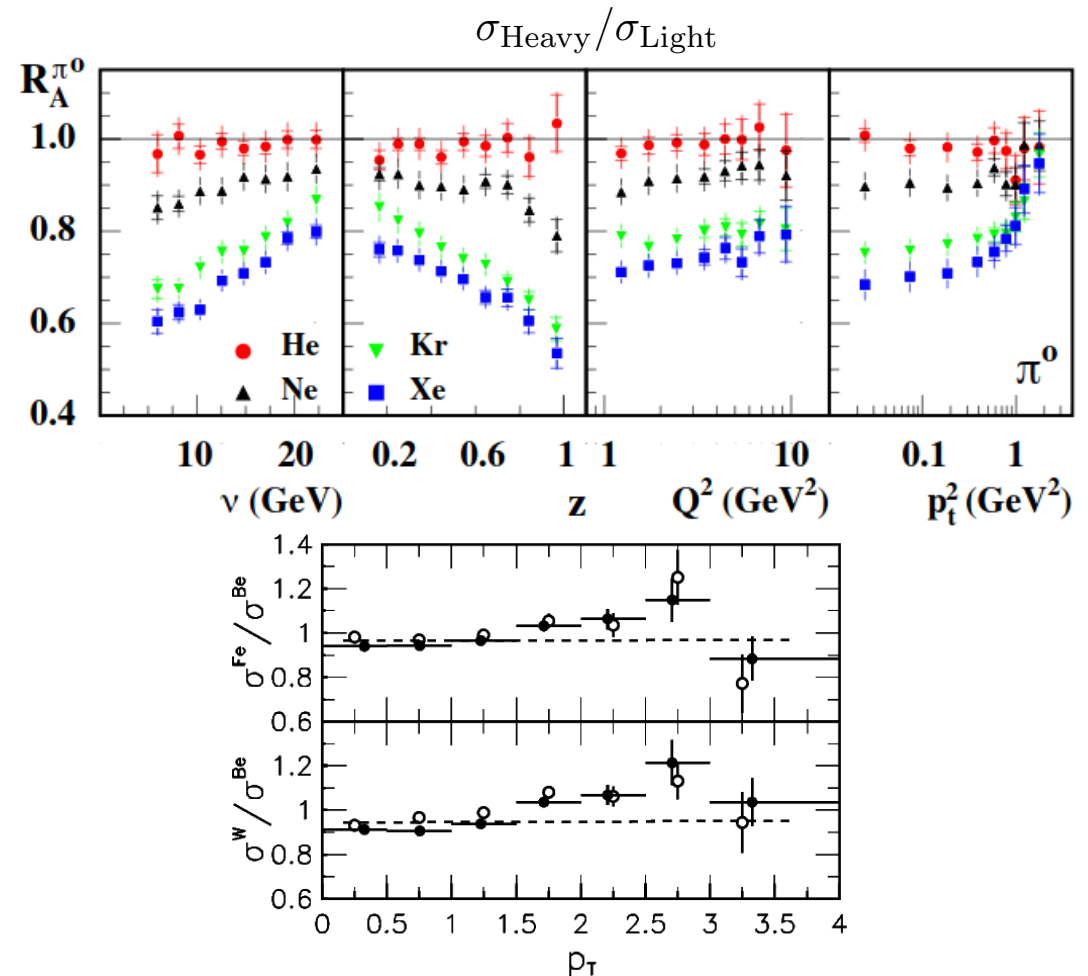
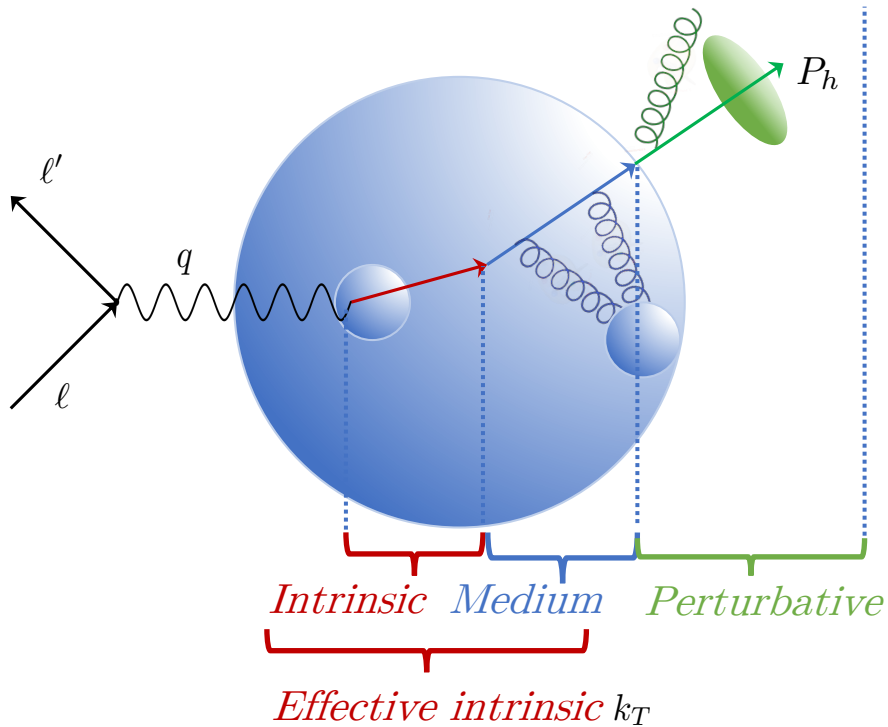
$$c_i \rightarrow c_i + c_{i,1} (1 - A^{c_{i,2}})$$



Abelev et al. (STAR) (2010)
Adams et al. (STAR) (2006)
Adare et al. (2013)
Airapetian et al. (HERMES) (2007)

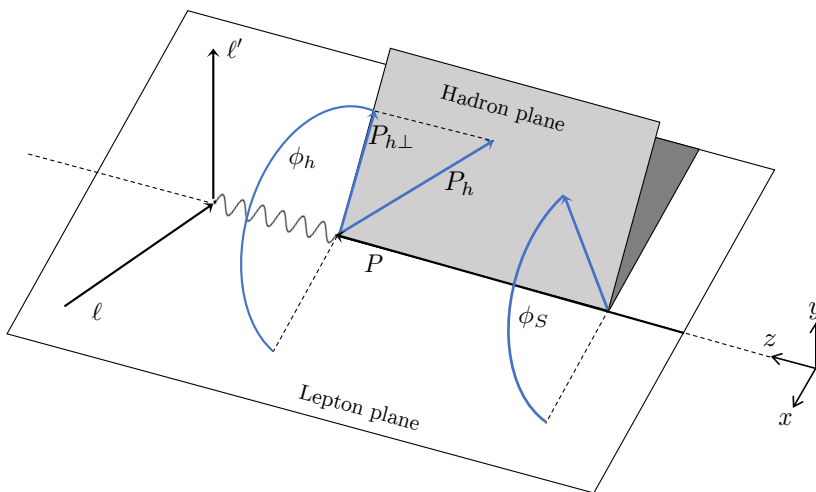
Effective treatment of the transverse momentum broadening

Interaction between partons and interact with the nuclear medium via Glauber exchange



Available data

Semi-Inclusive DIS for e-A collisions



Multiplicity ratio

$$R_A^h = \frac{d\sigma_A^h / \mathcal{PS}}{d\sigma_A / \mathcal{PS}} \frac{d\sigma_D / \mathcal{PS}}{d\sigma_D^h / \mathcal{PS} d^2 P_{h\perp}}$$

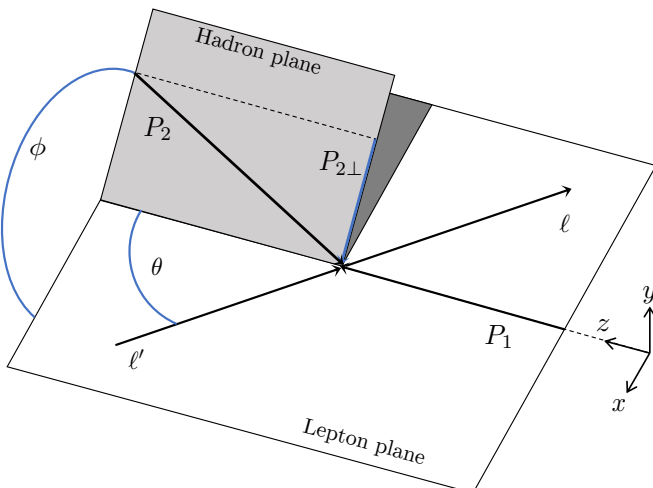
$$\text{SIDIS cross section } \frac{d\sigma_A^h}{\mathcal{PS} d^2 P_{h\perp}}$$

$$\text{DIS cross section } \frac{d\sigma_A}{\mathcal{PS}}$$

HERMES ratio for $A = \text{He, Ne, Kr, Xe}$
 $h = \pi^+, \pi^-, \pi^0, K^+, K^-, K^0$

Jefferson Lab ratio for $A = \text{C, Fe, Pb}$
 $h = \pi^+, \pi^-$

Drell-Yan production in p-A collisions



Cross section and cross section ratio
for p-A collisions

$$R_{AB} = \frac{d\sigma_A}{d\mathcal{PS} d^2 q_\perp} \frac{d\mathcal{PS} d^2 q_\perp}{d\sigma_B}$$

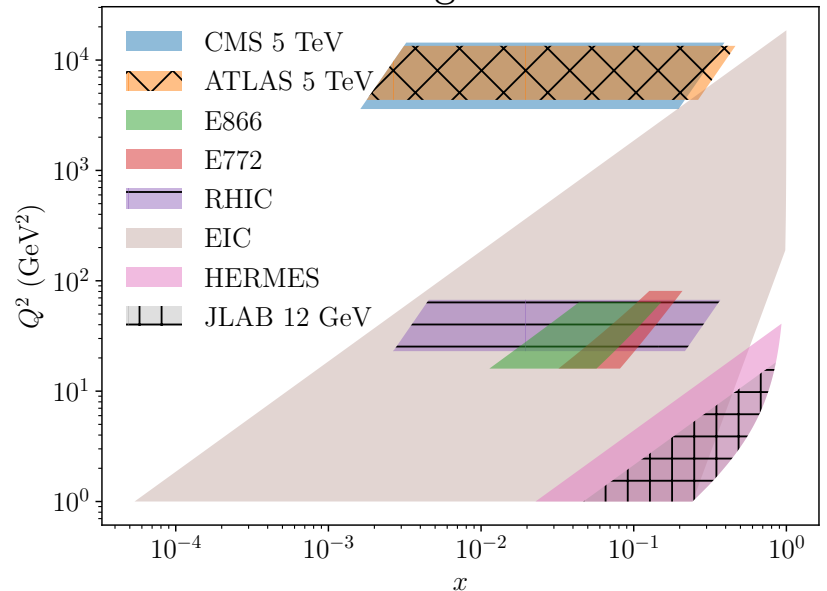
E772: $A = \text{C}; B = \text{D}$

E866: $A = \text{Fe, W}; B = \text{Be}$

RHIC: $A = \text{Au}; B = \text{p}$

ATLAS, CMS: q_\perp distribution p-Pb

Kinematic coverage of the data



Airapetian et al. (HERMES), Nucl. Phys. B 780, 1 (2007)

Dudek et al., Eur. Phys. J. A 48, 187 (2012)

Burkert, in CLAS 12 RICH Detector Workshop (2008)

Alde et al., Phys. Rev. Lett. 64, 2479 (1990)

Vasilev et al. (NuSea), Phys. Rev. Lett. 83, 2304 (1999)

Leung (PHENIX), PoS HardProbes2018, 160 (2018)

Khachatryan et al. (CMS), Phys. Lett. B 759, 36 (2016)

Aad et al. (ATLAS), Phys. Rev. C 92, 044915 (2015) 17/30

Available perturbative accuracy

Anomalous dimensions

$$\mu \frac{d}{d\mu} \ln F(Q, \mu, \nu) = \gamma_F^q(Q, \mu, \nu)$$

$$F \in \{H, f, D, S\}$$

$$\mu \frac{d}{d\nu} \ln G(Q, \mu, \nu) = \gamma_G^q(Q, \mu, \nu)$$

$$G \in \{f, D, S\}$$

Anomalous dimensions are almost known up to N⁴LL at this point (no 5-loop cusp)

Accuracy	H, \mathcal{J}	$\Gamma_{\text{cusp}}(\alpha_s)$	$\gamma_H^q(\alpha_s)$	$\gamma_r^q(\alpha_s)$	$\beta(\alpha_s)$
LL	Tree level	1-loop			1-loop
NLL	Tree level	2-loop	1-loop	1-loop	2-loop
NLL'	1-loop	2-loop	1-loop	1-loop	2-loop
NNLL	1-loop	3-loop	2-loop	2-loop	3-loop
NNLL'	2-loop	3-loop	2-loop	2-loop	3-loop
N ³ LL	2-loop	4-loop	3-loop	3-loop	4-loop
N ³ LL'	3-loop	4-loop	3-loop	3-loop	4-loop
N ⁴ LL	3-loop	5-loop	4-loop	4-loop	5-loop
N ⁴ LL'	4-loop	5-loop	4-loop	4-loop	5-loop

Lee, Smirnov, and Smirnov (2010)

Gehrmann, Glover, Huber, Ikizlerli, and Studerus (2010)

Ebert, Mistlberger, Vita (2020)

Ebert, Mistlberger, Vita (2020)

Agarwal, von Manteuffel, Panzer, and Schabinger (2021)

Duhr, Mistlberger, Vita (2022)

Moult, Zhu, Zhu (2022)

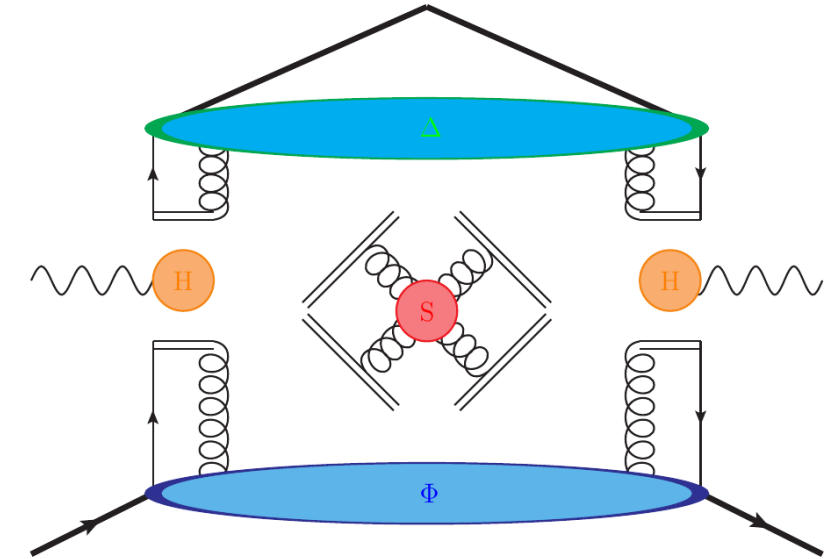
Herzog, Moch, Ruijl, Ueda, Vermaseren, and Vogt (2019)

Baikov, Chetyrkin, and Kuhn (2017)

Factorization and resummation in the medium

Differential cross section for Semi-Inclusive DIS is given by

$$\frac{d\sigma}{d\mathcal{PS} d^2 P_{h\perp}} = \sigma_0 \underbrace{H(Q; \mu)}_{\text{Hard}} \sum_q e_q^2 \int \frac{bdb}{2\pi} J_0 \left(\frac{bP_{h\perp}}{z} \right) \underbrace{f_{q/N}^A(x, b; \mu, \zeta_1)}_{nTMD PDF} \underbrace{D_{h/q}^A(z, b; \mu, \zeta_2)}_{nTMD FF}$$



TMDs can be matched onto the collinear distributions

$$f_{1q/A}(x, b, \mu, \zeta) = [C \otimes f]_{q/A}(x, b, \mu_i, \zeta_i) U(\mu_i, \mu; \zeta) Z(b, \zeta_i, \zeta; \mu_i) U_{NP}^{f^A}(x, b, \zeta, A)$$

$$D_{1h/q}^A(z, b, \mu, \zeta) = \frac{1}{z^2} [\hat{C} \otimes D^A]_{h/q}(z, b, \mu_i, \zeta_i) U(\mu_i, \mu; \zeta) Z(b, \zeta_i, \zeta; \mu_i) U_{NP}^{D^A}(z, b, \zeta, A)$$

Perturbative *Non-perturbative*

Large logarithms are resummed to all orders in the perturbative Sudakov

$$U(\mu_i, \mu; \zeta) = \exp \left[\int_{\mu_i}^{\mu} \frac{d\mu'}{\mu'} \gamma_{\mu}(\mu', \zeta) \right], Z(b, \mu_i, \mu; \zeta) = \left(\frac{\zeta}{\zeta_i} \right)^{\gamma_{\zeta}(b, \mu_i)}$$

Non-perturbative treatment

Non-perturbative contributions given by

$$f_{1q/A}(x, b, \mu, \zeta) = [C \otimes f]_{q/A}(x, b, \mu_i, \zeta_i) U(\mu_i, \mu; \zeta) Z(b, \zeta_i, \zeta; \mu_i) U_{\text{NP}}^{f^A}(x, b, \zeta, A)$$

$$D_{1h/q}^A(z, b, \mu, \zeta) = \frac{1}{z^2} [\hat{C} \otimes D^A]_{h/q}(z, b, \mu_i, \zeta_i) U(\mu_i, \mu; \zeta) Z(b, \zeta_i, \zeta; \mu_i) U_{\text{NP}}^{D^A}(z, b, \zeta, A)$$

EPPS21 In house FF (new), previous analysis used LIKEN

Non-perturbative Sudakov given by

$$U_{\text{NP}}^{f^A}(x, b, \zeta) = U_{\text{NP}}^f(x, b, \zeta) \exp \left\{ -g_q^A \left(A^{1/3} - 1 \right) b^2 \left(\frac{\zeta_A}{\zeta} \right)^\Gamma \right\}$$

$$U_{\text{NP}}^{D^A}(x, b, \zeta) = U_{\text{NP}}^D(x, b, \zeta) \exp \left\{ -g_h^A \left(A^{1/3} - 1 \right) \frac{b^2}{z^2} \left(\frac{\zeta_A}{\zeta} \right)^\Gamma \right\}$$

Parameterization for the medium modified fragmentation

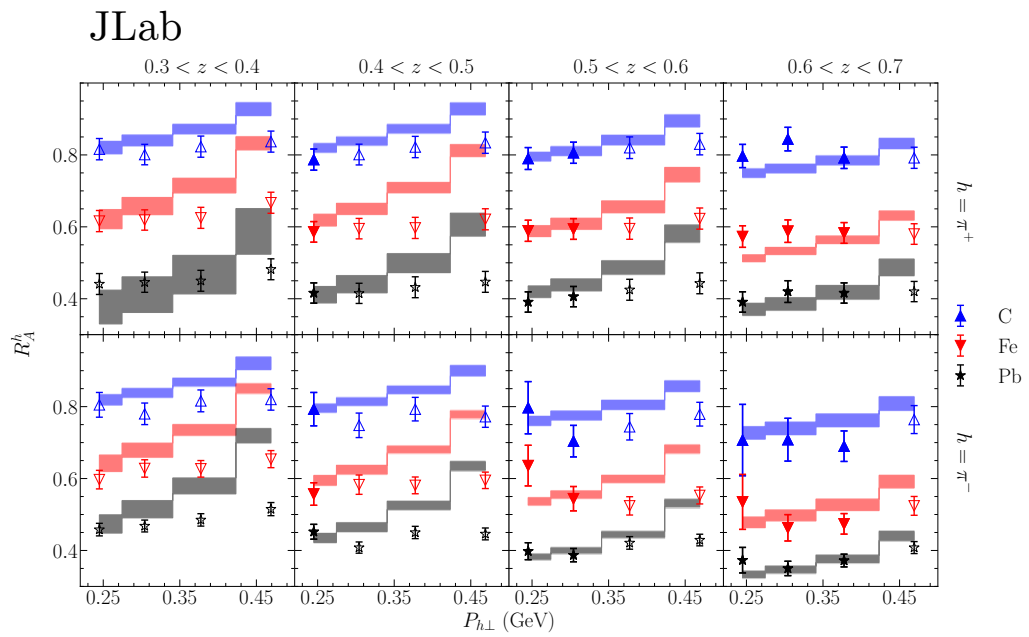
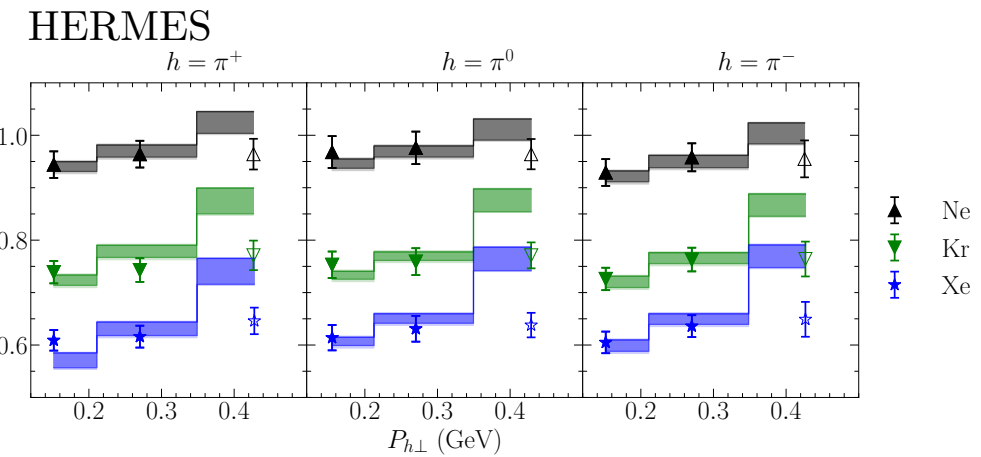
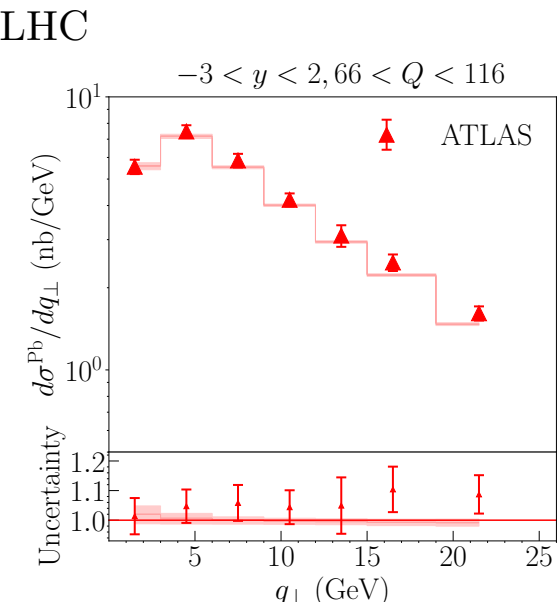
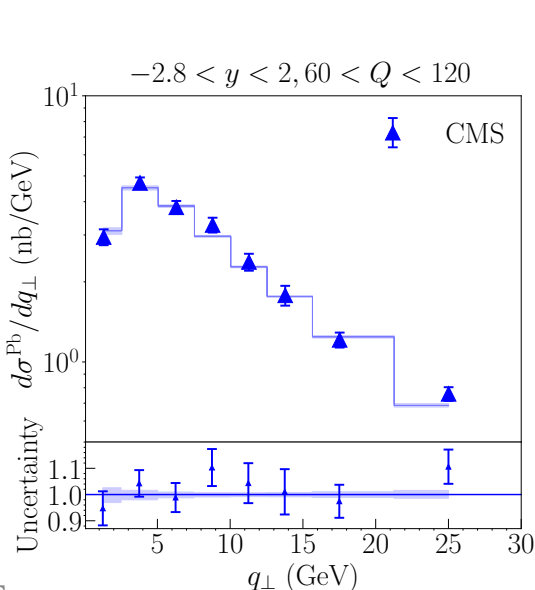
$$D_i^{\pi^+}(z, \mu_0) = \frac{N_i z^{\alpha_i} (1-z)^{\beta_i} [1 + \gamma_i (1-z)^{\delta_i}]}{B[2 + \alpha_i, \beta_i + 1] + \gamma_i B[2 + \alpha_i, \beta_i + \delta_i + 1]} .$$

$$\begin{aligned} \tilde{N}_i &\rightarrow \tilde{N}_i \left[1 + N_{i,1} (1 - A^{N_{i,2}}) \right] \\ c_i &\rightarrow c_i + c_{i,1} (1 - A^{c_{i,2}}) \end{aligned}$$

$$\mathbf{p} = \{N_{q1}, N_{q2}, \gamma_{q1}, \gamma_{q2}, \delta_{q1}, \delta_{q2}, g_q^A, g_h^A, \Gamma\} ,$$

Description of the experimental data

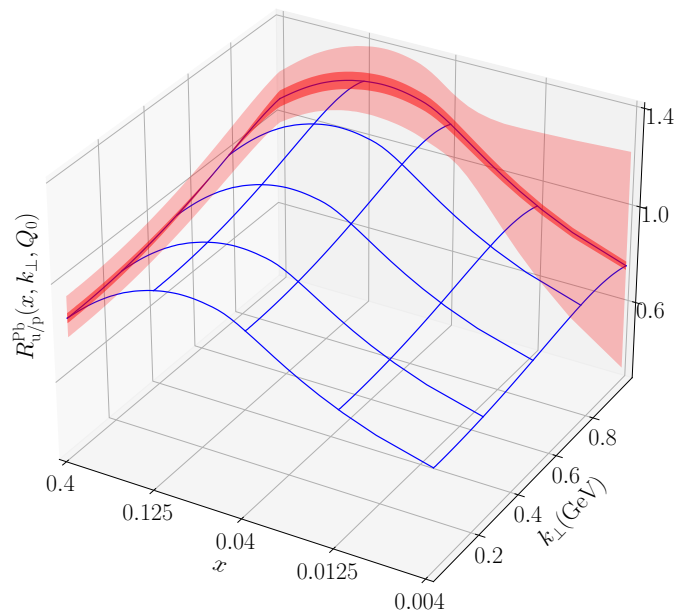
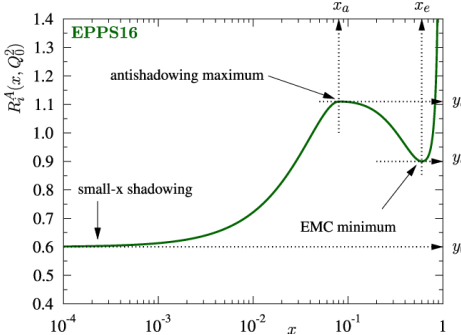
Collaboration	Process	Baseline	Nuclei	N _{data}	χ^2
JLAB [49]	SIDIS(π)	D	C, Fe, Pb	36	41.7
HERMES [40]	SIDIS(π)	D	Ne, Kr, Xe	18	10.2
RHIC [43]	DY	p	Au	4	1.3
E772 [41]	DY	D	C, Fe, W	16	40.2
E866 [42]	DY	Be	Fe, W	28	20.6
CMS [63]	γ^*/Z	N/A	Pb	8	10.4
ATLAS [83]	γ^*/Z	N/A	Pb	7	13.3
Total				117	137.8



Three-dimensional images

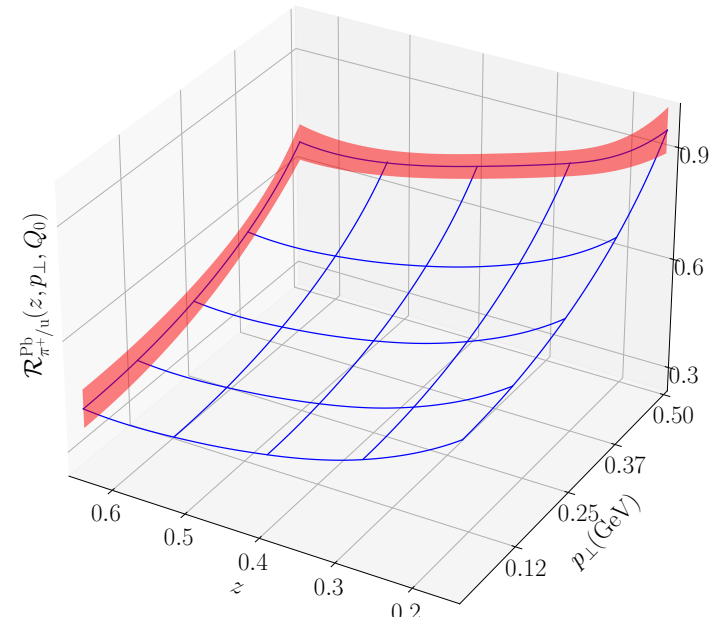
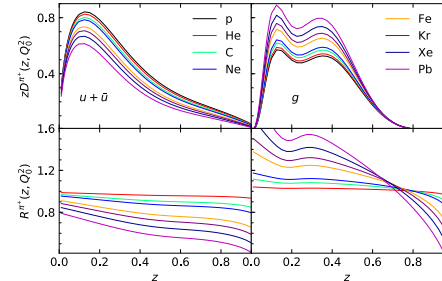
Ratios defined for nPDF and nFF

$$R_i^A(x, Q_0^2) = \frac{f_{i/p}^A(x, Q_0^2)}{f_{i/p}(x, Q_0^2)}$$



$$R_{u/p}^{Pb}(x, k_\perp, Q_0) = \frac{f_{u/p}^{Pb}(x, k_\perp, Q_0, Q_0^2)}{f_{u/p}(x, k_\perp, Q_0, Q_0, Q_0^2)}$$

$$R_i^A(z, Q_0^2) = \frac{D_{h/i}^A(z, Q_0^2)}{D_{h/i}(z, Q_0^2)}$$

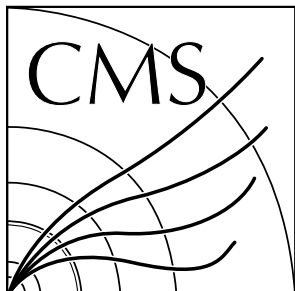
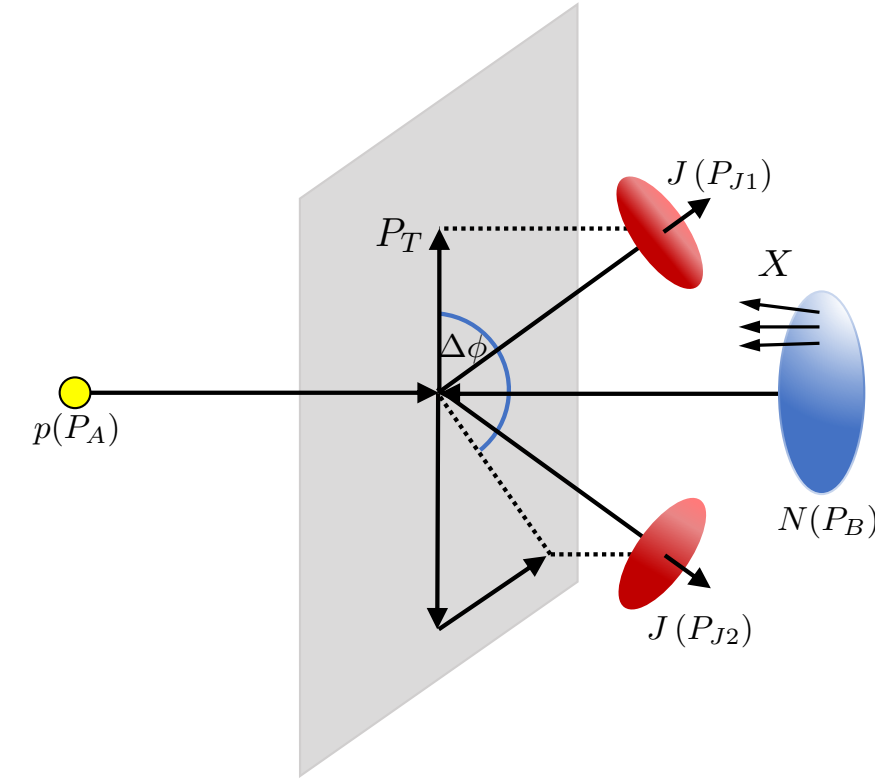


$$\mathcal{R}_{\pi^+/u}^{Pb}(z, p_\perp, Q_0) = \frac{D_{\pi^+/u}^{Pb}(z, p_\perp, Q_0, Q_0^2)}{D_{\pi^+/u}(z, p_\perp, Q_0, Q_0^2)}$$

Di-jet decorrelations in pp

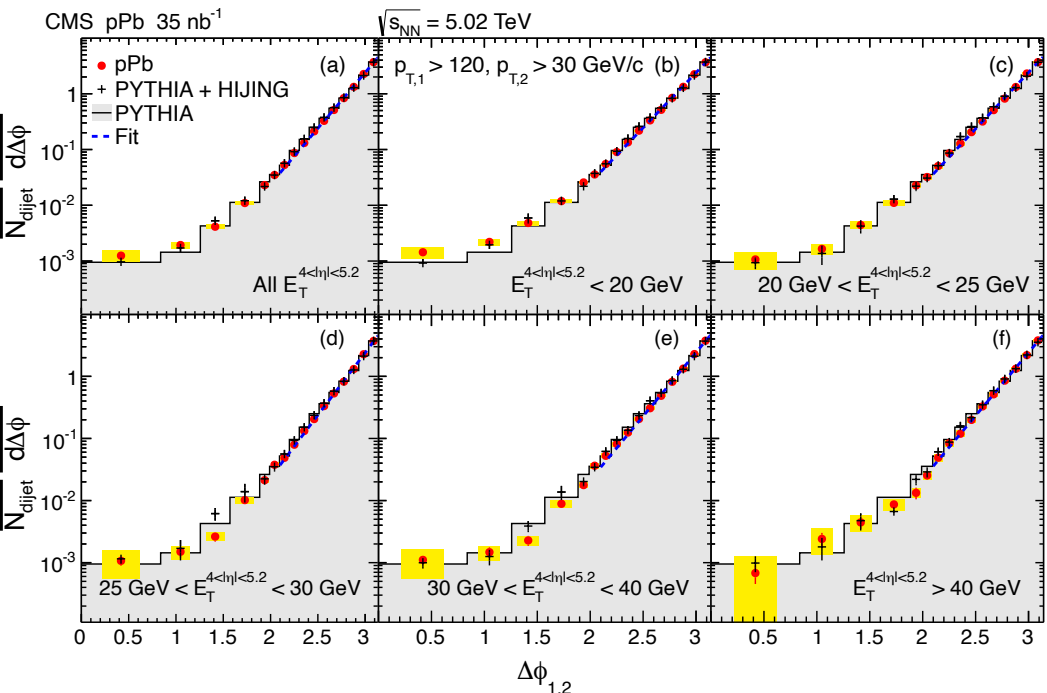
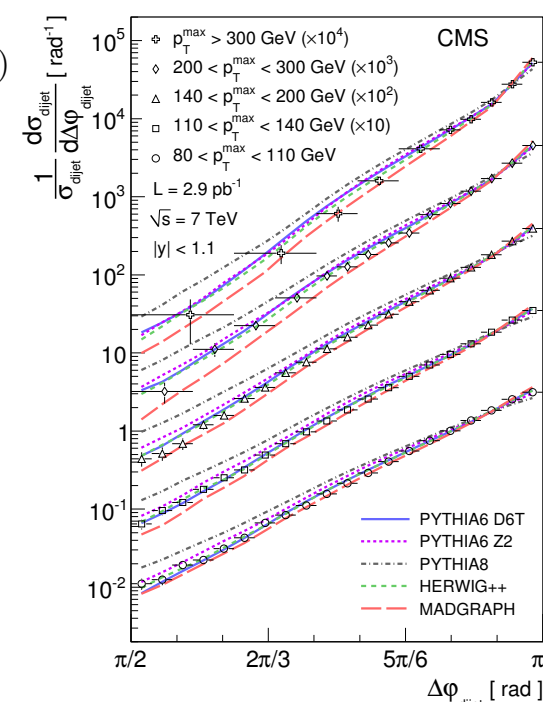
Azimuthal angle decorrelations of di-jets measured at the CMS, are sensitive to nTMDs

Back-to-back region is sensitive to the 1+1 dimensional TMDs



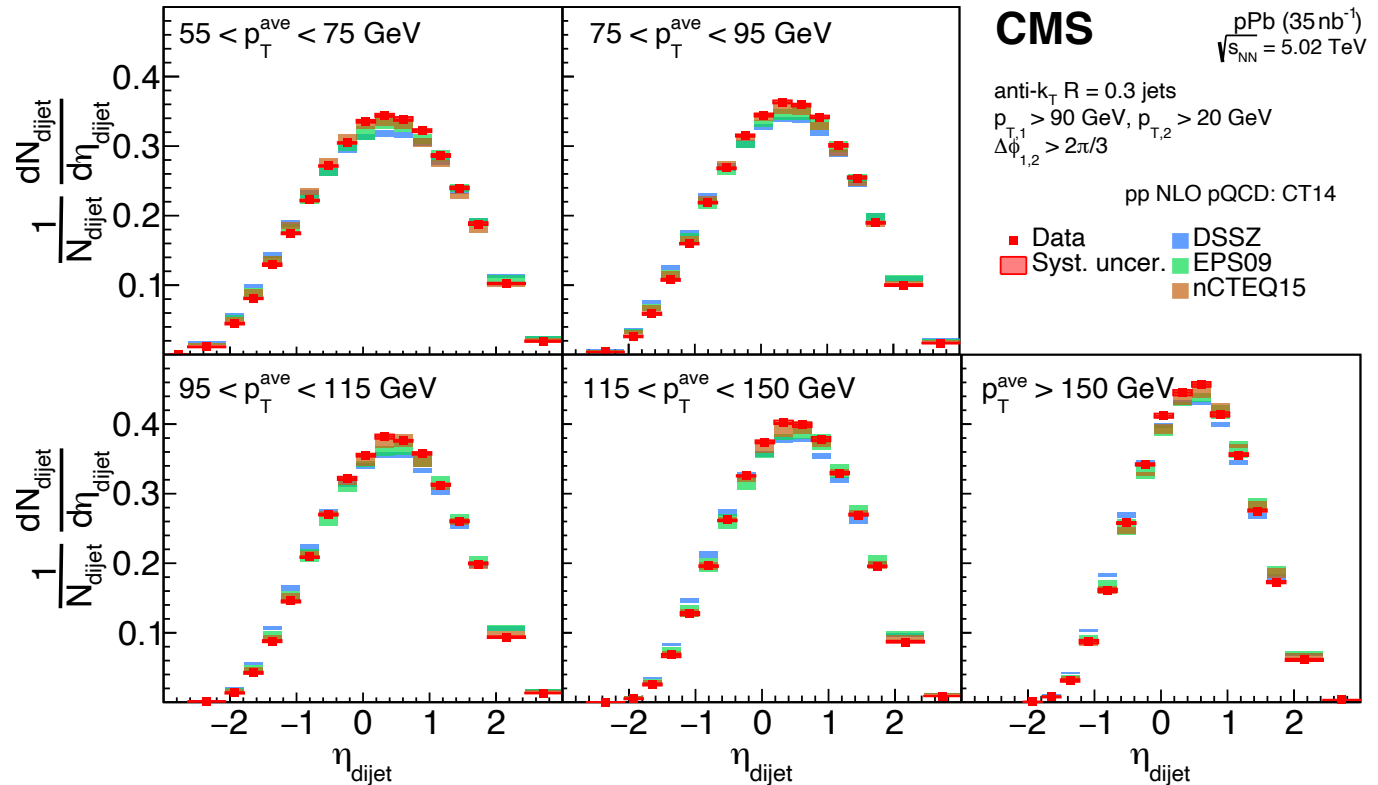
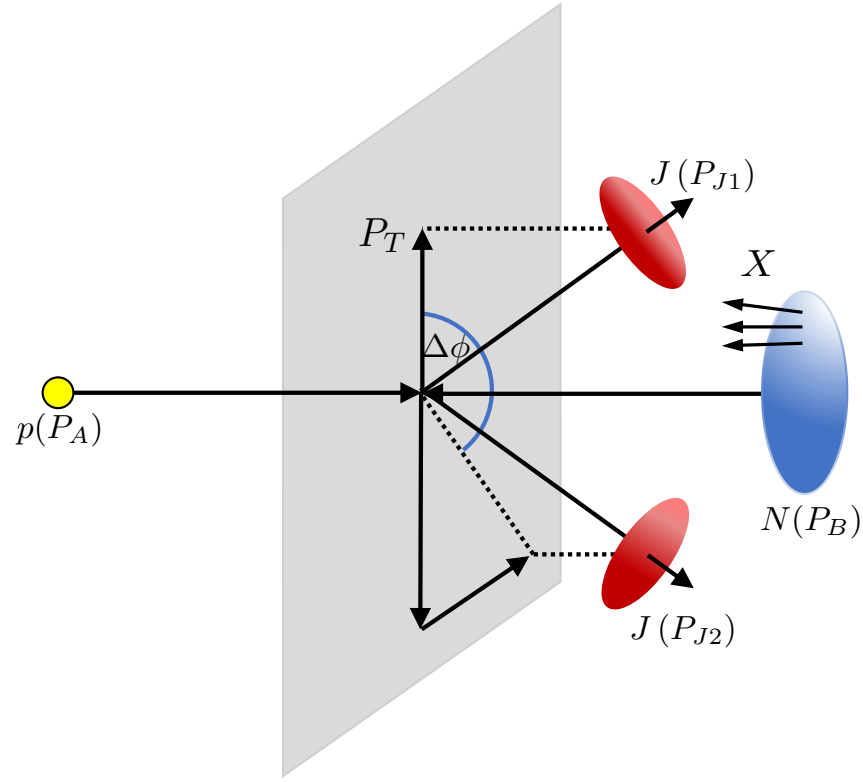
CMS Measurements in pp and pA collisions

[Phys.Rev.Lett.106:122003,2011](#)
[Eur. Phys. J. C 74 \(2014\) 2951](#)
[Phys. Rev. Lett. 121, 062002 \(2018\)](#)



Di-jet decorrelations in pp continued

Additional measurements of the integrated azimuthal angle decorrelation



Integration in region $\Delta\phi > 2\pi/3$ performed using a collinear approximation. However, there are issues with this approach as $\Delta\phi \rightarrow \pi$ due to large logarithms.

QCD modes in SCET

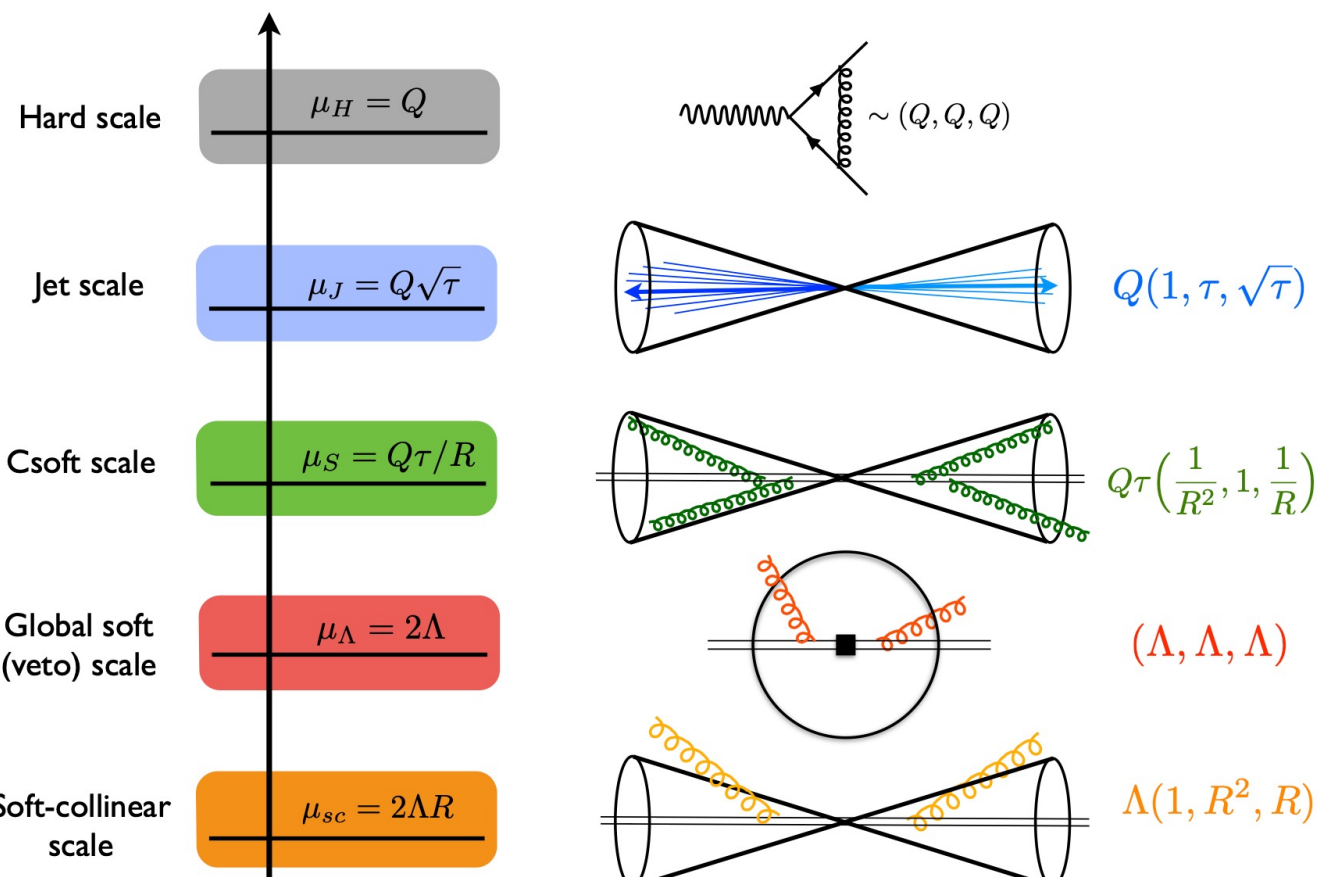
SCET is an EFT which captures soft and collinear emissions along the directions

$$\mathcal{L}_{\text{QCD}} = \sum_q \bar{\psi} i \not{D} \psi - \frac{1}{4} G_{\mu\nu}^A G^{A\mu\nu} + \mathcal{L}_{\text{gauge-fix}} + \mathcal{L}_{\text{ghost}}$$

$$\psi \rightarrow \psi_s + \psi_c \quad A^\mu \rightarrow A_s^\mu + A_c^\mu$$

$$\mathcal{L}_{\text{SCET}} = \bar{\psi}_s i \not{D}_s \psi_s - \frac{1}{4} G_{\mu\nu s}^A G_s^{A\mu\nu}$$

$$+ \xi \frac{\not{n}}{2} \left[i n \cdot D + i \not{D}_{c\perp} \frac{1}{i \bar{n} \cdot D_c} i \not{D}_{c\perp} \right] \xi - \frac{1}{4} G_{\mu\nu c}^A G_c^{A\mu\nu}$$



Bauer, Fleming, Luke 2000

Bauer, Fleming, Pirjol, Stewart 2001

Bauer, Stewart 2001

Bauer, Pirjol, Stewart 2002

Beneke, Chapovsky, Diehl, Feldmann 2002

Beneke, Feldmann 2003

Hill, Neubert 2003

Echevarria, Idilbi, Scimemi 2011

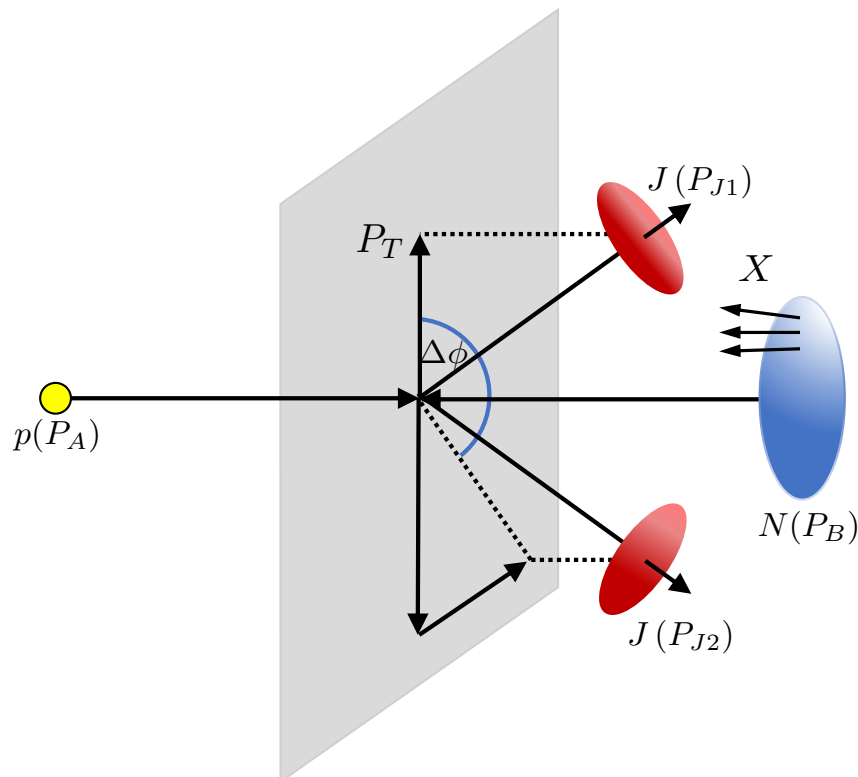
Chien, Hornig, Lee 2015

Factorization in SCET

Azimuthal angle decorrelations of di-jets measured at the CMS, are sensitive to nTMDs

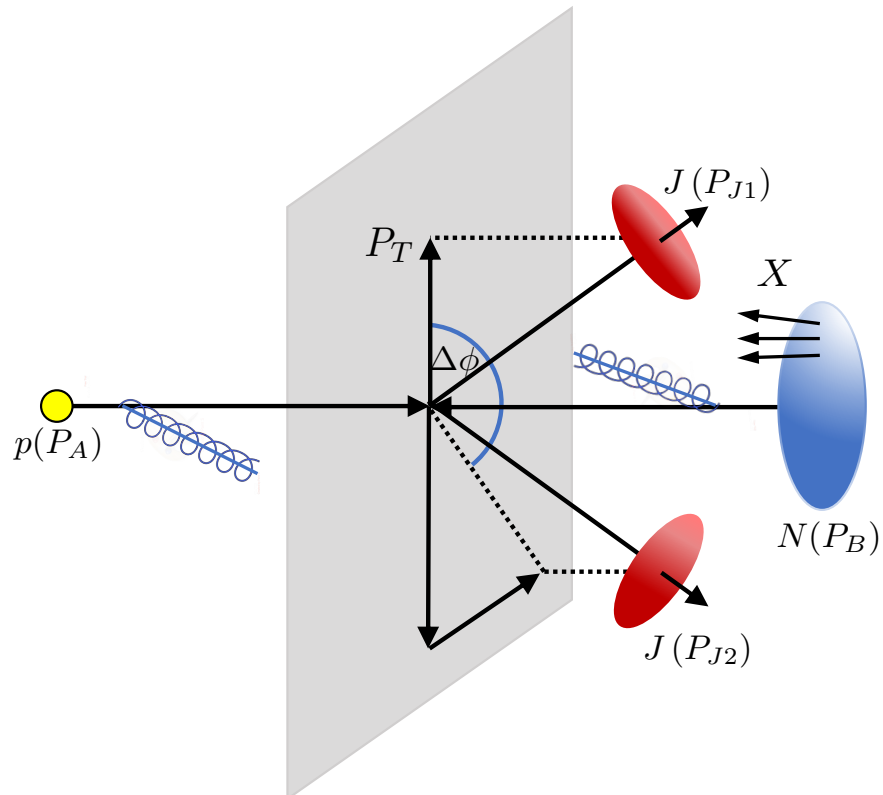
Factorization and resummation derived in a SCET framework

$$\text{hard} : p_h^\mu \sim p_T(1, 1, 1)$$



Factorization in SCET

Azimuthal angle decorrelations of di-jets measured at the CMS, are sensitive to nTMDs

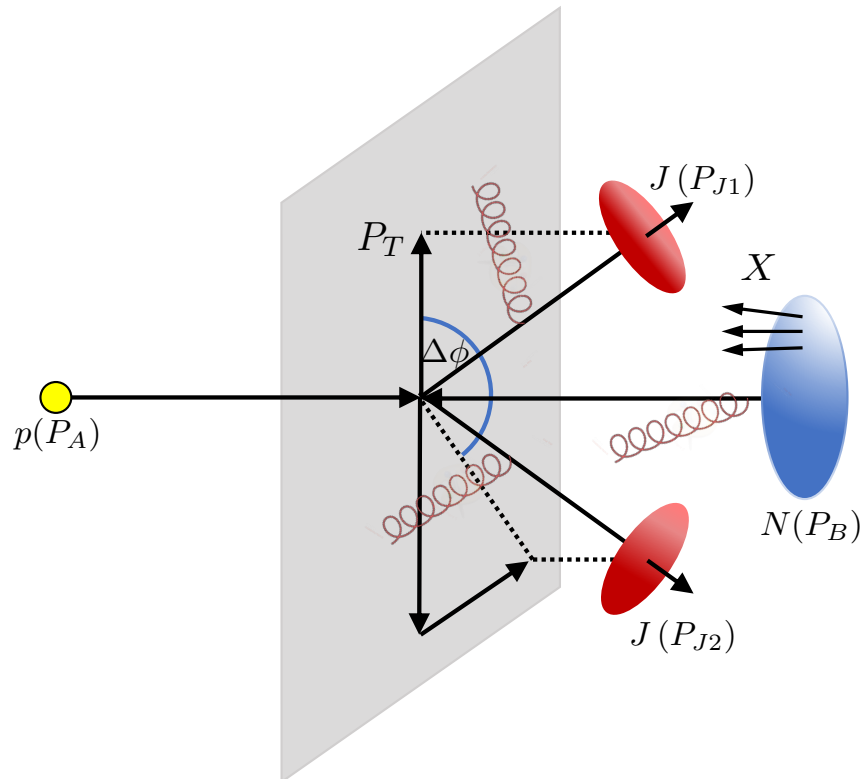


Factorization and resummation derived in a SCET framework

$$\begin{aligned}\text{hard : } p_h^\mu &\sim p_T(1, 1, 1) \\ n_{a,b}\text{-collinear : } p_{c_i}^\mu &\sim p_T(\delta\phi^2, 1, \delta\phi)_{n_i \bar{n}_i},\end{aligned}$$

Factorization in SCET

Azimuthal angle decorrelations of di-jets measured at the CMS, are sensitive to nTMDs

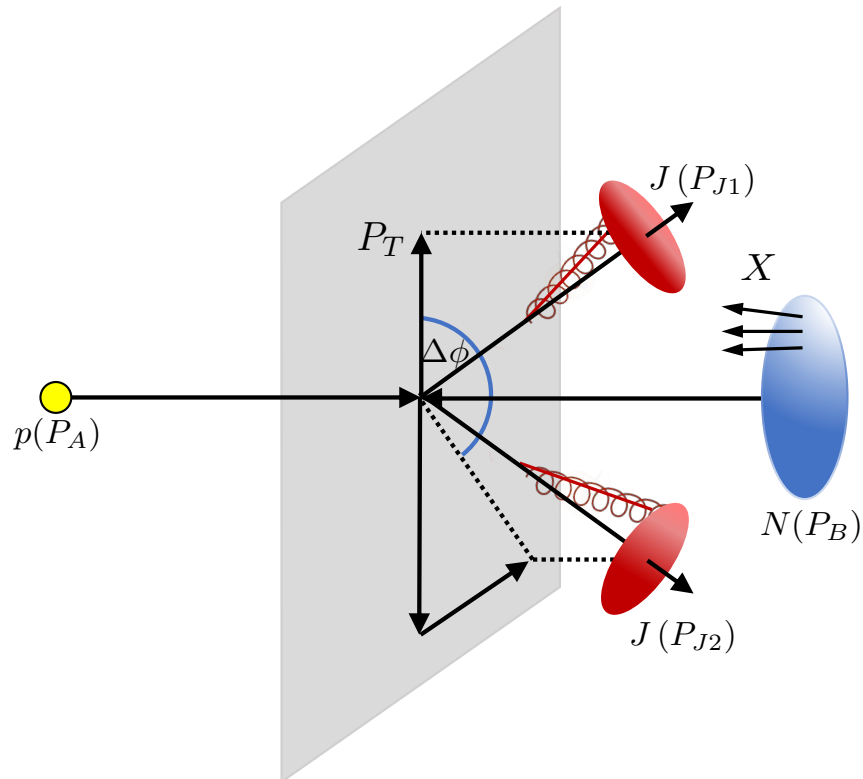


Factorization and resummation derived in a SCET framework

$$\begin{aligned}\text{hard : } p_h^\mu &\sim p_T(1, 1, 1) \\ n_{a,b}\text{-collinear : } p_{c_i}^\mu &\sim p_T(\delta\phi^2, 1, \delta\phi)_{n_i \bar{n}_i}, \\ \text{soft : } p_s^\mu &\sim p_T(\delta\phi, \delta\phi, \delta\phi),\end{aligned}$$

Factorization in SCET

Azimuthal angle decorrelations of di-jets measured at the CMS, are sensitive to nTMDs

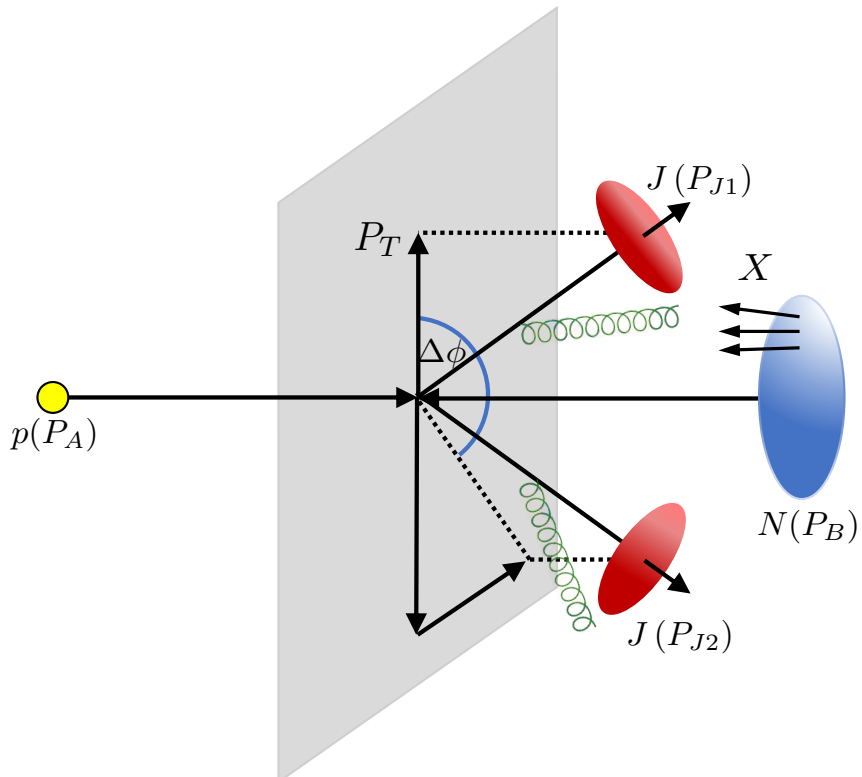


Factorization and resummation derived in a SCET framework

$$\begin{aligned}\text{hard} &: p_h^\mu \sim p_T(1, 1, 1) \\ n_{a,b}\text{-collinear} &: p_{c_i}^\mu \sim p_T(\delta\phi^2, 1, \delta\phi)_{n_i \bar{n}_i}, \\ \text{soft} &: p_s^\mu \sim p_T(\delta\phi, \delta\phi, \delta\phi), \\ n_{c,d}\text{-jet} &: p_{c_i}^\mu \sim p_T(R^2, 1, R)_{n_i \bar{n}_i},\end{aligned}$$

Factorization in SCET

Azimuthal angle decorrelations of di-jets measured at the CMS, are sensitive to nTMDs



Factorization and resummation derived in a SCET framework

$$\text{hard} : p_h^\mu \sim p_T(1, 1, 1)$$

$$n_{a,b}\text{-collinear} : p_{c_i}^\mu \sim p_T(\delta\phi^2, 1, \delta\phi)_{n_i \bar{n}_i},$$

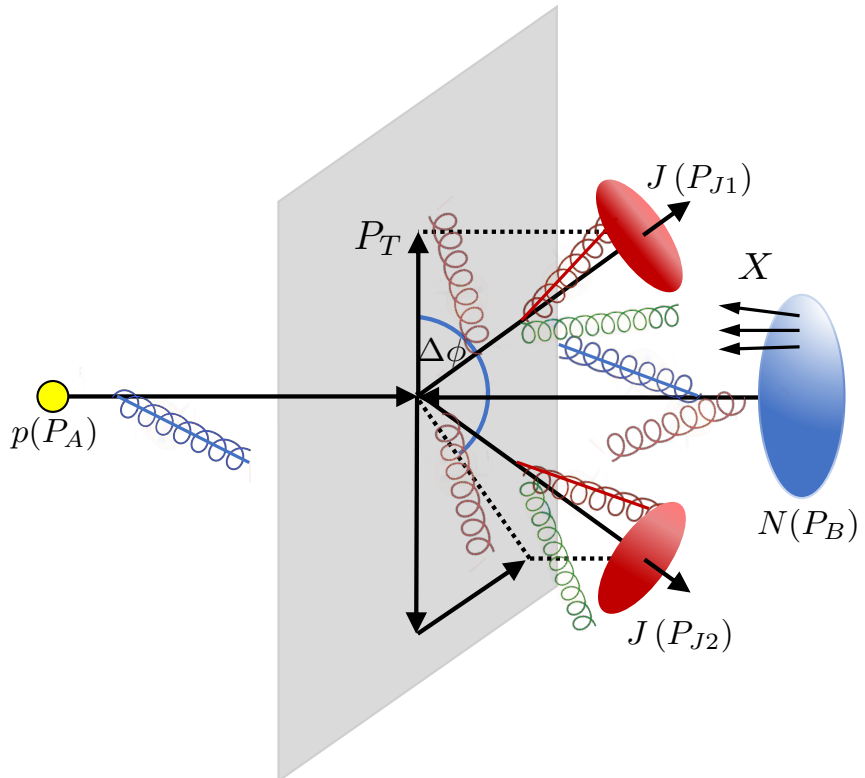
$$\text{soft} : p_s^\mu \sim p_T(\delta\phi, \delta\phi, \delta\phi),$$

$$n_{c,d}\text{-jet} : p_{c_i}^\mu \sim p_T(R^2, 1, R)_{n_i \bar{n}_i},$$

$$n_{c,d}\text{-collinear-soft} : p_{cs_i}^\mu \sim \frac{p_T \delta\phi}{R} (R^2, 1, R)_{n_i \bar{n}_i},$$

Factorization in SCET

Azimuthal angle decorrelations of di-jets measured at the CMS, are sensitive to nTMDs



Factorization and resummation at NLL:

Factorization and resummation derived in a SCET framework

$$\begin{aligned}
 \text{hard} &: p_h^\mu \sim p_T(1, 1, 1) \\
 n_{a,b}\text{-collinear} &: p_{c_i}^\mu \sim p_T(\delta\phi^2, 1, \delta\phi)_{n_i \bar{n}_i}, \\
 \text{soft} &: p_s^\mu \sim p_T(\delta\phi, \delta\phi, \delta\phi), \\
 n_{c,d}\text{-jet} &: p_{c_i}^\mu \sim p_T(R^2, 1, R)_{n_i \bar{n}_i}, \\
 n_{c,d}\text{-collinear-soft} &: p_{cs_i}^\mu \sim \frac{p_T \delta\phi}{R} (R^2, 1, R)_{n_i \bar{n}_i},
 \end{aligned}$$

$$\begin{aligned}
 \frac{d^4\sigma_{pp}}{dy_c dy_d dp_T^2 d\delta\phi} &= \sum_{abcd} \frac{p_T}{16\pi\hat{s}^2} \frac{1}{1 + \delta_{cd}} \int_0^\infty \frac{2db}{\pi} \cos(bp_T\delta\phi) x_a \tilde{f}_{a/p}(x_a, \mu_{b_*}) x_b \tilde{f}_{b/p}(x_b, \mu_{b_*}) \\
 &\times \exp \left\{ - \int_{\mu_{b_*}}^{\mu_h} \frac{d\mu}{\mu} \left[\gamma_{\text{cusp}}(\alpha_s) C_H \ln \frac{\hat{s}}{\mu^2} + 2\gamma_H(\alpha_s) \right] \right\} \\
 &\times \sum_{KK'} \exp \left[- \int_{\mu_{b_*}}^{\mu_h} \frac{d\mu}{\mu} \gamma_{\text{cusp}}(\alpha_s) (\lambda_K + \lambda_{K'}^*) \right] H_{KK'}(\hat{s}, \hat{t}, \mu_h) W_{K'K}(b_*, \mu_{b_*}) \\
 &\times \exp \left[- \int_{\mu_{b_*}}^{\mu_j} \frac{d\mu}{\mu} \Gamma^{J_c}(\alpha_s) - \int_{\mu_{b_*}}^{\mu_j} \frac{d\mu}{\mu} \Gamma^{J_d}(\alpha_s) \right] U_{\text{NG}}^c(\mu_{b_*}, \mu_j) U_{\text{NG}}^d(\mu_{b_*}, \mu_j) \\
 &\times \exp \left[-S_{\text{NP}}^a(b, Q_0, \sqrt{\hat{s}}) - S_{\text{NP}}^b(b, Q_0, \sqrt{\hat{s}}) \right].
 \end{aligned}$$

Do we observe factorization breaking effects?

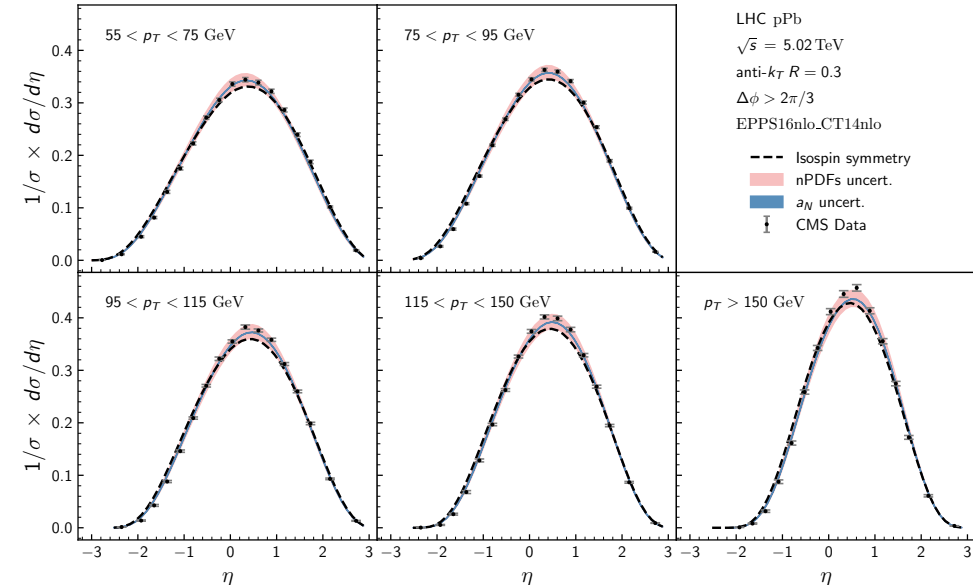
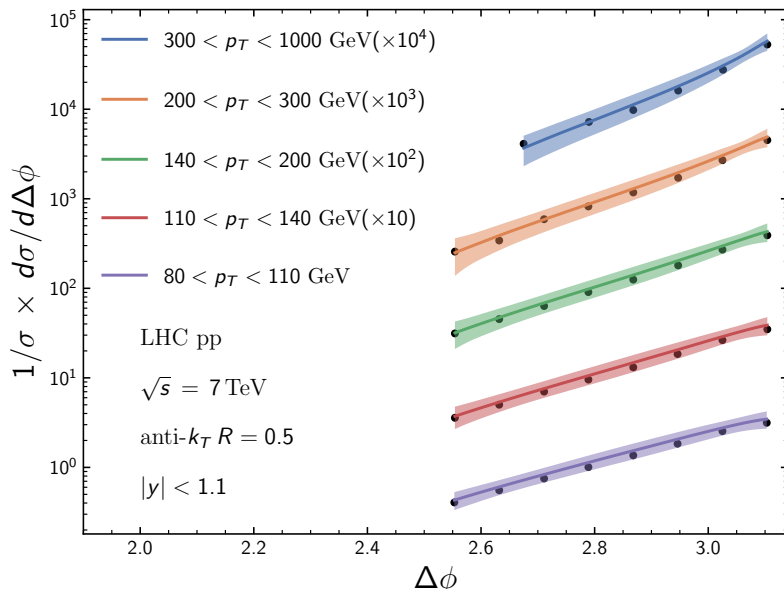
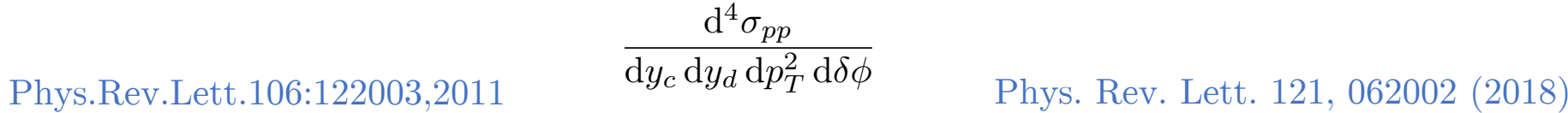
Glauber mode note treated in our paper

$$\begin{aligned}
 \text{hard} &: p_h^\mu \sim p_T(1, 1, 1) \\
 n_{a,b}\text{-collinear} &: p_{c_i}^\mu \sim p_T(\delta\phi^2, 1, \delta\phi)_{n_i \bar{n}_i}, \\
 \text{soft} &: p_s^\mu \sim p_T(\delta\phi, \delta\phi, \delta\phi), \\
 n_{c,d}\text{-jet} &: p_{c_i}^\mu \sim p_T(R^2, 1, R)_{n_i \bar{n}_i}, \\
 n_{c,d}\text{-collinear-soft} &: p_{cs_i}^\mu \sim \frac{p_T \delta\phi}{R} (R^2, 1, R)_{n_i \bar{n}_i}, \\
 n_G\text{-Glauber} &: p_G^\mu \sim p_T(\delta\phi^2, \delta\phi^2, \delta\phi)_{n_i \bar{n}_i}
 \end{aligned}$$

Factorization breaking effects in dijet production studied in

Collins, Qiu Phys.Rev.D75:114014,2007
Collins (2007)

The experimental data is well-described by the theoretical prediction in the back-to-back region, within the error bars



Nuclear modifications to this process

Azimuthal angle decorrelations of di-jets measured at the CMS, are sensitive to nTMDs

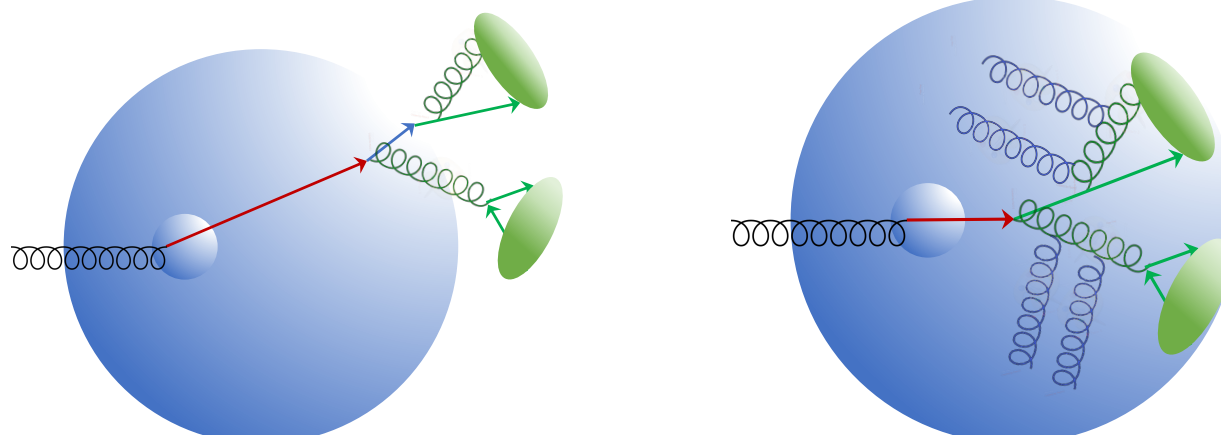
nTMDs can be matched onto the collinear distributions

$$f_{q/N}^A(b, x; \mu, \zeta_1) = [C \otimes f](x; \mu_i) \exp \left[-S_{\text{pert}}(b; \mu_i, \mu, \zeta_i, \zeta_1) - S_{\text{NP}}^{fA}(b; Q_0, \mu, \zeta_i, \zeta) \right]$$

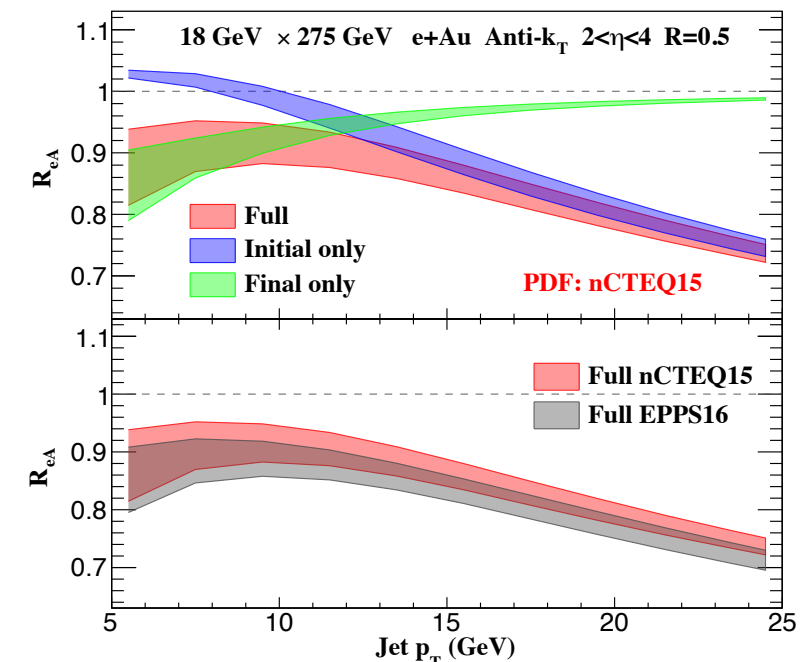
Perturbative *Non-perturbative: Contains all medium contributions*

We ignore all final-state interactions between the jets and the medium.

High energy jets are not expected to be affected by the medium

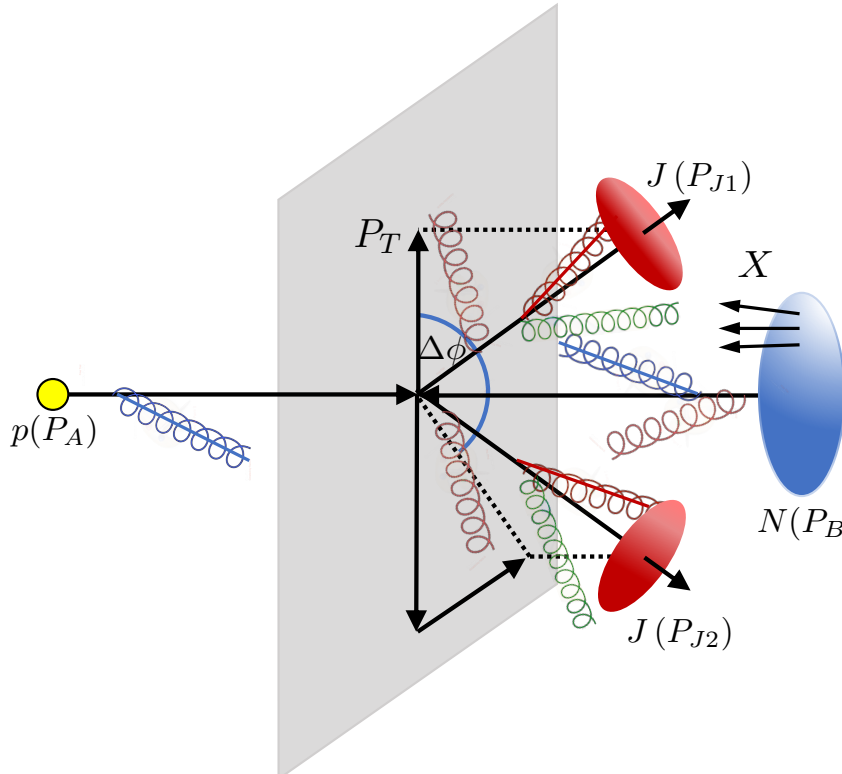


Li, Vitev (2021)



Factorization in pA

Azimuthal angle decorrelations of di-jets measured at the CMS, are sensitive to nTMDs



Factorization and resummation:

Factorization and resummation derived in a SCET framework

$$\text{hard} : p_h^\mu \sim p_T(1, 1, 1)$$

$$n_{a,b}\text{-collinear} : p_{c_i}^\mu \sim p_T(\delta\phi^2, 1, \delta\phi)_{n_i \bar{n}_i},$$

$$\text{soft} : p_s^\mu \sim p_T(\delta\phi, \delta\phi, \delta\phi),$$

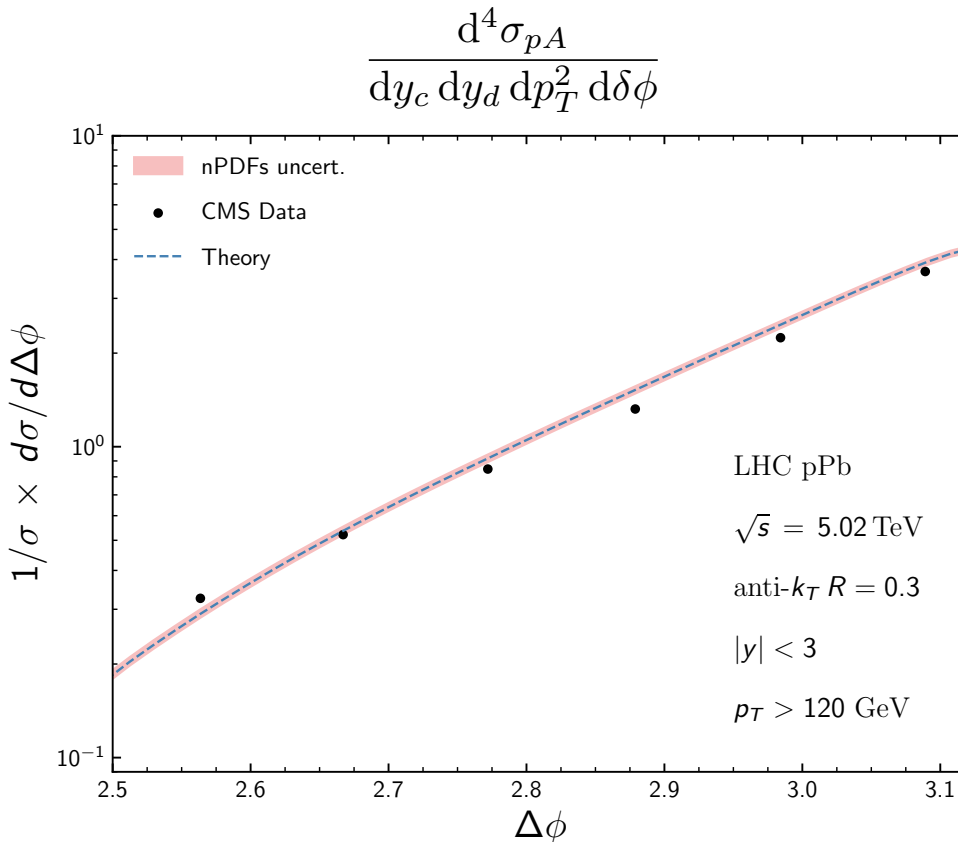
$$n_{c,d}\text{-jet} : p_{c_i}^\mu \sim p_T(R^2, 1, R)_{n_i \bar{n}_i},$$

$$n_{c,d}\text{-collinear-soft} : p_{cs_i}^\mu \sim \frac{p_T \delta\phi}{R} (R^2, 1, R)_{n_i \bar{n}_i},$$

$$\begin{aligned} \frac{d^4\sigma_{pA}}{dy_c dy_d dp_T^2 d\delta\phi} &= \sum_{abcd} \frac{p_T}{16\pi\hat{s}^2} \frac{1}{1 + \delta_{cd}} \int_0^\infty \frac{2db}{\pi} \cos(bp_T\delta\phi) x_a \tilde{f}_{a/p}(x_a, \mu_{b_*}) x_b \tilde{f}_{b/A}(x_b, \mu_{b_*}) \\ &\times \exp \left\{ - \int_{\mu_{b_*}}^{\mu_h} \frac{d\mu}{\mu} \left[\gamma_{\text{cusp}}(\alpha_s) C_H \ln \frac{\hat{s}}{\mu^2} + 2\gamma_H(\alpha_s) \right] \right\} \\ &\times \sum_{KK'} \exp \left[- \int_{\mu_{b_*}}^{\mu_h} \frac{d\mu}{\mu} \gamma_{\text{cusp}}(\alpha_s) (\lambda_K + \lambda_{K'}^*) \right] H_{KK'}(\hat{s}, \hat{t}, \mu_h) W_{K'K}(b_*, \mu_{b_*}) \\ &\times \exp \left[- \int_{\mu_{b_*}}^{\mu_j} \frac{d\mu}{\mu} \Gamma^{J_c}(\alpha_s) - \int_{\mu_{b_*}}^{\mu_j} \frac{d\mu}{\mu} \Gamma^{J_d}(\alpha_s) \right] U_{\text{NG}}^c(\mu_{b_*}, \mu_j) U_{\text{NG}}^d(\mu_{b_*}, \mu_j) \\ &\times \exp \left[-S_{\text{NP}}^a(b, Q_0, \sqrt{\hat{s}}) - S_{\text{NP}}^{b,A}(b, Q_0, \sqrt{\hat{s}}) \right] \end{aligned}$$

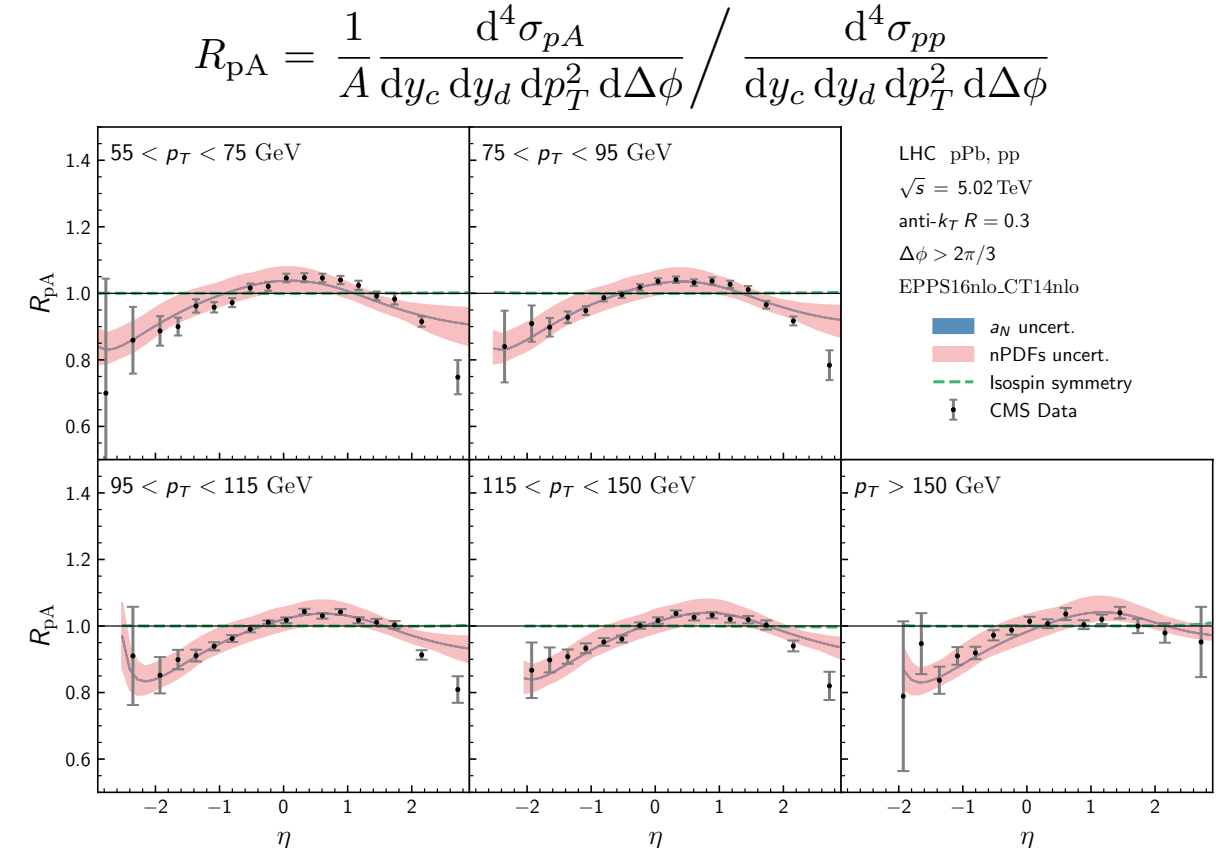
Description of pA data

Strong consistency with the CMS measurements of the azimuthal angle decorrelation in pA and the ratio of the integrated azimuthal angle decorrelation.



Eur. Phys. J. C 74 (2014) 2951

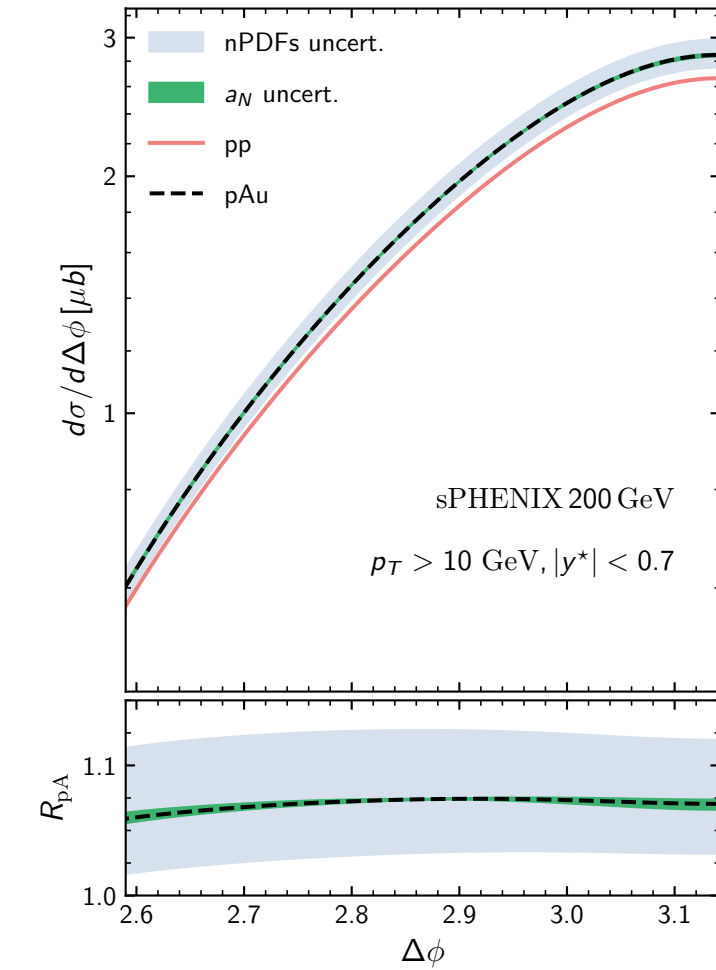
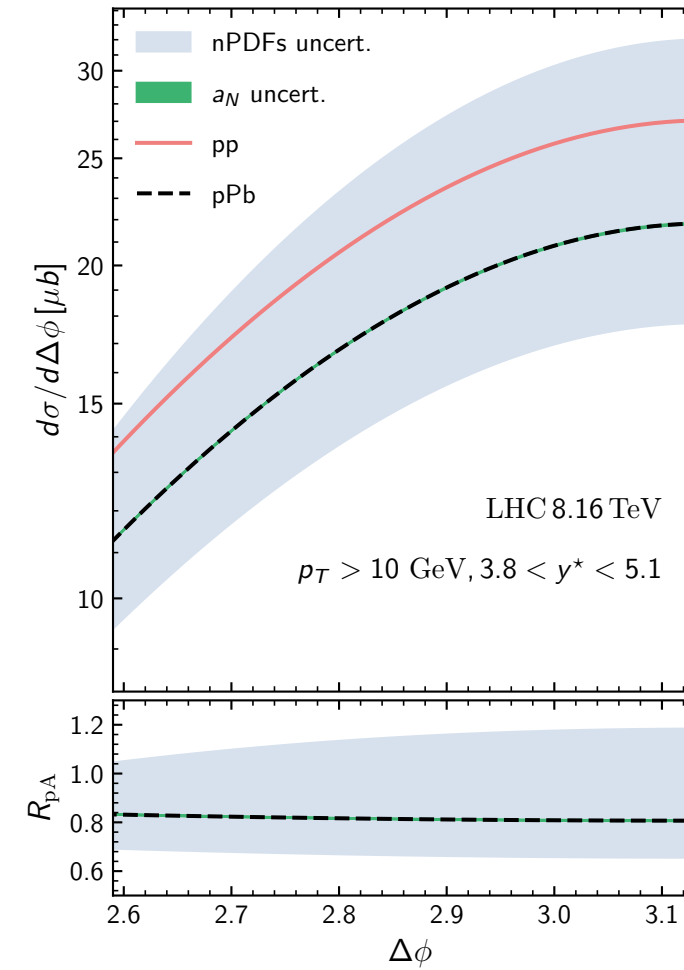
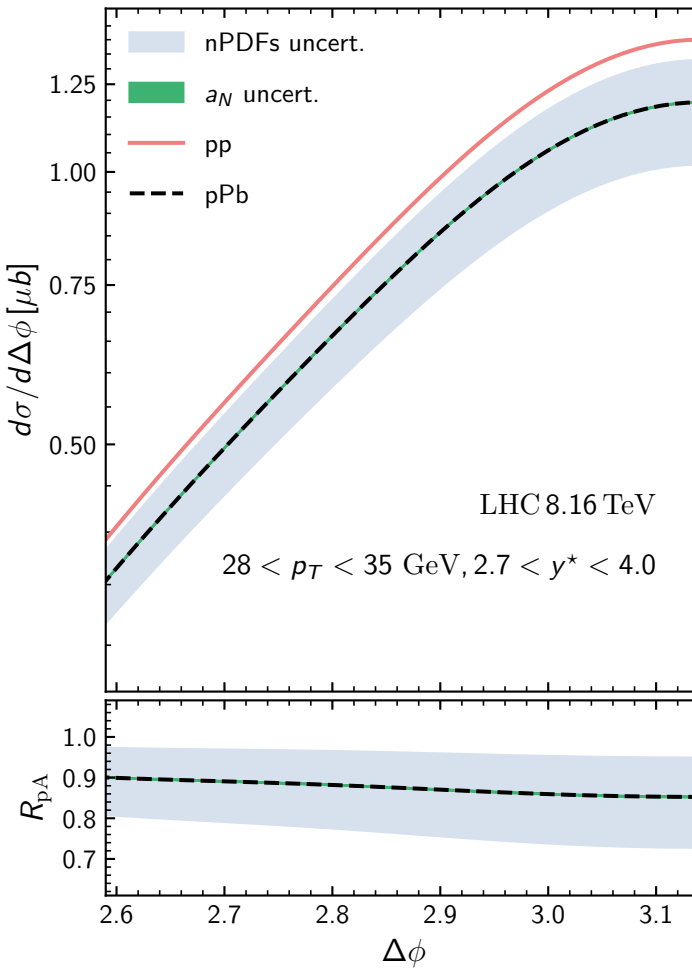
Red band is the uncertainty from the EPPS sets, small blue band from the uncertainty of the nTMDs and is very small for high pT jet production.



Phys. Rev. Lett. 121, 062002 (2018)

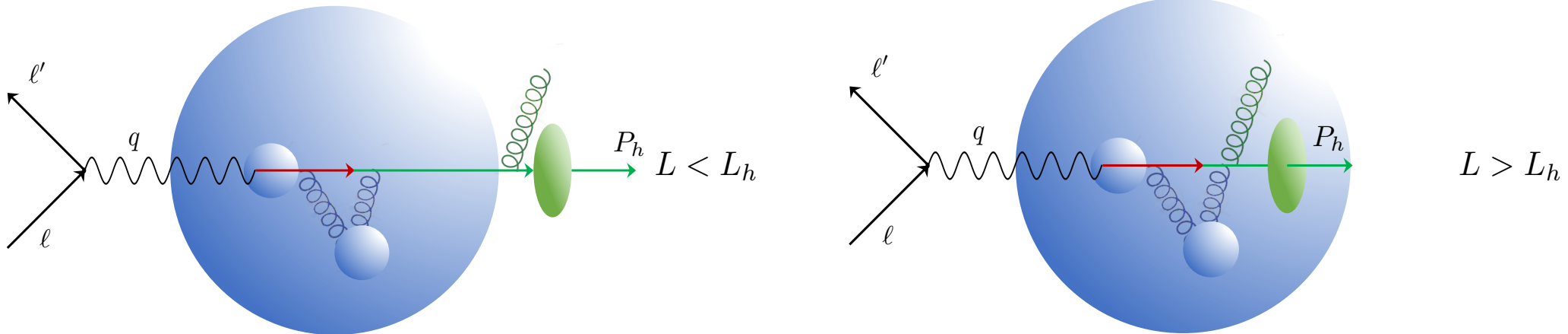
Predictions at ATLAS, ALICE, and sPHENIX

At the LHC, the collinear uncertainties are more dominant due to the large perturbative transverse momenta that are generated. Uncertainty band of the broadening becomes larger at lower center of mass energies



Fragmentation in the medium from first principles

Medium introduces three length scales to the problem $L \sim A^{1/3}/\Lambda_{\text{QCD}}$ $L_h \sim \nu/m_h^2$ λ



Thin medium: NP input only from medium properties

Large medium: requires additional NP input from hadronization
also require input from hadronic collisions

Number of collisions goes like $\chi = L/\lambda$

Dilute limit: Opacity expansion or higher twist $\chi \lesssim 1$

Gyulassy-Levai-Vitev (2000) Guo, Wang (2000)

Dense limit: Opacity expansion or higher twist $\chi \gg 1$

Baier, Dokshitzer, Mueller, Peigné, Schiff (1996) Zakharov (1997)

Can be treated in Glauber SCET

Ovanesyan and Vitev (2011)

$$p_G^\mu \sim Q(\lambda^2, \lambda^2, \lambda)$$

$$A_1^{(0)q} = \begin{array}{c} \text{J} \\ \xrightarrow{x_0} \end{array} \xrightarrow{p}$$

$$A_1^{(2)q} = \begin{array}{c} \text{J} \\ \xrightarrow{x_0} \end{array} \xrightarrow{q_1} \xrightarrow{q_2} \xrightarrow{p}$$

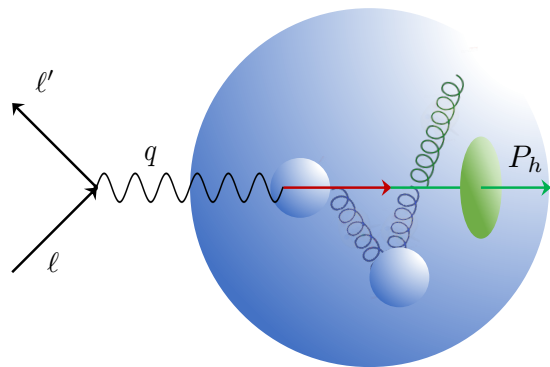
$\otimes_1 \quad \otimes_2$

$$A_1^{(1)q} = \begin{array}{c} \text{J} \\ \xrightarrow{x_0} \end{array} \xrightarrow{q_1} \xrightarrow{p}$$

\otimes_1

Medium modified DGLAP evolution

Previous work has been done in QCD and SCET to derive medium modified evolution equations



$$\frac{\partial \tilde{D}_{h/j}(z; \mu)}{\partial \ln \mu^2} = \frac{\alpha_s(\mu)}{2\pi} \sum_i \left[\tilde{P}_{ij} \otimes \tilde{D}_{h/i} \right] (z; \mu)$$

$$\tilde{P}_{ij}(z; \mu) = \tilde{P}_{ij}(z) + \Delta \tilde{P}_{ij}(z; \mu)$$

$$\begin{aligned} \frac{dN}{dx} \sim & \left| \begin{array}{c} \text{Diagram 1} \\ + \end{array} \right. + \left| \begin{array}{c} \text{Diagram 2} \\ + \end{array} \right. + \left| \begin{array}{c} \text{Diagram 3} \\ \otimes \end{array} \right|^2 \\ & + 2\text{Re} \left[\begin{array}{c} \text{Diagram 4} \\ + \end{array} \right. + \left. \begin{array}{c} \text{Diagram 5} \\ + \end{array} \right] \times \left| \begin{array}{c} \text{Diagram 6} \\ \otimes \end{array} \right| \end{aligned}$$

Ovanesyan, Vitev (2012)

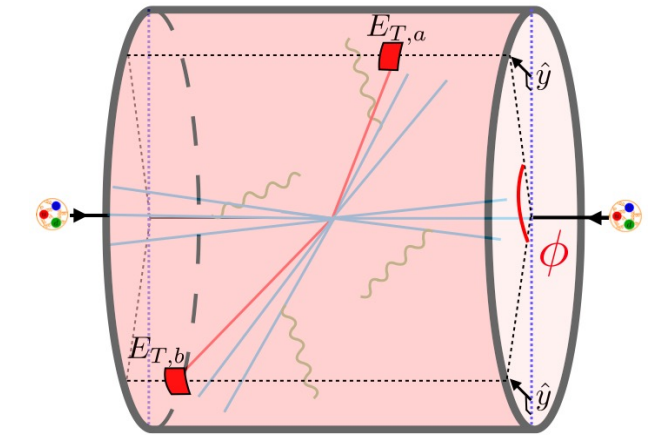
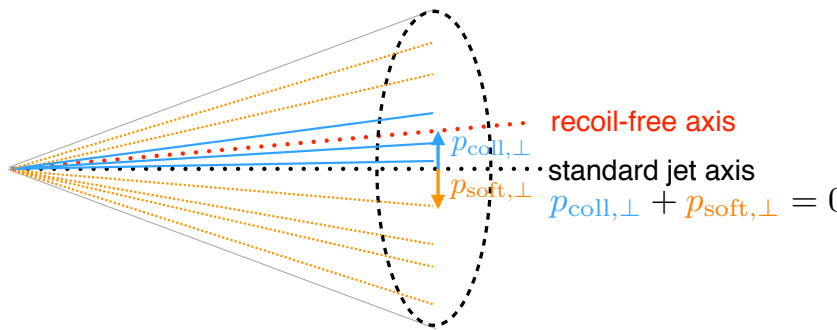
Medium modification can be implemented into the fit, but introduces additional scales. Future work in this community will involve including the medium modified DGLAP into the fit, as well as calculating the medium modifications to the RG and Collins-evolution of the TMDs.

Future work

Graphs for medium modified evolution can be applied to final-state functions for TMD measurements (exclusive jet functions, EECs)

$$\frac{dN}{dx} \sim \left| \begin{array}{c} \text{graph 1} \\ + \text{graph 2} \\ + \text{graph 3} \end{array} \right|^2$$

$$+ 2\text{Re} \left[\begin{array}{c} \text{graph 4} \\ + \text{graph 5} \\ + \text{graph 6} \end{array} \right] \times \text{graph 7}$$

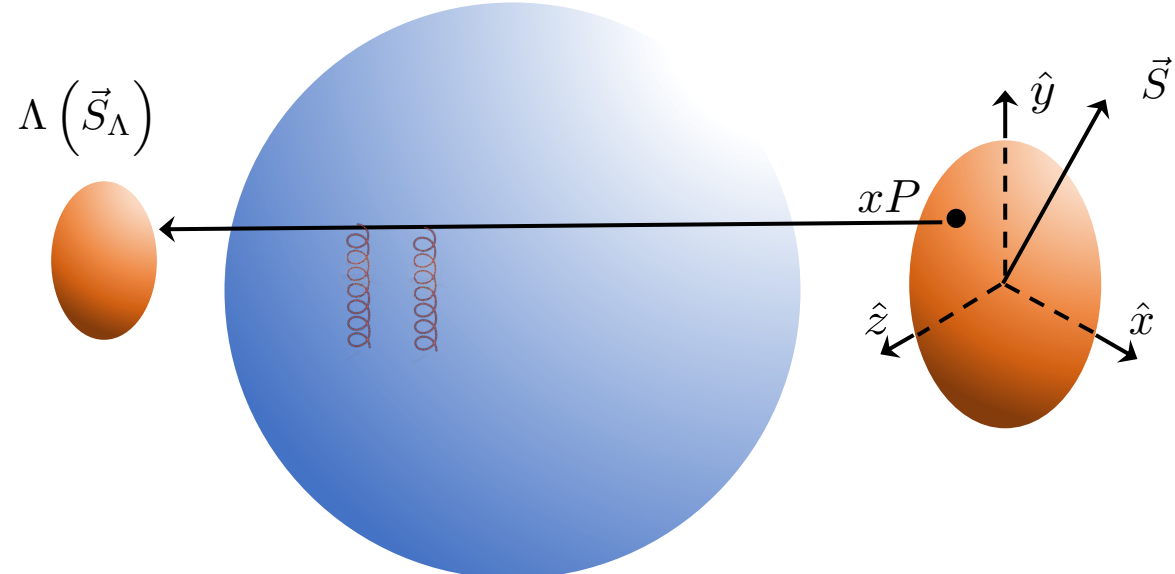


Medium modified DGLAP can be applied in a global analysis

$$\frac{\partial \tilde{D}_{h/j}(z; \mu)}{\partial \ln \mu^2} = \frac{\alpha_s(\mu)}{2\pi} \sum_i \left[\tilde{P}_{ij} \otimes \tilde{D}_{h/i} \right](z; \mu)$$

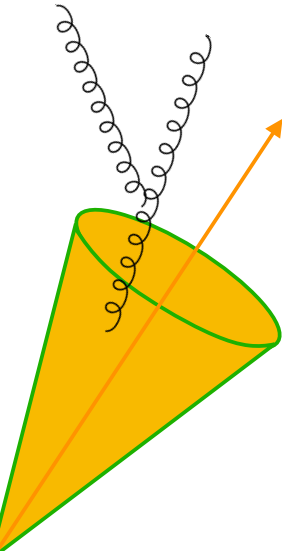
$$\tilde{P}_{ij}(z; \mu) = \tilde{P}_{ij}(z) + \Delta \tilde{P}_{ij}(z; \mu)$$

Medium modified spin physics as a new probe of medium properties



Non-global logs

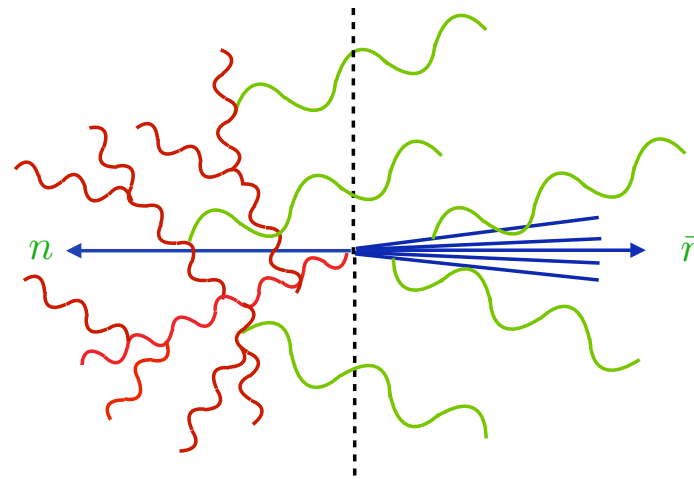
Standard jets complicate resummation



$$-\frac{C_A C_a}{2} \left(\frac{\alpha_s}{\pi} \right)^2 \frac{\pi^2}{24} \ln^2 \left(\frac{P_\perp^2}{\mu_b^2} \right)$$

Dasgupta, Salam (2001)

$$m_H \gg m_L$$



Larkoski, Moult, Neill (2016)

NGLs for jet at NLL is the same as jet mass in e+ e-

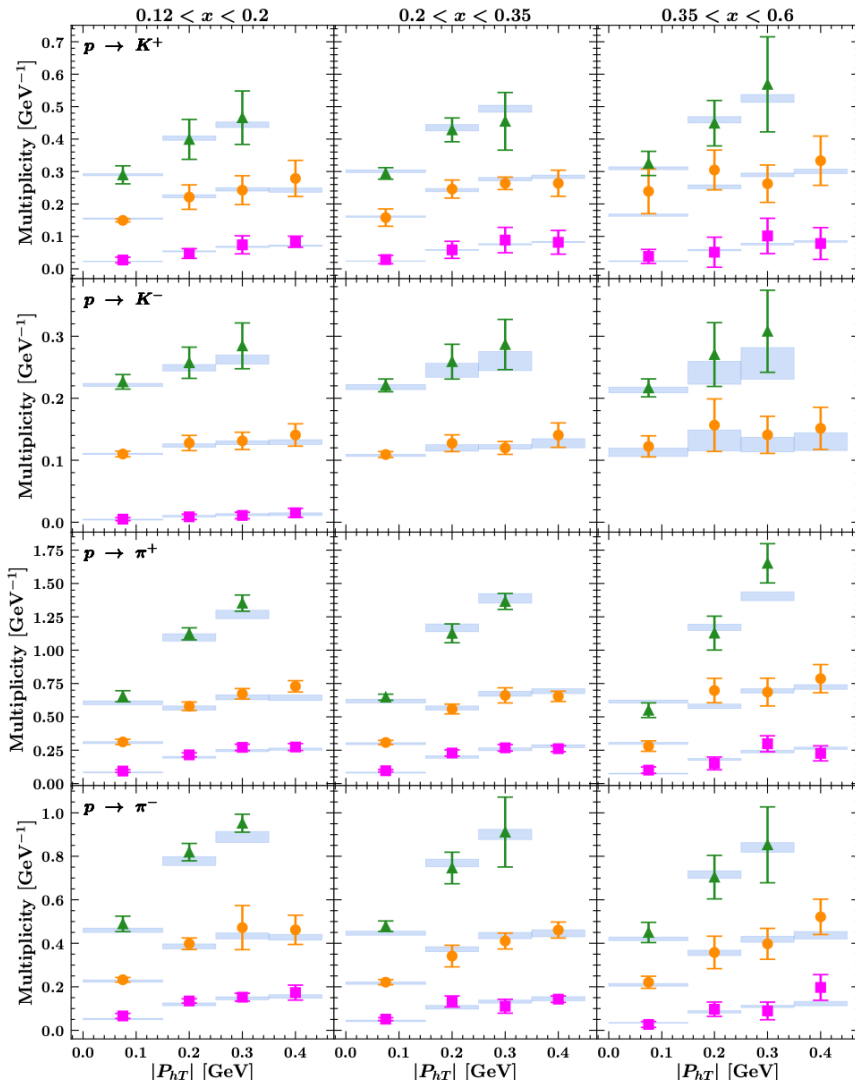
Becher, Neubert, Rothen and Shao (2016)

$$U_{\text{NG}}^k(\mu_{cs}, \mu_j) = \exp \left[-C_A C_k \frac{\pi^2}{3} u^2 \frac{1 + (au)^2}{1 + (bu)^c} \right],$$

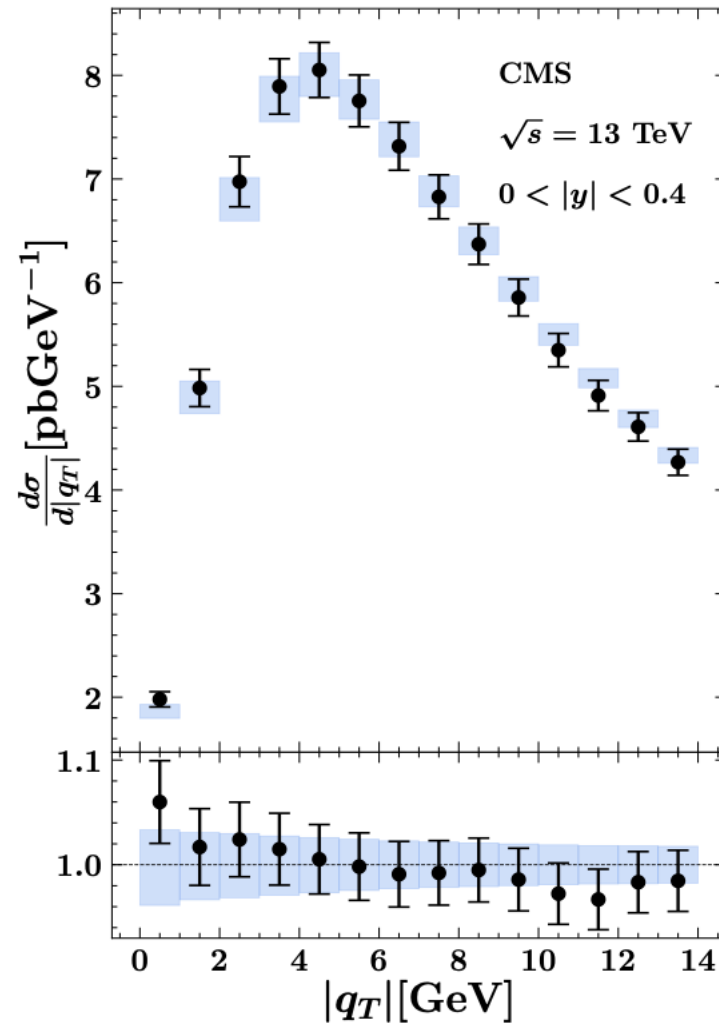
Map Collaboration

Extraction at NNLO+N³LL, SIDIS+DY

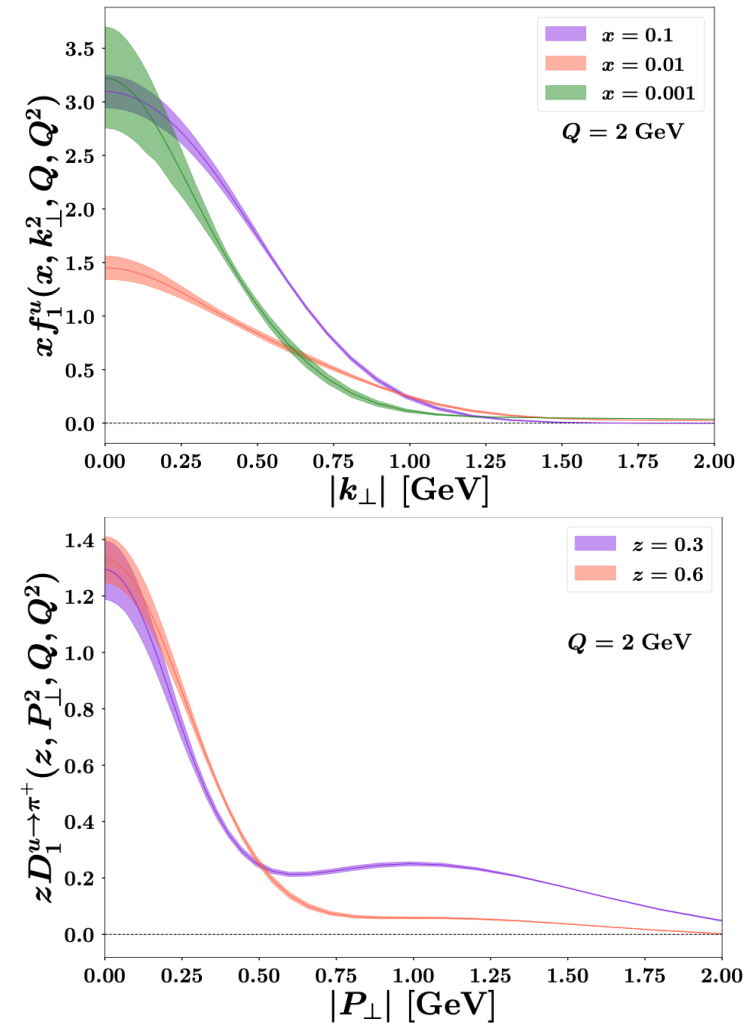
Hermes multiplicity data



CMS q_\perp distribution



TMDs

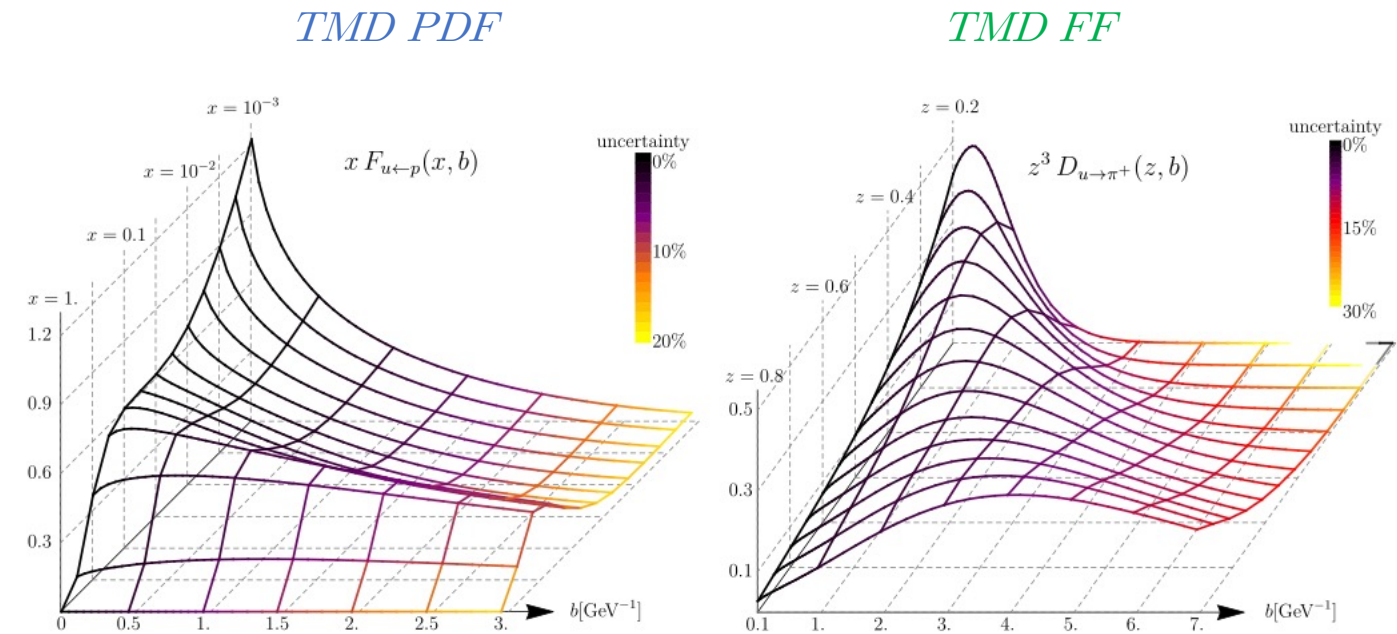
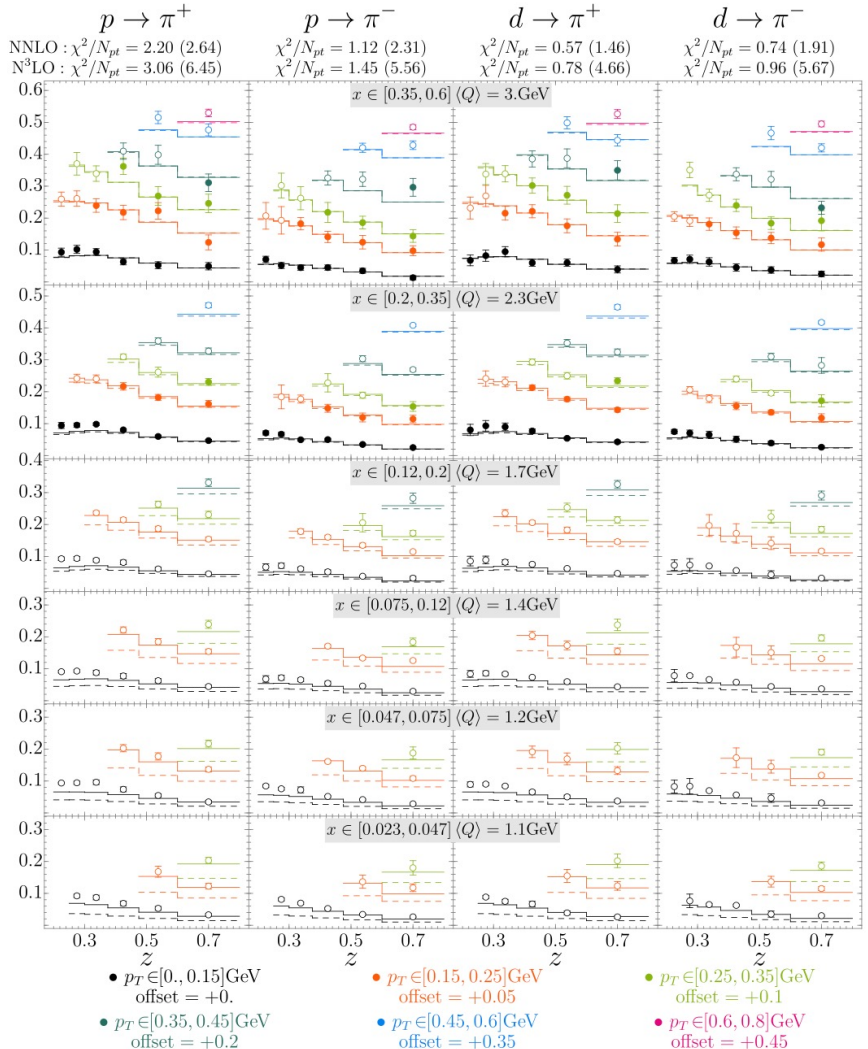


Artemides

Extraction obtained at NNLO+N³LL, SIDIS+DY

$$\Phi_n = 1 - \frac{\sin\left(\frac{\mathbf{Q}_n^2 L^+}{2x(1-x)p_1^+}\right)}{\frac{\mathbf{Q}_n^2 L^+}{2x(1-x)p_1^+}}$$

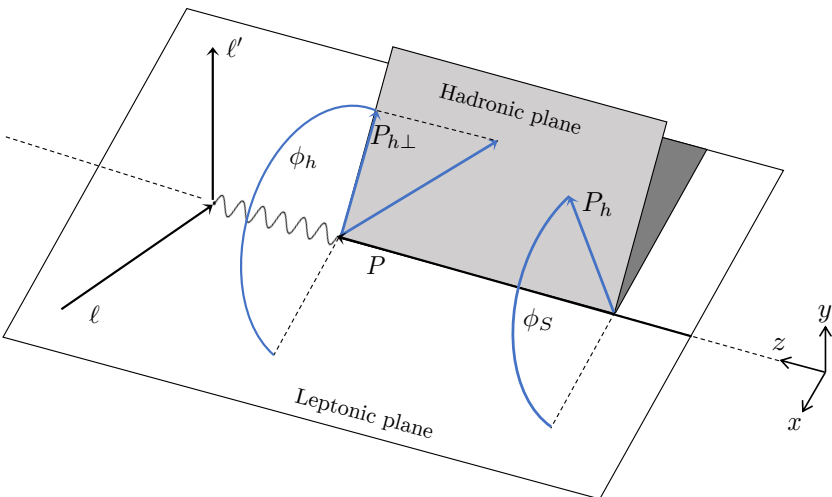
Hermes Multiplicity data



$$b \sim 1/q_T$$

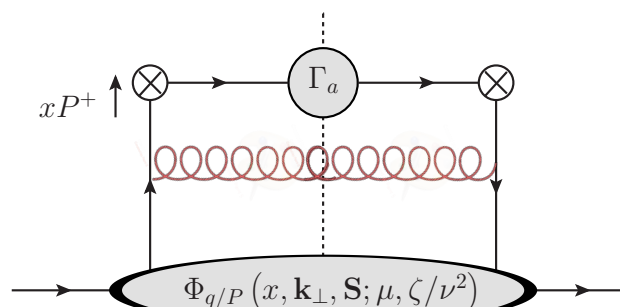
Factorization of physics at different scales

Factorization of the cross section in an OPE



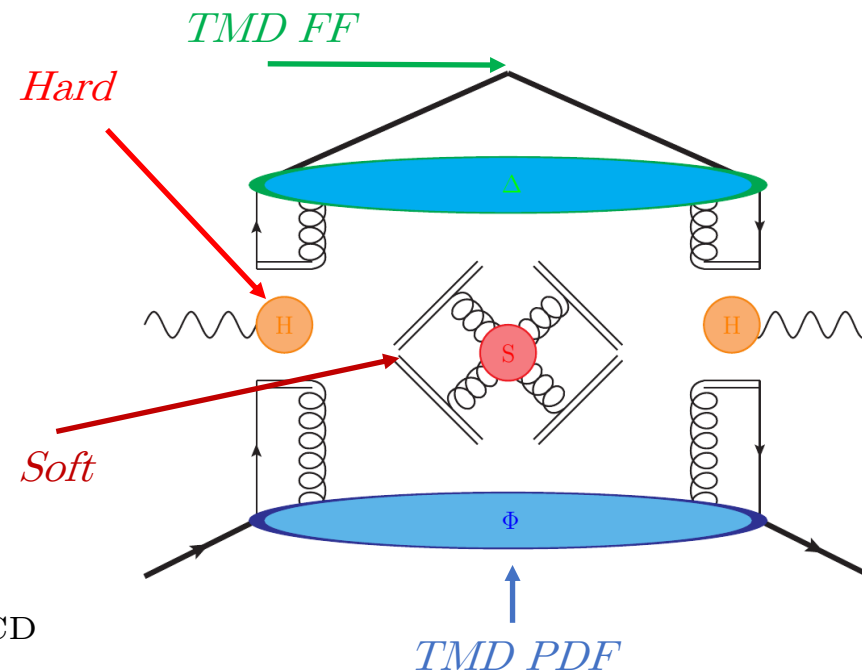
Factorization of IR modes

$$q_T \gtrsim \Lambda_{\text{QCD}}$$



John Terry (Los Alamos National Lab)

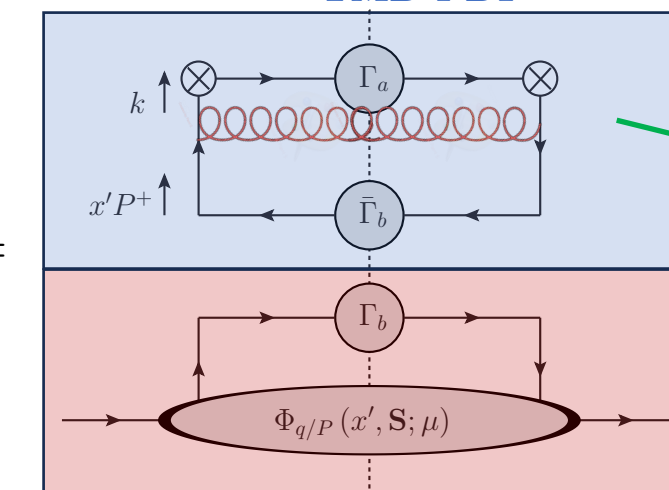
$$Q \gg q_T \gtrsim \Lambda_{\text{QCD}}$$



$$d\sigma \sim \sum_i |C(Q; \mu)| f \otimes D \otimes S(q_T, \mu)$$

Contains fixed order and large logs

$$\ln \left(\frac{Q}{\mu} \right)$$



Matching coefficient contains fixed order and large logs

$$\ln \left(\frac{q_T}{\mu} \right)$$

$$f(x, q_T, \mu) \sim [C \otimes f](x, q_T, \mu)$$

Collinear PDF

Soft-Collinear Effective Theory

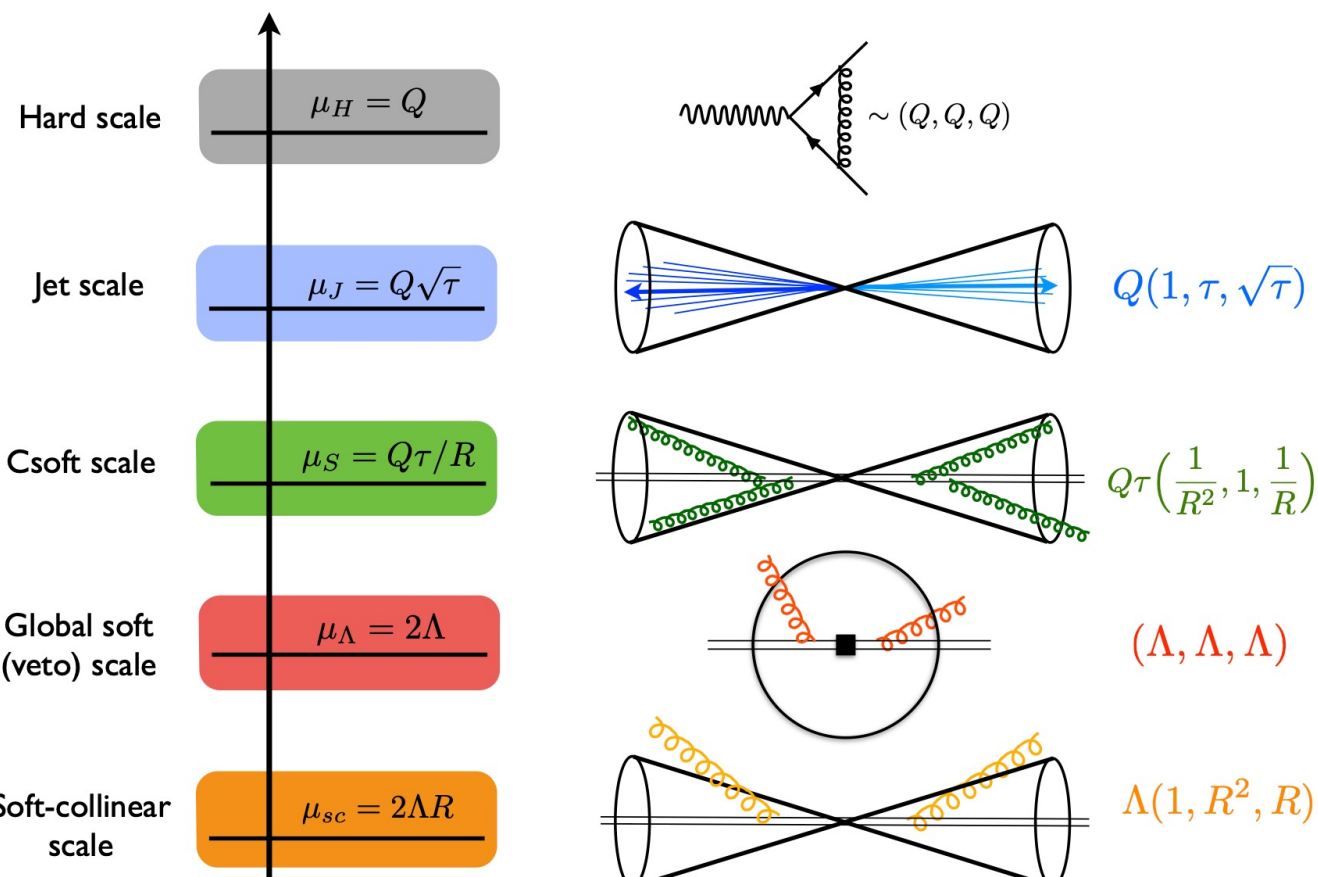
SCET is an EFT which captures soft and collinear emissions along the directions

$$\mathcal{L}_{\text{QCD}} = \sum_q \bar{\psi} i \not{D} \psi - \frac{1}{4} G_{\mu\nu}^A G^{A\mu\nu} + \mathcal{L}_{\text{gauge-fix}} + \mathcal{L}_{\text{ghost}}$$

$$\psi \rightarrow \psi_s + \psi_c \quad A^\mu \rightarrow A_s^\mu + A_c^\mu$$

$$\mathcal{L}_{\text{SCET}} = \bar{\psi}_s i \not{D}_s \psi_s - \frac{1}{4} G_{\mu\nu s}^A G_s^{A\mu\nu}$$

$$+ \xi \frac{\not{n}}{2} \left[i n \cdot D + i \not{D}_{c\perp} \frac{1}{i \bar{n} \cdot D_c} i \not{D}_{c\perp} \right] \xi - \frac{1}{4} G_{\mu\nu c}^A G_c^{A\mu\nu}$$



Bauer, Fleming, Luke 2000

Bauer, Fleming, Pirjol, Stewart 2001

Bauer, Stewart 2001

Bauer, Pirjol, Stewart 2002

Beneke, Chapovsky, Diehl, Feldmann 2002

Beneke, Feldmann 2003

Hill, Neubert 2003

Echevarria, Idilbi, Scimemi 2011

Back-to-back lepton-jet production

Process proposed by: [Liu, Ringer, Vogelsang, Yuan \(2019\)](#)

Less sensitive to non-perturbative physics

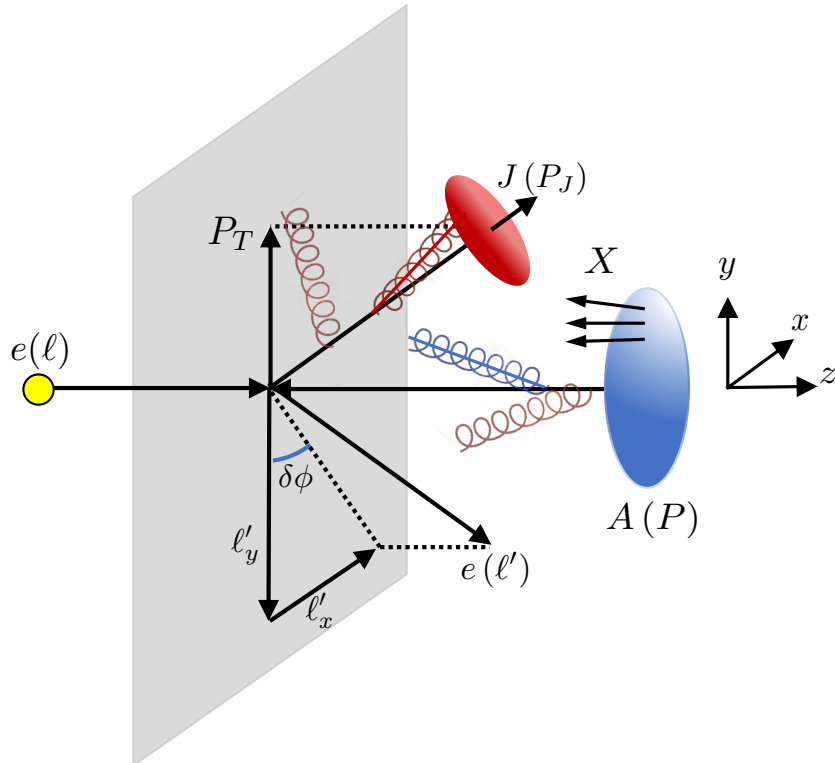
Lepton-jet transverse momentum imbalance

$$\vec{q}_T = \vec{P}_{JT} + \vec{\ell}_T$$

TMD region

$$\frac{|\vec{q}_T|}{|\vec{P}_{JT}|} \ll 1$$

Better than SIDIS in that there is no sensitivity to FFs
Worse due to the perturbative accuracy



Novel factorization using recoil-free jets

Hard: $P_{JT} (1, 1, 1)$

Collinear: $P_{JT} (\lambda^2, 1, \lambda)$

Jet: $P_{JT} (1, \lambda^2, \lambda)$

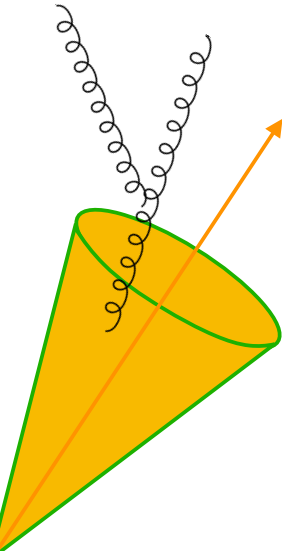
Global soft: $P_{JT} (\lambda, \lambda, \lambda)$

$$\frac{d\sigma_p}{d^2\ell'_T dy d\delta\phi} = \frac{\sigma_0 \ell'_T}{1-y} H(Q, \mu_H) \int \frac{db}{2\pi} \cos(b\ell'_T \delta\phi) \sum_q e_q^2 f_{q/p}(x_B, b, \mu_H, \zeta_B) \mathcal{J}_q(b, \mu_H, \zeta_J)$$

$$\frac{d\sigma_A}{d^2\ell'_T dy d\delta\phi} = \frac{\sigma_0 \ell'_T}{1-y} H(Q, \mu_H) \int \frac{db}{2\pi} \cos(b\ell'_T \delta\phi) \sum_q e_q^2 f_{q/A}(x_B, b, \mu_H, \zeta_B) \mathcal{J}_q^A(b, \mu_H, \zeta_J)$$

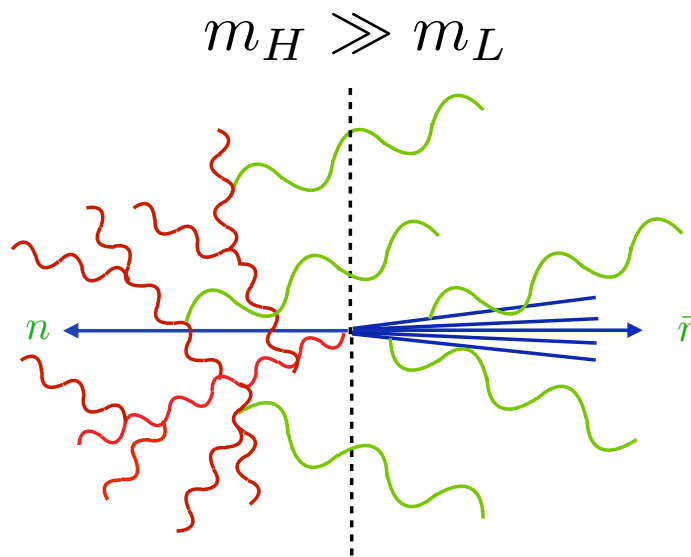
Non-global logs

Standard jets complicate resummation



$$-\frac{C_A C_a}{2} \left(\frac{\alpha_s}{\pi} \right)^2 \frac{\pi^2}{24} \ln^2 \left(\frac{P_\perp^2}{\mu_b^2} \right)$$

Dasgupta, Salam (2001)



Larkoski, Moult, Neill (2016)

$$m_H \gg m_L$$

NGLs for jet at NLL is the same as jet mass in e+ e-

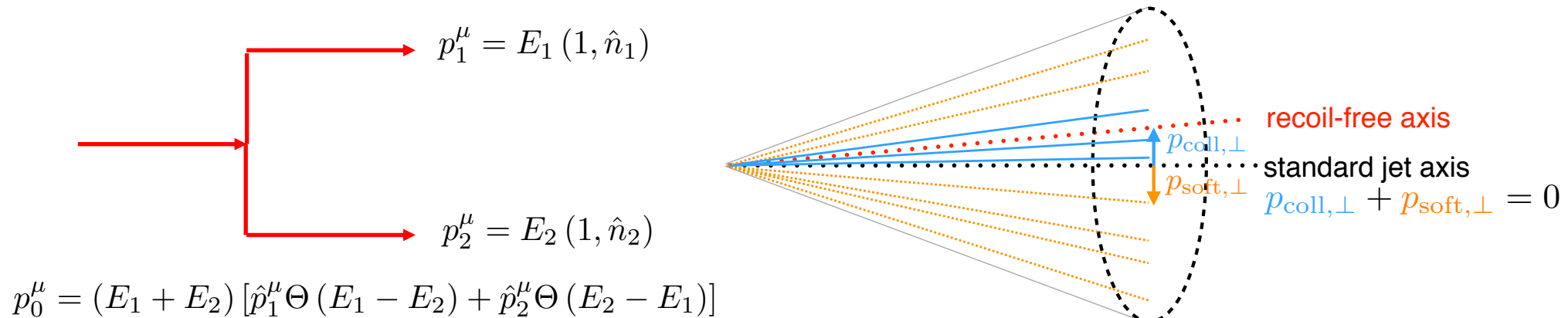
Becher, Neubert, Rothen and Shao (2016)

$$U_{\text{NG}}^k(\mu_{cs}, \mu_j) = \exp \left[-C_A C_k \frac{\pi^2}{3} u^2 \frac{1 + (au)^2}{1 + (bu)^c} \right],$$

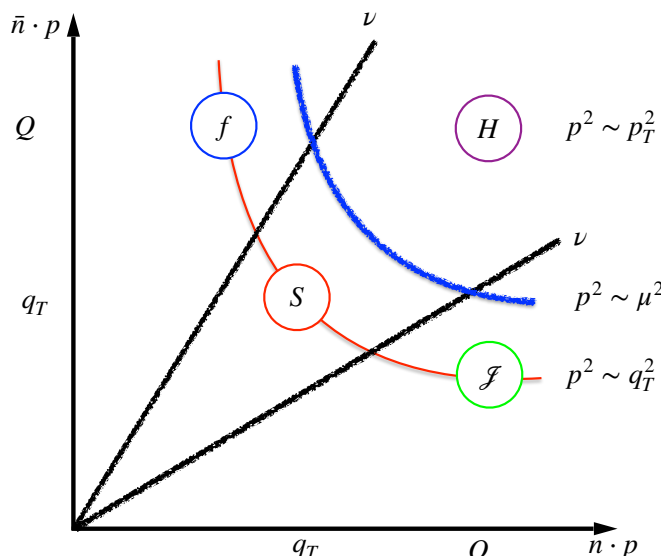
Winner take all jet axis

Direction of recoil-free jet is insensitive to all soft emissions, jet points in direction of most energetic hadron. Thus no NGLS

Larkoski, Neill, and Thaler (2014)



Direction of jet and total jet momentum have a transverse momentum relative to one another, contains rapidity divergence



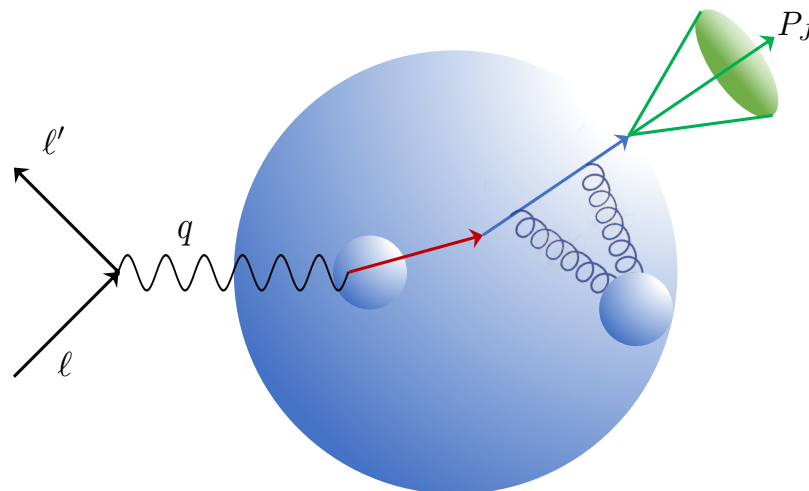
$$\begin{aligned} \mu \frac{d}{d\mu} \ln \mathcal{J}(Q, \mu, \nu) &= \gamma_{J\mu}^q(Q, \mu, \nu) & \gamma_{J\mu}^q(Q, \mu, \nu) &= \gamma_{D\mu}^q(Q, \mu, \nu) \\ \nu \frac{d}{d\nu} \ln \mathcal{J}(Q, \mu, \nu) &= \gamma_{J\nu}^q(Q, \mu, \nu) & \gamma_{J\nu}^q(Q, \mu, \nu) &= \gamma_{D\nu}^q(Q, \mu, \nu) \end{aligned}$$

$$\mathcal{J}_q(b, \mu, \zeta_J/\nu^2) = 1 + \frac{\alpha_s C_F}{4\pi} \left[3L + 2L \ln \left(\frac{\nu^2}{\zeta_J} \right) + 7 - \frac{2\pi^2}{3} - 6 \ln 2 \right] + \mathcal{O}(\alpha_s^2)$$

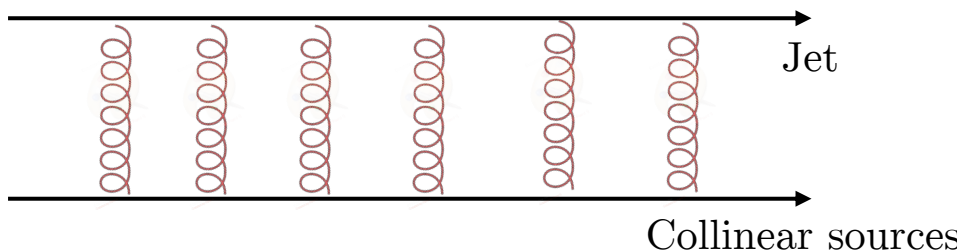
Treatment of medium modifications to the jet

We want to take the jets to be energetic so that

$$L/L_h \sim \frac{A^{1/3} \Lambda_{\text{QCD}}}{\nu} \ll 1$$



We consider an infinite chain of Glauber gluons



Modification to the jet

$$\mathcal{J}_q^A(b, \mu, \nu) = \frac{d\sigma_{n \rightarrow \infty}}{db} \mathcal{J}_q(b, \mu, \nu)$$

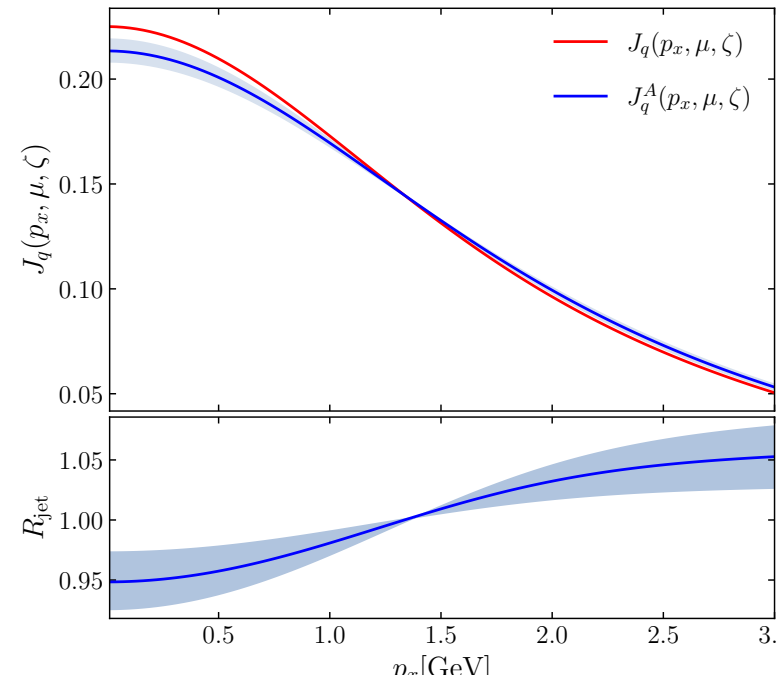
Single gluon exchange

$$\frac{d\sigma}{d^2 q_T} = \frac{\alpha_s C_F}{\pi} \frac{1}{(q_T^2 + m^2)^2}$$

Infinite number of gluon exchanges

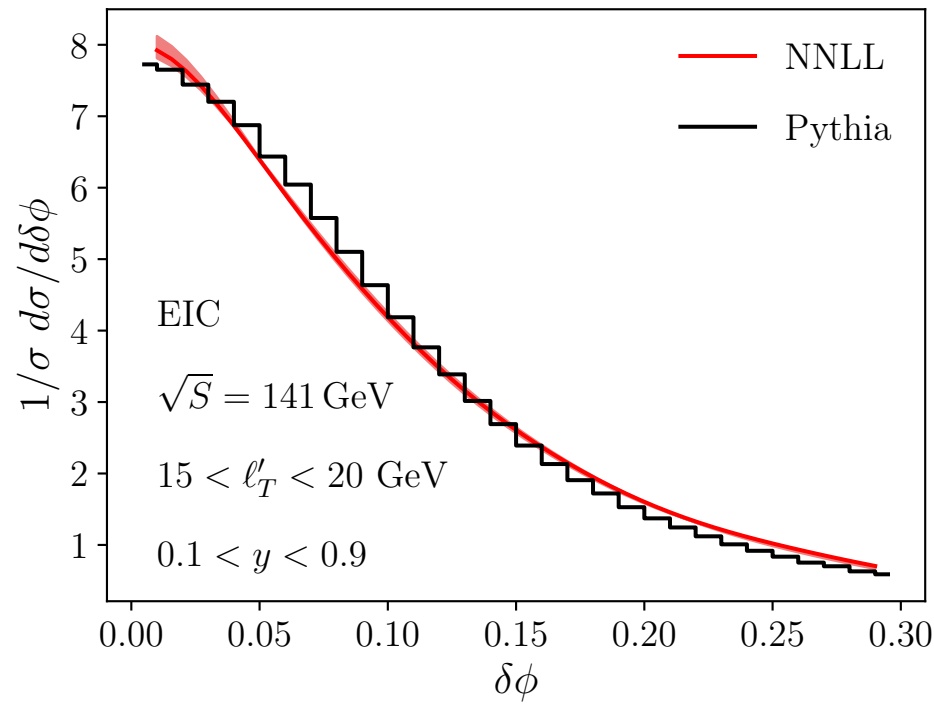
$$\frac{d\sigma_{n \rightarrow \infty}}{db} = \exp \left(\frac{\rho_G L}{m^2} \alpha_s C_F (mb K_1(mb) - 1) \right)$$

Modified jet function under this approximation

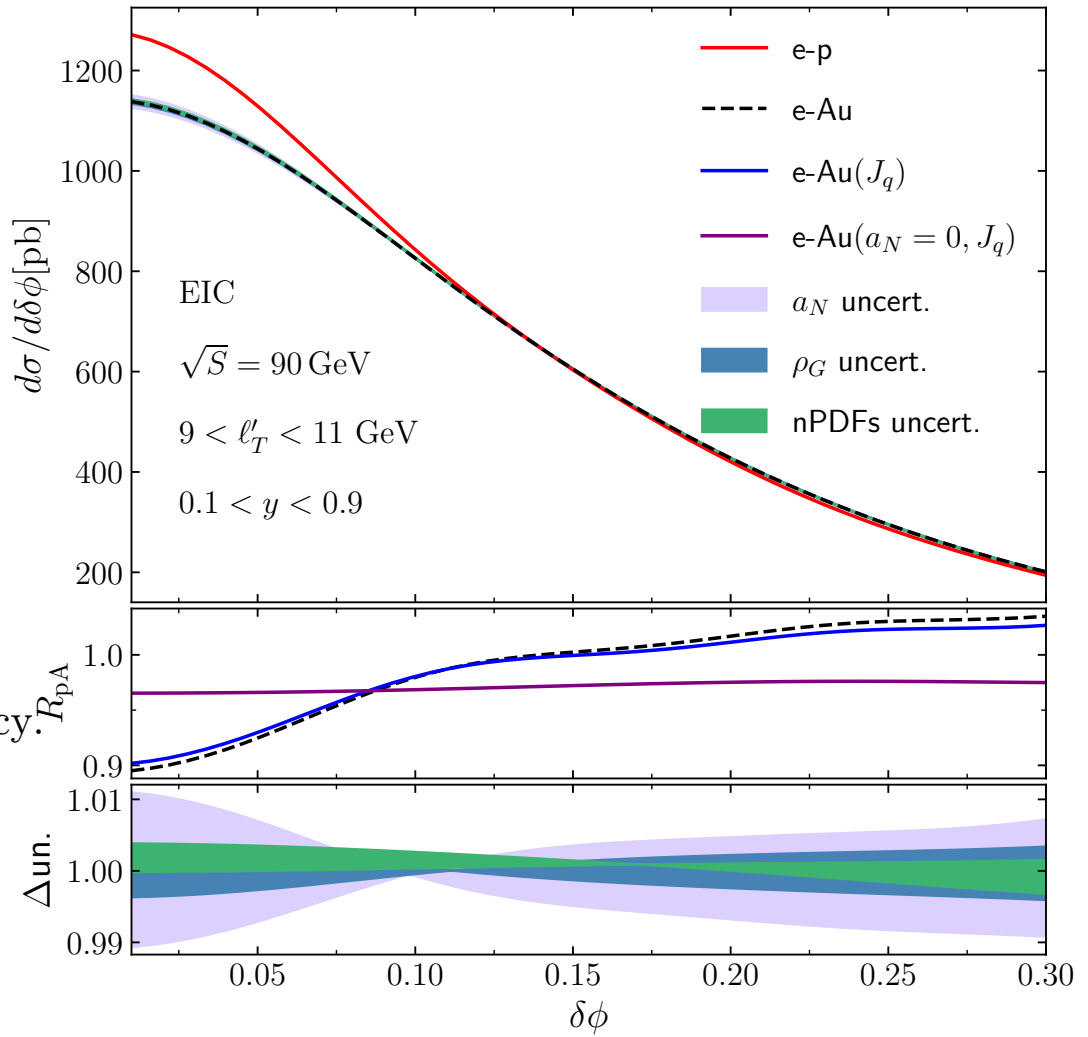


Predictions at the EIC

Comparison of our results with Pythia at NNLL

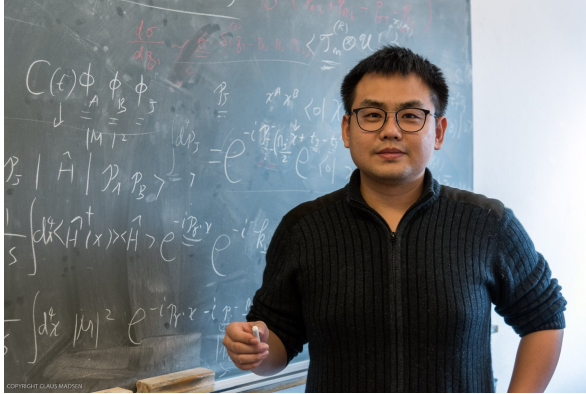


Perturbative ingredients are known to have N3LL accuracy.
Only missing the 3-loop jet function and the 5-loop
cusp anomalous dimension to reach N4LL

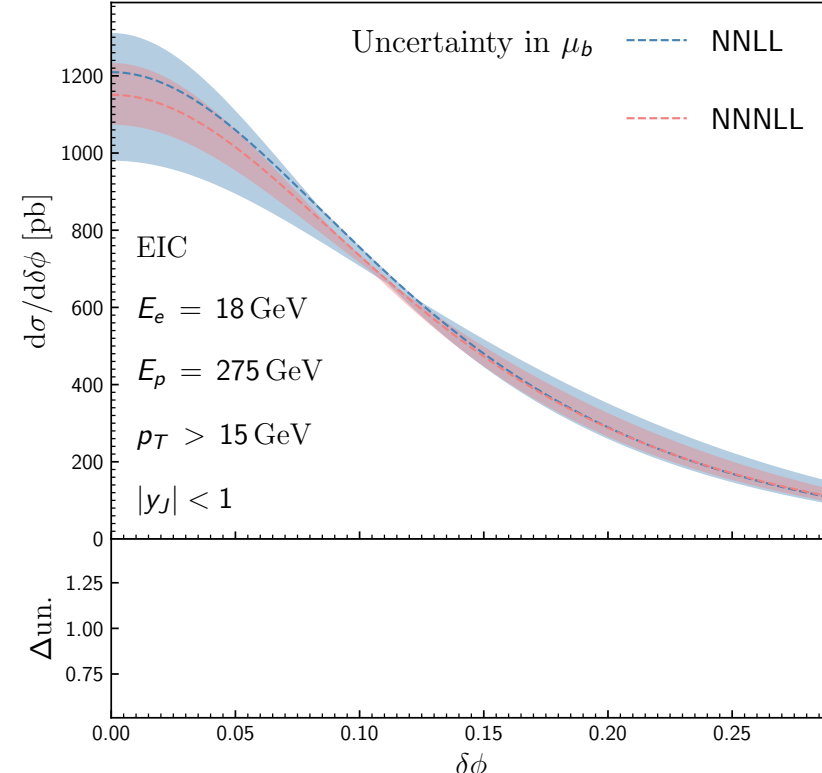


Higher order results

Results have been taken one step higher by *Fang, Gao, Li, Shao (2024)*

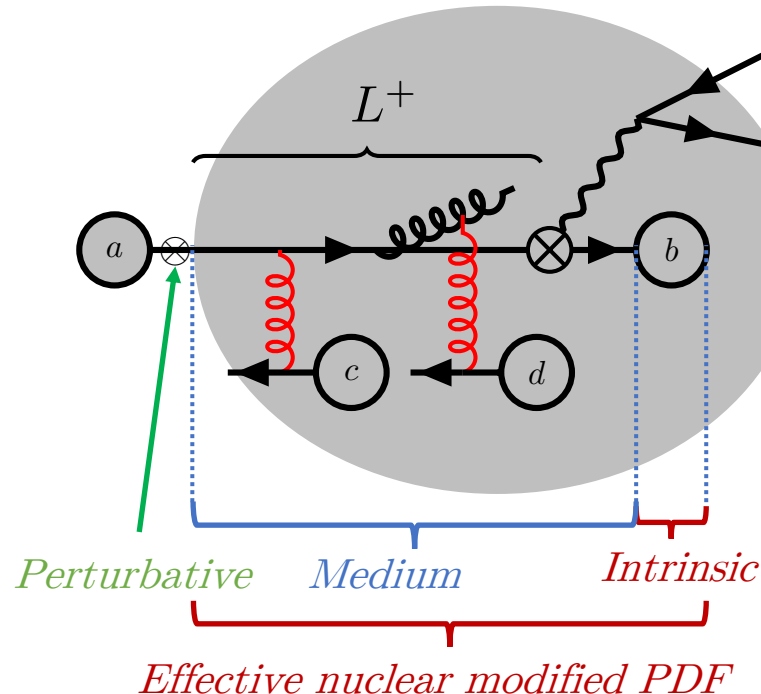


$$\begin{aligned}
 J_q(b, \mu, \zeta) = & 1 + \frac{\alpha_s C_F}{4\pi} \left[-L_b^2 + L_b(3 + 2L_\zeta) - \frac{5\pi^2}{6} + 7 - 6\ln 2 \right] \\
 & + \left(\frac{\alpha_s}{4\pi} \right)^2 \left\{ C_F^2 \left[\frac{L_b^4}{2} - L_b^3(3 + 2L_\zeta) + L_b^2 \left(2L_\zeta^2 + 6L_\zeta - \frac{5}{2} + 6\ln 2 + \frac{5\pi^2}{6} \right) \right. \right. \\
 & + L_b \left(L_\zeta \left(14 - 12\ln 2 - \frac{5\pi^2}{3} \right) + \frac{45}{2} - 18\ln 2 - \frac{9\pi^2}{2} + 24\zeta_3 \right) \left. \right] \\
 & + C_F C_A \left[-\frac{22}{9} L_b^3 + L_b^2 \left(\frac{11}{3} L_\zeta - \frac{35}{18} + \frac{\pi^2}{3} \right) + L_\zeta \left(\frac{404}{27} - 14\zeta_3 \right) \right. \\
 & + L_b \left(L_\zeta \left(\frac{134}{9} - \frac{2\pi^2}{3} \right) + \frac{57}{2} - 22\ln 2 - \frac{11\pi^2}{9} - 12\zeta_3 \right) \left. \right] \\
 & + C_F T_F n_f \left[\frac{8}{9} L_b^3 + L_b^2 \left(\frac{2}{9} - \frac{4}{3} L_\zeta \right) + L_b \left(-\frac{40}{9} L_\zeta - 10 + 8\ln 2 + \frac{4\pi^2}{9} \right) \right. \\
 & \left. \left. - \frac{112}{27} L_\zeta \right] + j_2 \right\}, \quad \text{Constant that was obtained numerically}
 \end{aligned}$$

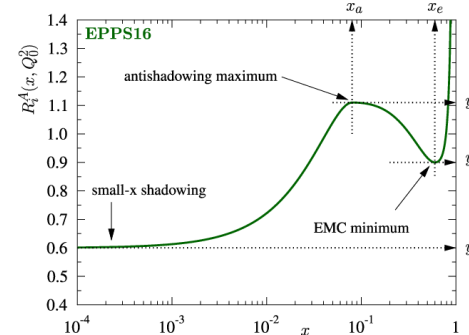


The structure of matter in the medium: an efficient approximation

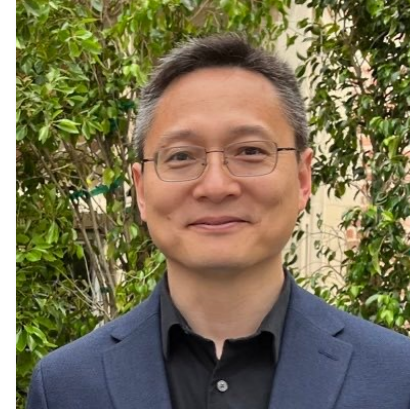
nTMDs were originally defined using an approximate scheme by these two



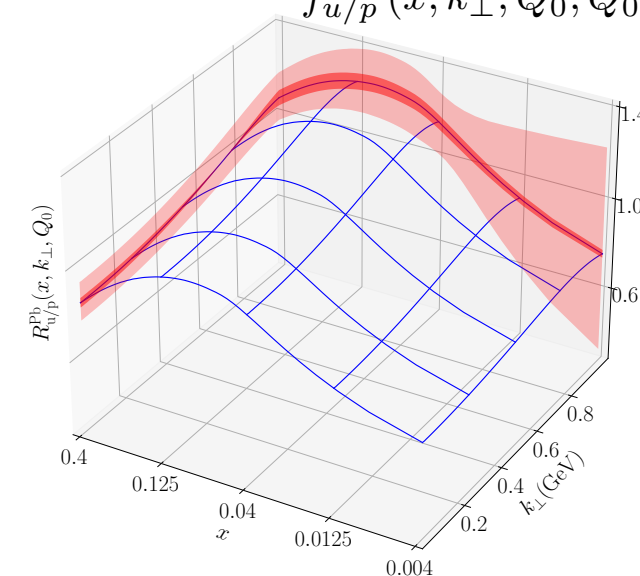
$$R_i^A(x, Q_0^2) = \frac{f_{i/p}^A(x, Q_0^2)}{f_{i/p}(x, Q_0^2)}$$



Alrashed, Kang, JT, Xing et al (2022)
Alrashed, Kang, JT, Xing et al (2023)



$$R_{u/p}^{\text{Pb}}(x, k_\perp, Q_0) = \frac{f_{u/p}^{\text{Pb}}(x, k_\perp, Q_0, Q_0^2)}{f_{u/p}(x, k_\perp, Q_0, Q_0, Q_0^2)}$$



Power counting

Power counting the observable requires examining several scales

$$\tau_f = \frac{1}{p^-} = \frac{x(1-x)p^+}{\mathbf{p}^2}$$

$$e^{iL^+/\tau_f}$$

$$\tau_f \ll L^+$$

LPM phase rapidly oscillates

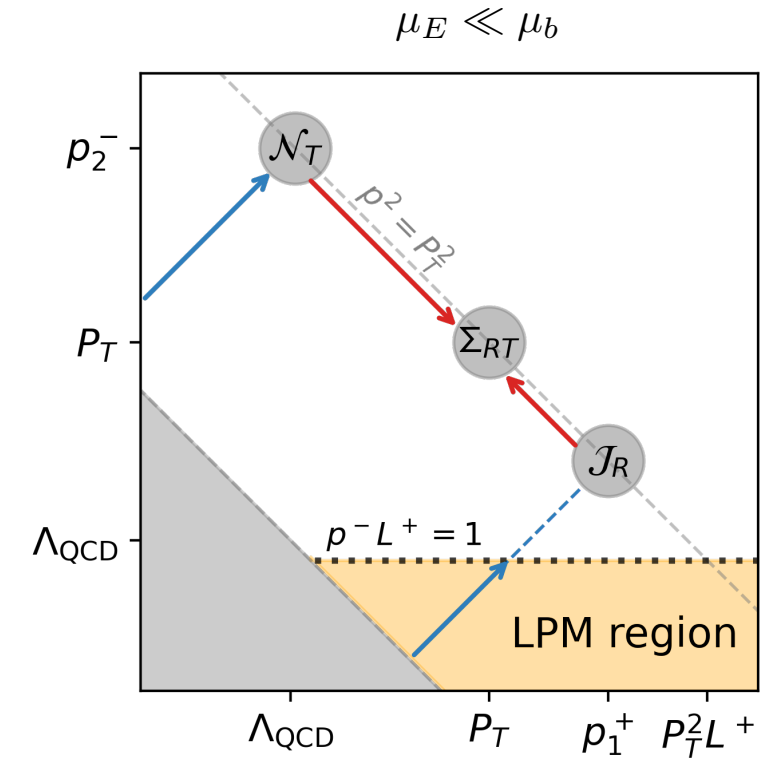
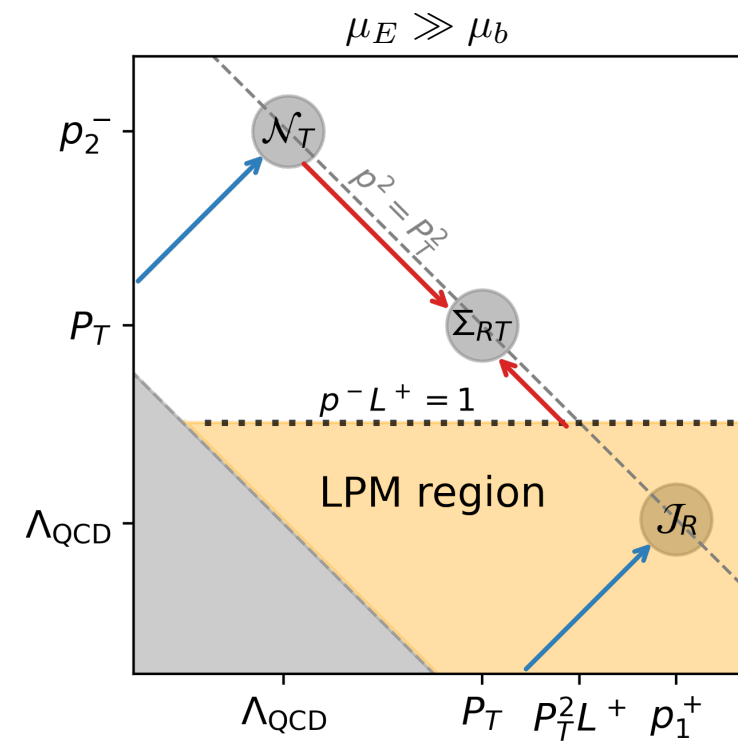
$$\tau_f \gg L^+$$

LPM phase contributes

Power counting the observable requires examining several scales. Collinear logs are different in these cases

$$\Lambda_{\text{QCD}}^2 \ll \mu_E^2 \ll Q^2$$

$$\mu_E^2 = p_1^+ / L^+$$

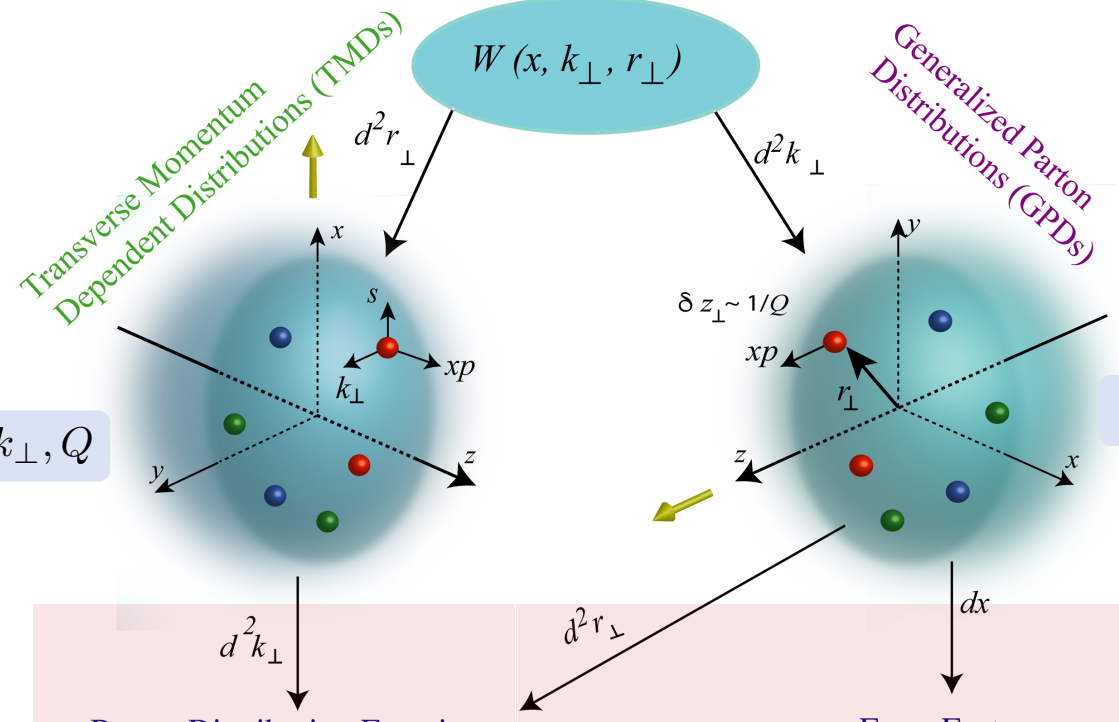


The structure of matter: Nuclear matter

Distributions of partons in hadrons

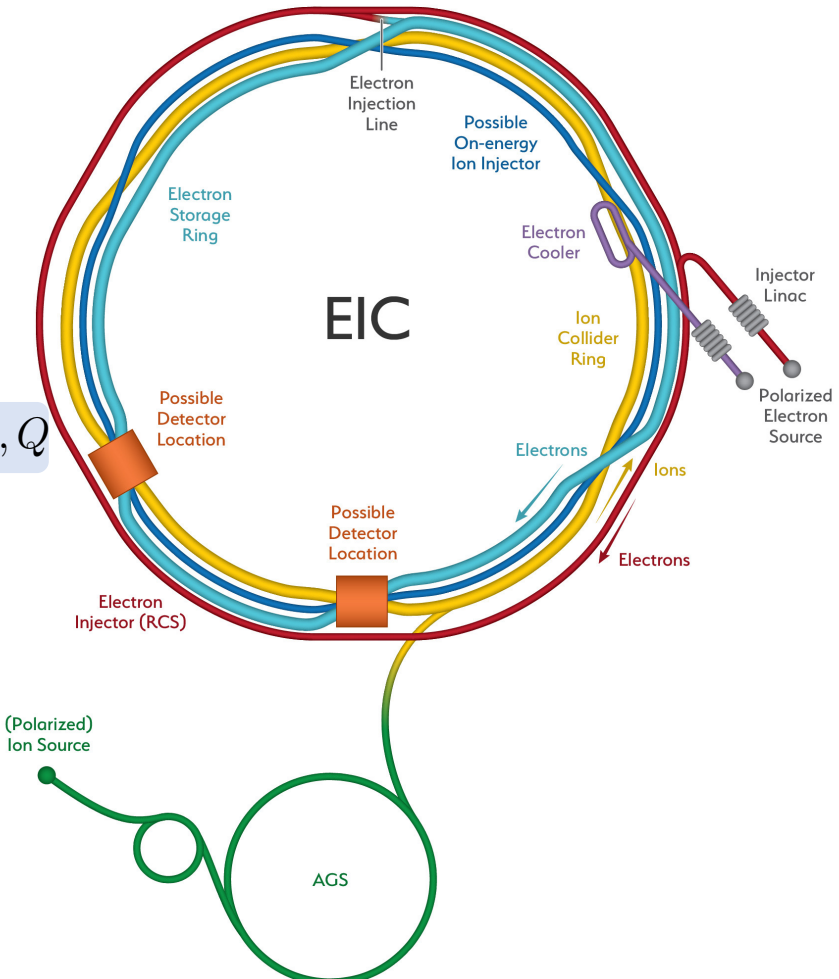
Wigner Distributions

$\Lambda_{\text{QCD}}, k_\perp, 1/r_\perp, Q$



The reach of EFTs

Highly differential distributions require high luminosity

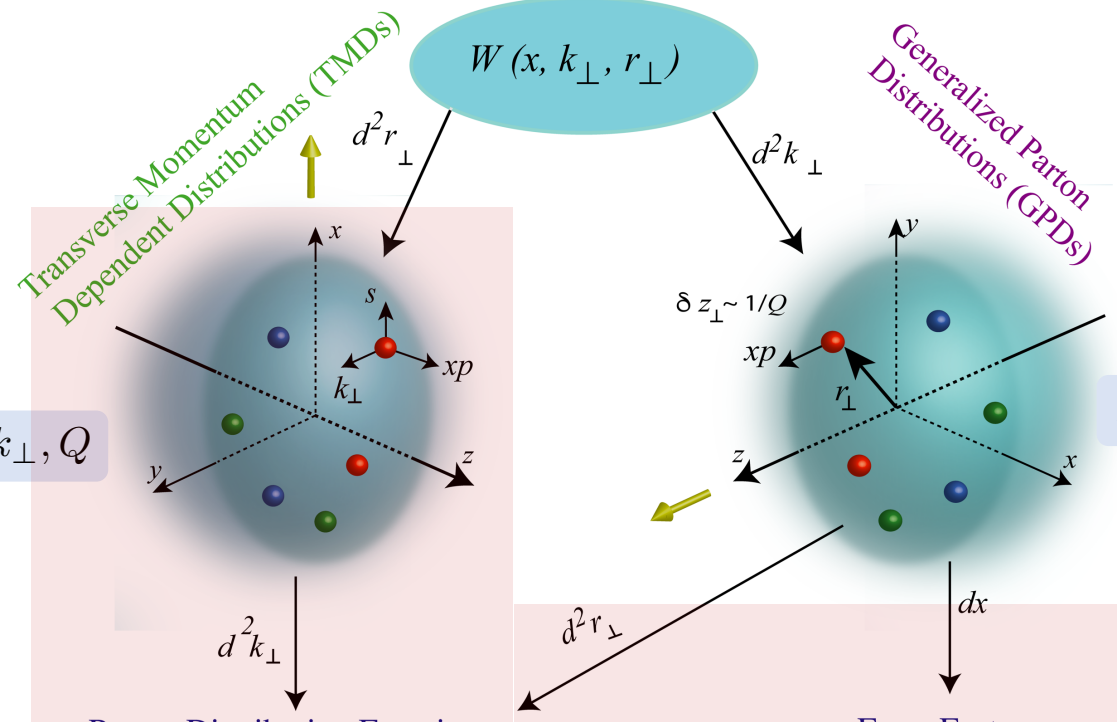


The structure of matter in the vacuum

Distributions of partons in hadrons

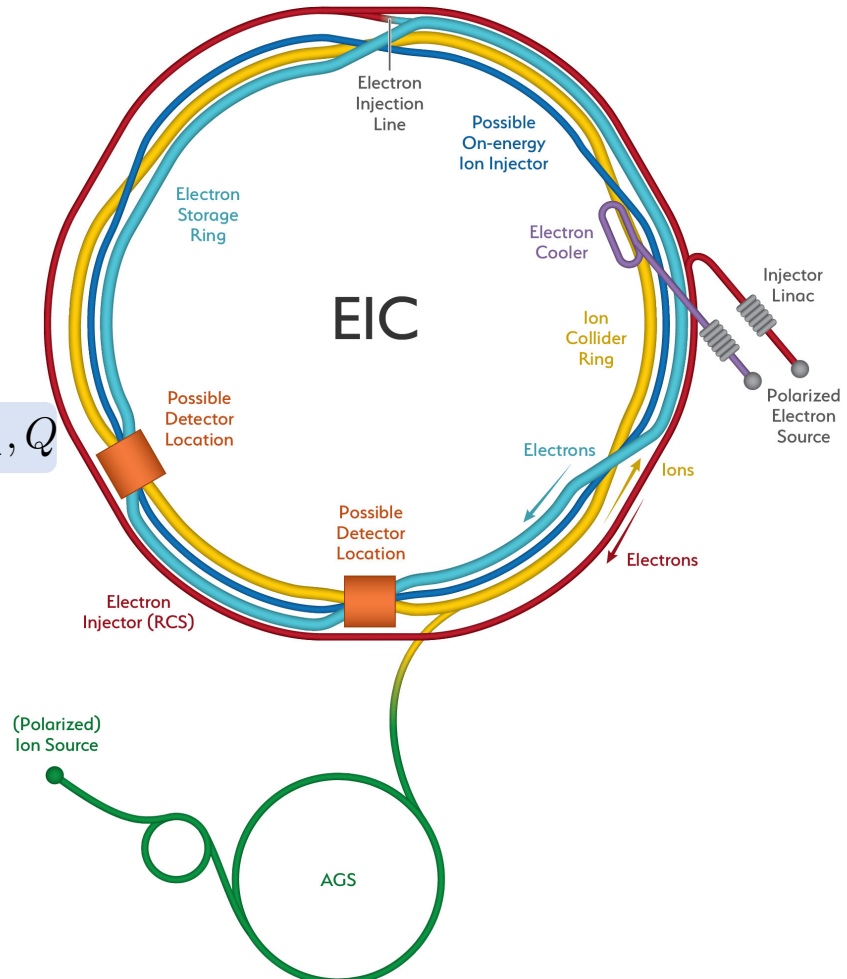
Wigner Distributions

$\Lambda_{\text{QCD}}, k_\perp, 1/r_\perp, Q$



The reach of EFTs

Highly differential distributions require high luminosity



Medium induced collinear divergences

The one-loop computation yields a medium-induced collinear divergence

$$\sum_{T,j} x f_{q/p}(x) \otimes \mathcal{J}_{q/q,F}^{(1),\text{coll}} \otimes_{\perp} \Sigma_{FT}^{(0)} \otimes_{\perp} \mathcal{N}_{j,T}^{(0)} \otimes f_{j/N} \rho_0^- L^+ \quad \text{Medium-induced collinear divergence}$$

$$= \frac{\alpha_s^2(\mu^2) \rho_G^- L^+}{8\mu_E^2} B(w) \left(\frac{1}{2\epsilon} + \ln \frac{\mu^2}{\gamma(w)\mu_E^2} \right) 2C_F \left(\frac{2C_A + C_F}{x} - 2C_A \frac{d}{dx} \right) [xf_{q/a}(x)]$$

Collinear divergences give rise to a medium modified DGLAP evolution equation

Flavor non-singlet ($q - \bar{q}$)

Flavor singlet ($q + \bar{q}, g$)

$$\frac{\partial F_{q-\bar{q}}}{\partial t_\mu} = \left(4C_F C_A \frac{\partial}{\partial x} - \frac{4C_F C_A + 2C_F^2}{x} \right) F_{q-\bar{q}}$$

$$\frac{\partial F_{q+\bar{q}}}{\partial t_\mu} = \left(4C_F C_A \frac{\partial}{\partial x} - \frac{4C_F C_A + 2C_F^2}{x} \right) F_{q+\bar{q}} + C_F \frac{F_g}{x}$$

$$\frac{\partial F_g}{\partial t_\mu} = \left(4C_A^2 \frac{\partial}{\partial x} - \frac{2N_f C_F}{x} \right) F_g + 2C_F^2 \sum_q \frac{F_{q+\bar{q}}}{x}$$

